INFORMATION TO USERS

This material was produced from a microfilm copy of the original document. While the most advanced technological means to photograph and reproduce this document have been used, the quality is heavily dependent upon the quality of the original submitted.

The following explanation of techniques is provided to help you understand markings or patterns which may appear on this reproduction.

1. The sign or "target" for pages apparently lacking from the document photographed is "Missing Page(s)". If it was possible to obtain the missing page(s) or section, they are spliced into the film along with adjacent pages. This may have necessitated cutting thru an image and duplicating adjacent pages to insure you complete continuity.

2. When an image on the film is obliterated with a large round black mark, it is an indication that the photographer suspected that the copy may have moved during exposure and thus cause a blurred image. You will find a good image of the page in the adjacent frame.

3. When a map, drawing or chart, etc., was part of the material being photographed the photographer followed a definite method in "sectioning" the material. It is customary to begin photoing at the upper left hand corner of a large sheet and to continue photoing from left to right in equal sections with a small overlap. If necessary, sectioning is continued again — beginning below the first row and continuing on until complete.

4. The majority of users indicate that the textual content is of greatest value, however, a somewhat higher quality reproduction could be made from "photographs" if essential to the understanding of the dissertation. Silver prints of "photographs" may be ordered at additional charge by writing the Order Department, giving the catalog number, title, author and specific pages you wish reproduced.

5. PLEASE NOTE: Some pages may have indistinct print. Filmed as received.

Xerox University Microfilms
300 North Zeeb Road
Ann Arbor, Michigan 48106

Downloaded from SHAREOK. Persistent Handle URL: https://hdl.handle.net/11244/3591

73-31,485

NESKORA, Daniel Ray, 1941-
COPPER AND NICKEL PRODUCTION BY CONTINUOUS STEADY-STATE HYDROGEN REDUCTION FROM AQUEOUS IONIC SALT SOLUTIONS.

The University of Oklahoma, Ph.D., 1973
Engineering, metallurgy

University Microfilms, A XEROX Company, Ann Arbor, Michigan

© 1973

DANIEL RAY NESKORA

ALL RIGHTS RESERVED

THIS DISSERTATION HAS BEEN MICROFILMED EXACTLY AS RECEIVED.

THE UNIVERSITY OF OKLAHOMA

GRADUATE COLLEGE

COPPER AND NICKEL PRODUCTION BY CONTINUOUS STEADY-STATE HYDROGEN REDUCTION FROM AQUEOUS IONIC SALT SOLUTIONS

A DISSERTATION

SUBMITTED TO THE GRADUATE FACULTY

in partial fulfillment of the requirements for the

degree of

DOCTOR OF PHILOSOPHY

BY

DANIEL RAY NESKORA

Norman, Oklahoma

1973

COPPER AND NICKEL PRODUCTION BY CONTINUOUS STEADY-STATE HYDROGEN REDUCTION FROM AQUEOUS IONIC SALT SOLUTIONS

APPROVED BY

C. M. Sliepcevich

William R. Huff

K E Starling

F M Townsend

William Marshall

DISSERTATION COMMITTEE

ABSTRACT

Hydrogen reduction of pure metals from aqueous solutions dates back to the middle 1800's but commercial application of this technology was not initiated until the middle 1900's. The past experimental and commercial applications by hydrogen reduction have all been based on batch or semi-continuous reaction systems.

This work explored the feasibility of using continuous, steady-state, hydrogen reduction processing to recover metallic copper and nickel from their respective aqueous ionic salt solutions. A small (100 gram per minute nominal capacity) continuous, processing facility was designed and constructed for this purpose. Aqueous metal ion feed solutions, including feed obtained from an acid leach of copper ore, were processed over a wide range of operating conditions.

The results of this work indicate the effective mechanism for continuous copper and nickel reduction is essentially heterogeneous. The corresponding rate limiting step for producing metallic copper is the subsequent reduction of intermediate basic salts of copper. Nickel reduction from ammine solutions requires a heteronucleating catalyst to form initial nickel seed particles. The active nickel seed

Copyright © 1973 by
Daniel Ray Neskora

Printed and bound in the United States of America.

All rights reserved. No part of this dissertation may be reproduced in any form or by any means, electronic or mechanical, including photocopying, recording, or by any information storage and retrieval system, without permission in writing from the author.

ACKNOWLEDGMENTS

It is difficult to acknowledge all the individuals who have contributed to the completion of this research effort. The author is especially indebted to his committee chairman, Dr. C. M. Sliepcevich, for his interest, inspiration, and continual guidance throughout the author's graduate work, to Dr. R. C. Jerner and Dr. K. E. Starling for their assistance during the author's graduate studies, and to the other members of my committee, Dr. William N. Huff, Dr. W. E. Martinsen, and Dr. F. M. Townsend.

My sincerest appreciation is extended to my colleagues, Mr. Robert L. Brown for his valuable background work in this challenging field, Mrs. Judy Homer for assistance in the analytical work, and Dr. Olmedo Kieswetter for his cooperation and suggestions during this work.

The efforts of Ms. Bobbie Everidge and Mrs. Carlotta Wood, who typed the manuscript, and Mr. Gregory Puckett and Mr. Steve Presson who handled the graphical work, are appreciated.

Special thanks is due to Dr. J. L. Lott, who undertook the proof reading of this dissertation and Mr. W. H. Bellis

who provided numerous hours of assistance in X-ray diffraction and electron microscope analyses.

The author is extremely grateful to University Engineers, Inc., for financial support during this research work and to my colleagues with Esso Research and Engineering Company, who encouraged my continued education.

Finally, I wish to acknowledge the contributions of my family. To my wife, Tena, and my children, who provided the incentive for this work and sacrificed the most, and to my parents, who appreciate the value of an education, a sincere thanks.

Daniel Ray Neskora

TABLE OF CONTENTS

		Page
LIST OF TABLES		viii
LIST OF ILLUSTRATIONS		ix
Chapter		
I.	INTRODUCTION	1
II.	PREVIOUS WORK	3
III.	SUPPORTING THEORY	22
IV.	DESCRIPTION OF EXPERIMENTAL EQUIPMENT	46
V.	EXPERIMENTAL PROCEDURE	66
VI.	ANALYTICAL PROCEDURE	80
VII.	METHOD OF DATA ANALYSIS	84
VIII.	EXPERIMENTAL RESULTS AND DISCUSSION	99
IX.	CONCLUSIONS	124
NOMENCLATURE		126
BIBLIOGRAPHY		129
APPENDICES		132

LIST OF TABLES

Table		Page
1.	Commercial Hydrometallurgical Plants of the Fifties	10
2.	Commercial Hydrometallurgical Plants of the Sixties	16
3.	Dissociation Constants and Standard Potentials of Copper Solutions at 25°C	29
4.	Analytical Techniques Used for Various Sample Phases	81
5.	Product Nickel Wet Analyses, Adjusted Nickel Content and Nickel Conversion Results	91
6.	Summary of Continuous Operations	100
7.	Run 13 Data Sheet	191

LIST OF ILLUSTRATIONS

Illustration		Page
1.	Potential at varying molar Metal Solutions and Hydrogen Potential at Varying pH (25°C)	26
2.	Schematic Diagram-Continuous Hydrogen Reduction Processing System	47
3.	Feed System Accumulator	49
4.	High Pressure Feed Pump, Reactor and Separator	50
5.	Continuous Hydrogen Reduction System Control Panel	53
6.	Feed Preheater	56
7.	Continuous Hydrogen Reduction Tabular Reactor	59
8.	Dilution Effect at Start of Run	88
9.	Fraction of Original Copper Ions in Amine Solution Precipitated by Pretreatment With Concentrated Sulfuric Acid	92
10.	Fraction of Original Nickel Ions in Ferrous Sulfate Acid Solution Precipitated by Pretreatment With Ammonium Hydroxide	93
11.	Nickel and Iron Composition of Synthetic Nickel Feed Precipitate	95
12.	Arrhenius Plot - Group I Copper Runs	105
13.	Arrhenius Plot - Group II Copper Runs	106
14.	Arrhenius Plot - Group III Copper Runs	109

LIST OF ILLUSTRATIONS (continued)

Illustration		Page
15.	Nickel Product Sieve Analyses	116
16.	Electron Micrograph of Run Minus 250 Mesh Nickel Product (X 14,000)	118
17.	Electron Micrograph of Run 16 Product Nickel (X 24,250)	120
18.	Arrhenius Plot - Nickel Runs	123
19.	Lapse Time versus Depletion (Run 1)	135
20.	Lapse Time versus Depletion (Run 2)	137
21.	Lapse Time versus Depletion (Run 3)	139
22.	Lapse Time versus Depletion (Run 4)	141
23.	Lapse Time versus Depletion (Run 5)	143
24.	Lapse Time versus Depletion (Run 6)	145
25.	Lapse Time versus Depletion (Run 7)	147
26.	Lapse Time versus Depletion (Run 8)	149
27.	Lapse Time versus Depletion (Run 9)	151
28.	Lapse Time versus Depletion (Run 11)	154
29.	Lapse Time versus Depletion (Run 12)	156
30.	Lapse Time versus Depletion (Run 13)	158
31.	Lapse Time versus Depletion (Run 14)	160
32.	Lapse Time versus Depletion (Run 15)	162
33.	Lapse Time versus Depletion (Run 16)	164
34.	Lapse Time versus Depletion (Run 17)	166
35.	Lapse Time versus Depletion (Run 18)	168
36.	Lapse Time versus Depletion (Run 19)	171

LIST OF ILLUSTRATIONS (continued)

Illustration		Page
37.	Lapse Time versus Depletion (Run 20)	173
38.	Lapse Time versus Depletion (Run 21)	175
39.	Lapse Time versus Depletion (Run 22)	178
40.	Pretreatment Accumulator Calibration	187
41.	Feed Hydrogen Rotometer Calibration	188
42.	High Pressure Separator Liquid Volume Calibration	189
43.	Non-isothermal Reactor Temperature Profile (Run 13)	192

CHAPTER I

INTRODUCTION

The precipitation of a pure metal product from a pregnant leach solution of metal ions is a critical step in all hydrometallurgical processes for recovering metals. The ability to precipitate a pure metal efficiently and economically is the distinguishing characteristic among currently available precipitation techniques.

Hydrogen reduction of aqueous metal ion solutions to produce pure metal powders offers an attractive alternative to the currently popular electrowinning precipitation techniques. Based on the efficiencies of converting fuel to hydrogen and to electricity, current batch hydrogen reduction techniques are capable of producing two to three times more metal per unit of fuel than electrowinning. Capitalizing on the enhanced efficiency of a continuous processing system, hydrogen reduction could produce four to six times more metal per unit of input fuel than electrowinning.

The objectives of this investigation were twofold: Design and construct a continuous hydrogen reduction processing facility, and develop preliminary experimental data to

determine the process feasibility. These objectives were accomplished by constructing and operating a micro-mini pilot plant having a nominal feed capacity of 100 cubic centimeters per minute. Aqueous synthetic metal ion feed solutions of copper and nickel were continuously reduced with hydrogen over a wide range of processing conditions. The continuous reduction studies were culminated with operations employing actual feed solutions derived from leaching of copper oxide ores.

CHAPTER II

PREVIOUS WORK

Experimental Work

Hydrogen reduction of aqueous ionic metal solutions to recover metal values dates back to the 19th century. In 1869, Academician M. N. Beketoff (1) was successful in displacing silver and mercury from their dilute metal salt solutions under ten atmospheres hydrogen pressure. Employing similar conditions, Beketoff was unable to displace copper or lead.

In 1892, Tammann and Nernst (32) attempted to displace copper from its copper sulfate solution with hydrogen. The experiments of Tammann and Nernst employed hydrogen pressures approaching forty atmospheres and were continually plagued with explosions. The experiments surviving the severe pressure conditions failed to precipitate copper from its ionic salt solution. Tammann and Nernst were the last investigators to contribute to the science of hydrogen reduction during the 19th century.

During the first decade of the 20th century, interest in hydrogen reduction to recover metals from aqueous solution

was renewed. In 1908, V. N. Ipatieff (16) initiated his experiments in the field of aqueous phase metal ion hydrogen reduction. Ipatieff's work was an outgrowth of his successful experimentation in the hydrogenation of organic compounds under pressure. Consequently, Ipatieff possessed the technical background in high pressure applications that previously hindered the progress of earlier investigators.

Ipatieff's first experiments involved the effects of hydrogen pressure on hydrogen reduction at room temperatures. Room temperature experiments conducted at hydrogen pressures of 200, 580, and 600 atmospheres failed to separate copper from its sulfate solution. Similar high pressure, room temperature, experiments were made with other salts of copper and the salts of nickel, cobalt, and cadmium. The results of these additional experiments also failed to separate the respective metal from their solutions.

In Ipatieff's subsequent batch hydrogen reduction experiments heat was applied to increase the reaction temperature. The results of increasing temperature in the copper sulfate - hydrogen system were dramatic. Deposits of copper, copper oxides, and copper basic salts immediately precipitated at the elevated temperature conditions. The composition of the deposits was directly related to the severity of the experiment. For example, copper sulfate experiments conducted at 90°C and 25 atmospheres hydrogen pressure initially produced the crystalline basic salt, antlerite. Continued

exposure of the basic salt solution revealed the presence of cuprous oxide and eventually after 40 to 50 hours at reaction conditions the presence of metallic copper was detected. Complete conversion to metallic copper was observed after seven days at 90°C and 25 atmospheres pressure. Ipatieff attributed the basic salt and metal oxide formations to hydrolysis of the salts and considered the pure metal precipitation by hydrogen a separate reaction. To prove his theory, Ipatieff added sulfuric acid to neutral solutions of copper sulfate and experimentally observed the precipitation of pure copper in the absence of hydrolysis.

Ipatieff's experiments showed that at atmospheric pressure an increase in temperature does not precipitate a metal and conversely at room temperature an increase in pressure does not precipitate a metal by hydrogen. The cooperative action of both temperature and pressure is essential for hydrogen reduction to take place. According to Ipatieff (16), each metal has a certain critical condition of temperature and pressure at which its displacement from solutions occurs. The definitions of critical temperature, according to Ipatieff, is the temperature at which a metal is precipitated from solution rapidly and completely at a minimum hydrogen pressure.

In 1926 (15), Ipatieff experimented with the hydrogen reduction of multi-metal ionic solutions. Initial experiments

using binary solutions of copper and zinc sulfates and of copper sulfate and iron salts separated metallic copper exclusively. However, the separation of copper occurred at temperatures and pressures slightly higher than those required for precipitation of copper from single copper solution.

V. V. Ipatieff, the son of the elder Ipatieff, pursued the multi-metal hydrogen reduction experiments which his father initiated. V. V. Ipatieff (16) was successful in completely separating arsenic from bismuth and antimony in acid solutions. The separation of antimony from bismuth was only partial due to the small difference in electropotential between the two metals. According to the elder Ipatieff, V. V. Ipatieff conducted additional experiments involving the separation of metals in the platinum family. However, details of this additional work were not reported.

V. N. Ipatieff concluded the initial phase of his work with hydrogen reduction in 1930. Twenty-two years later, the eighty-five year old Russion-born scientist renewed his interest in hydrogen reduction; however, he was only able to review his past work briefly prior to his untimely death in 1952.

The pioneer work of the Ipatieffs has been continued both here and abroad. Beginning in the nineteen fifties, numerous investigations extending the initial work of Ipatieff have been published. The majority of publications are related to the industrial efforts of the Chemical Construction

Corporation and Sherritt Gordon Mines, Ltd. Notable exceptions are the Russian studies of Dobrokhotov (6) and Sobol (31) and the contributions of university research groups.

The contributions of university research groups may be narrowed down to three major sources. The continuing work of Halpern (13) and Peters (26) at the University of British Columbia provides the majority of the university research group contributions. Halpern and his co-workers have been primarily concerned with the catalytic activation of molecular hydrogen by metal ions and complexes. Peters and his co-workers have been primarily concerned with the mechanism and kinetics of copper reduction from various solutions.

At the University of Utah, Kaneko and Wadsworth (34) have studied the applications of nucleation catalyst to the hydrogen reduction of ammine-cobaltous sulfate solutions.

Beginning in 1965 the University of Oklahoma initiated work in the field of hydrogen reduction. Brown (3) performed a comprehensive study of the copper sulfate - hydrogen system. Many of Brown's findings confirm the earlier findings of Ipatieff. In conjunction with Brown's study an in-depth investigation of the thermodynamics of the system was made by Conner (4). Conner applied a systematic computer solution to the multivariable copper sulfate - ammonium sulfate system and successfully described the concentrations and activities of all ionic species involved.

In 1971 Kothari (18) studied the "critical reaction" temperatures of nickel sulfate systems. Kothari determined the reaction temperatures for buffered nickel sulfate solutions were between 375°F and 400°F. Similar operations using ferrous sulfate reached completion before 300°F.

In 1973 Kieswetter (17) studied the process variables of the copper and nickel sulfate systems. Kieswetter used an improved batch hydrogen reduction system to make reduced residence time studies. The investigation by Kieswetter provided sufficient observations and data to bridge the gap between batch hydrogen reduction and continuous hydrogen reduction.

Commercial Application

In the late nineteen forties and early nineteen fifties (23), Chemical Construction Corporation initiated the transition from batch laboratory experiments to batch commercial hydrogen reduction processes. Under the leadership of F. A. Schaufelberger, the critical engineering and technological solutions to commercial size batch hydrogen reduction problems were solved.

Application of hydrogen reduction technology developed by Chemical Construction Corporation depended on the successful development of a compatible hydrometallurgical leaching process. Such a process was simultaneously being developed by Sherritt Gordon Mines, Ltd. The combination of the

hydrometallurgical leaching and reduction processes was carried through by Sherritt Gordon (23) in their laboratory and in their pilot plant facilities. The resulting process combination, perfected by Sherritt Gordon, led to the world's first total hydrometallurgical processing operation.

Plants of the Nineteen Fifties

Four gaseous reduction hydrometallurgical plants were constructed and operated during the nineteen fifties. These plants are listed with brief details in Table I.

Sherritt Gordon plant: The first integrated hydrometallurgical hydrogen reduction commercial plant was fostered by the pilot plant work of Sherritt Gordon. The commercial plant is located at Fort Saskatchewan, Alberta. Feed to the Sherritt Gordon plant is a flotation concentrate of nickel-cobalt-copper sulfide. Nickel is the predominate product with lesser quantities of cobalt, copper sulfide and specialty powders being produced.

The feed concentrate is leached with air and ammonia under elevated pressure and temperature in a two-stage batch operation. Following leach purification and recovery of all copper in the copper sulfide form, the nickel and cobalt metal values are separately recovered by hydrogen reduction. Nickel is reduced in horizontal, agitated, batch autoclaves employing hydrogen at a total pressure of 450 pounds per square inch and operating temperatures of 350-400°F. The use of a catalyst

TABLE I

COMMERCIAL HYDROMETALLURGICAL PLANTS OF THE FIFTIES*

Status	Company	Years in Operation	Metals	Production lb/year	System	Refinery Feed Materials	Comments
Operating	Sherritt Gordon Mines, Ltd. Mines: Lynn Lake, Manitoba, Canada Refinery: Fort Saskatchewan, Alberta, Canada	1954 to date	Ni Co Cu Composite powders	30,000,000 1,000,000 Development quantities 100,000	Metal ammine sulfate solutions	1. Ni-Cu-Co sulfide flotation concentrates from Lynn Lake and elsewhere. 2. Ni matte from various sources. 3. High-temperature alloy scrap and other secondary materials.	
			Special powders	250,000	Nickel ammine carbonate solutions & basic salts		
Operating	Universal Minerals and Metals (formerly Whitaker Metals) Plant: Kansas City Missouri, U.S.A.	1954 to date	Cu	4,600,000	Copper ammine carbonate solutions	Copper scrap	
Shut down	Calera Mining Co. Mines: Blackbird, Idaho, U.S.A. Refinery: Garfield, Utah, U.S.A.	1953 to 1959	Co	2,500,000	Metal ammine sulfate solutions	Arsenical cobalt-iron sulfide flotation concentrates	Operating difficulties resulted in switch to electrolytic cobalt recovery in 1956. Shut down owing to shortage of ore.
Shut down	National Lead Co. Mines and Refinery: Fredericktown, Missouri, U.S.A.	1954 to 1960	Ni, Co	1,500,000 1,200,000	Metal ammine sulfate solutions	By-product Ni-Co-Cu sulfuric flotation concentrates from a Pb-Cu mining operation	Shut down owing to lack of feed.
			Cu	1,500,000 (impure)	Metal sulfate solutions		

*Source: Advances in Extractive Metallurgy, 1968, Reference No. 23.

is necessary to initiate the reduction cycle which includes three distinct operations:

1. Nucleation.
2. Densification.
3. Leaching.

The catalyst used to initiate the nucleation operation is ferrous sulfate and is added to provide 1.0 gram per liter of total reduction solution. The nucleation operation is performed with vigorous agitation and is completed in 30-40 minutes. When nucleation is complete, the depleted nickel solution is discharged from the autoclave leaving a very fine nucleated nickel powder. The autoclave is then refilled with the reduction feed solution and the first densification reduction is carried out. During this and subsequent densifications, nickel particles provide the catalytic surface required for nickel reduction to proceed. The initial, nucleated, nickel particles grow in size and increase in density with each densification operation. After 50-60 densification operations the nickel particles reach 200-250 microns in size and are discharged from the reduction autoclave.

During reduction, nickel plates out on the walls of the autoclave. Following the densification operation this plating is removed by air-ammonia leaching with an ammonia-ammonium sulfate solution. The leaching operation completes the reduction cycle.

The nickel reduction feed contains both nickel and cobalt. However, because of the difference in potential of the two metal ion solutions the nickel may be selectively reduced to a terminal concentration of 1.0 grams per liter. At this concentration cobalt reduction accounts for only 0.07 weight percent of the reduced metallic nickel. The depleted nickel reduction product solution, containing mostly cobalt, is purified using a soluble cobaltic pentammine process (23). The purified cobaltous diammine is reduced with hydrogen at 350°F and 500 pounds per square inch pressure using cobalt powder as a catalyst. Similar to the batch nickel reduction cycle, the cobalt particles increase with subsequent densification operations. Approximately 30 densification operations are performed before the cobalt powder is discharged from the batch autoclave. Plating of cobalt on the autoclave walls is less severe than during nickel reduction; therefore, leaching of the autoclave is only performed every third reduction cycle.

Universal Minerals and Metals plant: The Universal Minerals and Metals plant in Kansas City, Missouri, produces copper from an ammonia - ammonium carbonate leach of scrap and cement copper. The plant is an extremely efficient batch operation designed to operate on the small margin of profit associated with scrap copper recovery. Atmospheric pressure leaching at 120-140°F is practiced in rotating or agitated

batch systems. The resulting treated and purified leach solution is reduced in agitated, horizontal autoclaves at 400°F and hydrogen pressures of 900 pounds per square inch gauge. A reduction cycle consists of four batch reductions. No nucleation catalyst is required to initiate the homogeneous reduction; however, the presence of copper improves the rate of copper reduction (23). Ammonium polyacrylate is added to the reduction feed solution to control plastering effects on the autocalve walls. Consequently, a formal autoclave leaching procedure following a reduction cycle is not necessary.

The copper recovered from the fourth consecutive reduction is centrifuged and washed to remove surface impurities. Copper powder is then dried and sintered under hydrogen atmospheres at 1100-1300°F. During the sintering process, carbon derived from ammonium polyacrylate reacts with surface oxides to form gaseous oxides which are removed. The sintered copper cake is crushed, pulverized and air classified to produce the appropriate grade copper powder.

National Lead Company: The National Lead Company refinery located at Fredericktown, Missouri, is no longer in operation. It processed a cobalt-nickel-copper sulfide concentrate from a lead-copper operation. Following acid leaching and solution purification with limestone addition, the acid solution was hydrogen reduced in horizontal, agitated autoclaves. Eighty-five percent of the feed copper

concentration was recovered in a single batch reduction at 325°F and 600 pounds per square inch gauge total hydrogen pressure. The acid conditions employed provided selective separation of copper in the presence of nickel and cobalt ions. However, the high hydrogen ion concentration of the final reduction solution decreased the effective copper reduction rate. An iron cementation step was required to recover the remaining copper from reduction solution.

The copper stripped solution from cementation was purified with limestone to remove iron. The resultant solution, containing approximately equal concentrations of nickel and cobalt, was hydrogen reduced by a process similar to the Sherritt Gordon process previously described.

Calera Mining Company: The Calera Mining Company refinery, located at Garfield, Utah, is no longer in operation. It processed a arsenical cobalt concentrate. The high sulfur content (29 percent) concentrate was leached under acidic conditions in horizontal, stirred autoclaves at 375°F with air at 500 pounds per square inch pressure. Cobalt, nickel and copper passed into solution while most of the iron and arsenic were precipitated as basic sulfate and ferric arsenate.

The copper was stripped from the purified solution by cementation with recycled cobalt powder. The resulting cobalt and nickel solution was buffered with ammonia prior

to reduction by hydrogen to produce a high sulfur content cobalt powder. Reduction was accomplished with hydrogen at 375°F and 800 pounds per square inch pressure in vertical, stirred autoclaves. No efforts were made to separate nickel and cobalt during reduction. The reduction powder was melted with a high-lime slag to reduce the sulfur content before selling to the U.S. Government stock pile.

Plants of the Nineteen Sixites

During the nineteen sixties three additional gaseous reduction hydrometallurgical plants were constructed. Table II lists the plants of the sixties with brief details of their operations.

Freeport Nickel Company: The largest hydrometallurgical plant constructed during the nineteen sixties was ironically operated for the shortest length of time. The plant, operated by Freeport Nickel Company at Port Nickel, Louisiana, processed a rich nickel - cobalt sulfide prepared and shipped from Moa Bay, Cuba. The Cuban concentrate of mixed sulfides was acid leached at 500 pounds per square inch pressure and 350°F in stirred spherical autoclaves. Purification of the leach solution was carried out in two steps. Iron, chromium and aluminum hydroxides were precipitated by air oxidation and pH adjustment to 1.5 with ammonia. After adjusting the pH of the resulting filtered solution to a value of 1.5, the solution was reacted with

TABLE II

COMMERCIAL HYDROMETALLURGICAL PLANTS OF THE SIXTIES*

Status	Company	Years of Operation	Metals	Production lb/year	System	Refinery Feed Materials	Comments
In mothball storage	Freeport Nickel Co. Mines: Cuba Extraction plant: Moa Bay, Cuba Refinery: Port Nickel, Louisiana, U.S.A.	Six months (1959-60)	Ni, Co	50,000,000 5,500,000	Metal ammine sulfate solutions	Precipitated Ni-Co sulfide from Moa Bay laterite treatment plant	Extraction plant in Cuba currently operating at 50 percent capacity. Refinery shut down but continuously maintained.
Operating	Arizona Chemcopper Corporation Plant: Bagdad, Arizona, U.S.A.	1966 to date	Cu	16,500,000	Acid copper sulfate solutions	Cement copper	
Operating	Outokumpu Oy Plant: Kokkola, Finland	1967	Cu	3,000,000	Cobalt ammine sulfate solutions	Solution from aqueous leaching of sulfation-roasted cobaltiferous pyrite	

*Source: Advances in Extractive Metallurgy, 1968, Reference 23.

hydrogen sulfide gas to precipitate copper, lead and most of the zinc.

The purified solution was then hydrogen reduced in agitated, horizontal autoclaves at 375°F and 650 pounds per square inch gauge pressure. During reduction the pH was maintained between 0.9 and 1.8 by injection of ammonia. By maintaining the 0.9 to 1.8 pH range, 95 percent of the nickel was preferentially reduced. The extremely acid reduction conditions and resulting severe corrosion conditions led to the use of titanium-lined autoclaves and internals.

The depleted solution from the nickel reduction step was concentrated to 500 grams per liter ammonium sulfate, at which point the double salts of ammonium sulfate and nickel, cobalt and zinc sulfates precipitated. The mixed double salts were separated from the ammonium sulfate solution and were redissolved in water. The subsequent nickel - cobalt separation was achieved by means of the soluble cobaltic pentammine process previously described for the Sherritt Gordon plant. The final cobalt recovery was by batch hydrogen reduction at 350°F and 500 pounds per square inch gauge pressure.

Six months after the Freeport plant started operations the turn of political events severed the Cuban feed supply, thus forcing the plant to shut down.

Arizona Chemcopper Corporation: The Arizona Chemcopper Corporation plant located at Bagdad, Arizona, employs an acid-ammonium sulfate step to solubilize cement copper. The cement

copper is produced by dump leaching copper oxide ores with sulfuric acid and subsequent cementation of the 1.0 gram per liter copper leach solution using shredded tin cans.

The leach solution is filtered at a pH of 1.5-2.5 and is hydrogen reduced at 275°F and 425 pounds per square inch pressure. The stirred, horizontal reduction autoclaves are titanium lined to limit corrosion during the acid reduction operation. Polyacrylic acid is blended with the reduction feed solution to prevent plastering and to control resultant copper particle size. A drying, sintering, and classification system, similar to that described for the Universal Minerals and Metals plant, is used to obtain the desired product quality.

Outokumpu Oy: The Outokumpu Oy plant, located at Kokkola, Finland, processes a cobaltiferrous pyrite by-product from an adjacent plant. A pyrometallurgical roasting step followed by a quenching leach are used to produce a 20 gram per liter cobalt solution also containing nickel, copper and zinc. The cobalt solution is purified by selective hydrogen sulfide precipitation. Employing careful pH control the copper, zinc, nickel and cobalt sulfides are separately precipitated from solution. The cobalt sulfide is then suspended in water and leached at 285°F with 150 pounds per square inch gauge air pressure. The resulting cobalt solution is subjected to a final nickel and iron removal step. The purified cobalt solution is buffered with

ammonia and is hydrogen reduced at 375°F and 600 pounds per square inch gauge pressure.

Plants of the Nineteen Seventies

Seven gaseous hydrogen production plants were commissioned during the nineteen fifties and sixties. Of the original seven plants, four are currently operating, one is being re-activated under new management, and two have been shut down. The National Lead Fredericktown plant was shut down after six years of operation because of feed shortage. Likewise, the Freeport Nickel plant operation was terminated after only six months operation because of feed shortage. Consequently, of the seven original plants, only the Calera Mining plant at Garfield, Utah, was shut down for technological reasons.

The technological advances made in gaseous hydrogen reduction plants during the past two decades are being applied to three new plants this decade (23).

Union Corporation: Union Corporation has initiated operation of a new hydrometallurgical plant at Springs, Transvaal, South Africa. The Transvaal plant processes a depleted platinum sulfide ore containing nickel and copper values. Copper and nickel are separately leached from a matte which is later processed for precious metals recovery. Copper is recovered from its leach solution by electrowinning, and nickel is recovered by gaseous hydrogen reduction.

Filmed as received

without page(s) 20.

UNIVERSITY MICROFILMS.

The original experimental batch concepts used by Ipatieff at the turn of the century have been directly applied to commercial processes. Current designs for large capacity hydrometallurgical plants incorporate larger and improved batch designs. It appears that the batch or semi-continuous processing concepts will continue to predominate in hydrometallurgical plants of this decade.

CHAPTER III

SUPPORTING THEORY

Thermodynamic Considerations

The hydrogen reduction of a divalent metal ion from its aqueous solvent solution may be written as

$$M^{++} + H_2 \rightleftharpoons M^0 + 2H^+ \qquad \text{(III-1)}$$

where M^{++} is the metal ion, H_2 is the hydrogen reducing gas, M^0 is the product metal, and H^+ is the product hydrogen ions. The reversible half-cell electrode reactions which combine to form Equation III-1 are:

$$M^0 \rightleftharpoons M^{++} + 2e^- \qquad \text{(III-2)}$$

$$H_2 \rightleftharpoons 2H^+ + 2e^- \qquad \text{(III-3)}$$

The combined Gibbs free energy relationship for the reaction represented by Equation III-1 at temperature T may be written as

$$\Delta G_T - \Delta G_T^0 = RT \ln \frac{a_{M^{++}} \cdot a_{H_2}}{a_{M^0} \cdot a_{H^+}^2} \qquad \text{(III-4)}$$

where ΔG_T is the Gibbs free energy change, ΔG_T^0 is the standard state free energy change, R is the universal gas constant, T is the absolute temperature, and a represents the activities of the corresponding species. At equilibrium, $\Delta G_T \equiv 0$ and the ratio of activities in Equation III-4 may be expressed as

$$K_a = \frac{a_{M^{++}} \cdot a_{H_2}}{a_{M^0} \cdot a_{H^+}^2} \qquad \text{(III-5)}$$

where K_a is the equilibrium constant, expressed in terms of activities, for Equation III-1. The corresponding equilibrium Gibbs relationship may be written as

$$\Delta G_T^0 = -RT \ln K_a \qquad \text{(III-6)}$$

The Nernst relationship between electropotential and Gibbs free energy is

$$\Delta G = -nFE \qquad \text{(III-7)}$$

where n is the number of electrons transferred per mole of product formed, F is the Faraday equivalent, and E is the corresponding reaction electrode potential. In terms of electrode potential the non-equilibrium relation of Equation III-4 may be written as

$$E_{III-1} = E_{III-1}^0 + \frac{RT}{nF} \ln \frac{a_{M^{++}} \cdot a_{H_2}}{a_{M^0} \cdot a_{H^+}^2} \qquad \text{(III-8)}$$

For the corresponding half cell reactions of Equations III-2 and III-3, where $a_{M^0} = 1$, a_{H_2} = hydrogen partial pressure, and the ion activities are expressed by their respective concentrations, the following potential expressions apply:

$$E_M = E^0_{M^0} + \frac{RT}{nF} \ln \frac{1}{[M^{++}]} \qquad \text{(III-9)}$$

$$E_{H_2} = E^0_{H_2} - \frac{RT}{nF} \ln \frac{[H^+]^2}{P_{H_2}} \qquad \text{(III-10)}$$

By convention, the hydrogen reference electrode is taken as zero. Substitution of the pH equivalent for hydrogen ion concentration and setting n = 2 for a divalent metal ion gives

$$E_{H_2} = \frac{+2.303\ RT}{F} (pH) + \frac{RT}{2F} \ln (P_{H_2}) \qquad \text{(III-11)}$$

For the reaction represented by Equation III-1 to have a tendency to occur spontaneously without supplying work energy from an external source, the Gibbs free energy change for the overall reaction must satisfy the criteria

$$\Delta G_{III-1} < 0 \qquad \text{(III-12)}$$

On an electrical potential basis, Equation III-12 is equivalent to

$$E_{III-1} > 0 \qquad \text{(III-13)}$$

In terms of the difference in half cell potentials given for

Equations III-9 and III-11, Equation III-13 may be written as

$$E_{H_2} - E_{M^{++}} > 0 \qquad \text{(III-14)}$$

Equation III-14 sets the requirement for hydrogen reduction to occur; the hydrogen potential at a given temperature and pressure must exceed the potential of the ionic metal solution at the same conditions.

Figure 1 illustrates the variation of hydrogen potential with pH and pressure at 25°C temperature. The variation of the potentials of copper and nickel ion solutions as a function of concentration at 25°C are also shown in Figure 1.

The thermodynamic requirement for hydrogen reduction to occur was derived in Equation III-14. Based on Equation III-14 and the results shown in Figure 1 for a temperature of 25°C, cupric ions can theoretically be reduced by hydrogen over the entire range of pH and copper ion concentration shown. The lower pH limit, calculated at 1 atmosphere hydrogen pressure and 25°C temperature, for hydrogen reduction of cupric ion solution is approximately minus three. As illustrated in Figure 1, an increase in hydrogen pressure from 1 to 100 atmospheres will reduce the minimum theoretical pH below minus three.

The lower pH limits for hydrogen reduction of nickel ions at 25°C and 1 atmosphere hydrogen pressure, shown in Figure 1, is approximately 4 to 5 over the given concentration

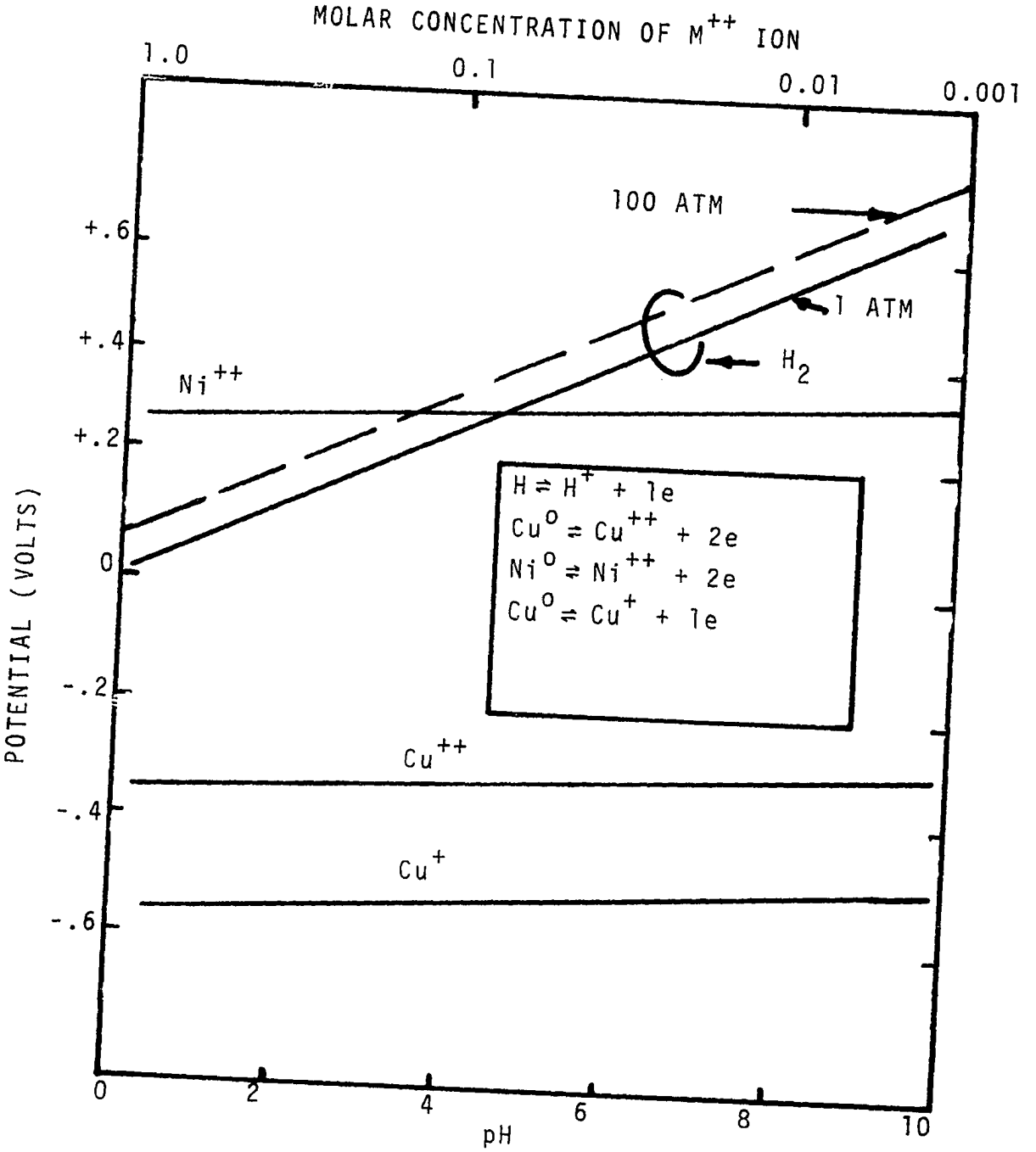

Figure 1. Potential at Varying Molar Metal Solutions and Hydrogen Potential at Varying pH (25°C)

range. Increasing hydrogen pressure from 1 to 100 atmospheres reduces this lower limit approximately one pH unit.

According to Figure 1, a decrease in metal ion concentration from 1.0 to 0.001 results in a corresponding increase in metal ion potential of less than 0.1 volts. However, in real solutions, the concentrations are replaced by metal ion activities which are more sensitive to variations in corresponding processing conditions.

The upper values of pH shown in Figure 1 appear to be unlimited. However, the steeply increasing hydrogen potential is partially compensated by a corresponding increase in metal ion solution potential. This increased metal ion solution potential in ammonia systems, for example, is caused by complex formations. Complexes of ammonia and divalent metals form according to

$$M^{++} + xNH_3 \rightleftharpoons M(NH_3)_x^{++} \qquad \text{(III-15)}$$

The dissociation constant for the complex formed in Equation III-15 may be written as

$$k_x = \frac{[M^{++}][NH_3]^x}{[M(NH_3)_x^{++}]} \qquad \text{(III-16)}$$

where k_x is the dissociation constant and the terms in brackets are the activities of the reactants and products. Consequently increasing the pH of a divalent metal solution results in a decreased metal ion concentration which is dependent on the dissociation constant expressed in Equation III-16.

To illustrate the effects of the complexing reaction, Table III gives a partial listing of dissociation constants and corresponding solution potentials for the copper - ammonia systems at 25°C. The cuprous ion shown in Table III is unstable in its pure ionic form. However, in the presence of various ions or molecules, such as ammonia, the cuprous state is stabilized.

The reduction of divalent metals from ammonia solutions may be generally written for solutions containing more than 2 moles ammonia per mole of metal as:

$$M^{++} + xNH_3 + H_2 \rightarrow M^0\downarrow + xNH_4^+ + (x-2)NH_3\uparrow, \quad x \geq 2 \tag{III-17}$$

where the terms are represented by respective activities or partial pressures. The equilibrium constant for the reactions of Equation III-17 may be written as

$$K_{III-17} = \frac{[NH_4^+]^x [NH_3]^{x-2}}{[M^{++}] [NH_3]^x P_{H_2}} \tag{III-18}$$

Incorporating the dissociation constant relation given by Equation III-16, Equation III-18 becomes

$$K_{III-17} = \frac{[NH_4^+] [NH_3]^{x-2}}{k_x [M(NH_3)_x^{++}] P_{H_2}} \tag{III-19}$$

Evaluation of Equation III-19 at operating conditions reveals the impact of ammonia on the equilibrium of ammoniacal hydrogen reduction systems. The presence of k_x in the denominator

TABLE III*

DISSOCIATION CONSTANTS AND STANDARD POTENTIALS OF COPPER SOLUTIONS AT 25°C

Solution	Dissociation Constant, k_x	Standard Potential E (volts)
Cu^{++} (ionic)	--	-0.337
Cu^{+}	--	-0.521
$Cu^{+} \rightarrow Cu^{++}$	1.6×10^{6}	--
$Cu(NH_3)_2^{+}$	1.35×10^{-11}	+0.120
$Cu(NH_3)_4^{++}$	4.7×10^{-15}	+0.050

*From Reference 29.

of Equation III-19 indicates the reductions of weak complexes such as $Cu(NH_3)_4^{++}$, shown in Table III, are favored. Excess concentrations of ammonium salts and free ammonia above the equilibrium concentrations determined from Equation III-19 adversely effect the reduction equilibrium (29).

Kinetic Considerations

Thermodynamic considerations of the hydrogen reduction reaction not only verify its feasibility but also develop general conditions necessary for the reaction to proceed. The rate of the hydrogen reduction reaction and its actual application in practice are controlled by the kinetics of the system. The kinetics are intimately related to the mechanisms by which the reaction proceeds. Consequently, an

understanding of the possible mechanisms occurring during hydrogen reduction is a prerequisite for efficient process utilization.

Hydrogen reduction of metal ions from solution generally consist of nucleation, growth, and agglomeration phenomena (29). Nucleation is the homogeneous formation of the smallest stable metal particle from its metal ion counterpart.

Growth is the atom-by-atom reduction of solution metal ions on a solid surface. The resulting formation of metal on the solid surface usually adheres to form uniform surface deposits and increasingly larger particle sizes. In systems using vigorous agitation the freshly formed particles may be dislodged to form new solid surfaces for subsequent reductions. This process is known as ancillary nucleation. Although growth is normally associated with reduction of ions on their metal counterpart, reduction of metal ions by the growth phenomenon may also occur on foreign surfaces.

Agglomeration is perhaps the least important phenomenon in regard to the actual reduction of metal ions from solution. Agglomeration is the clustering of two or more metal particles resulting in the formation of a larger aggregate particle. The agglomerated aggregate may contribute to the growth phenomenon; however, the more active smaller particles usually promote growth more effectively.

In an initially homogeneous operation, nucleation is the only phenomenon that can occur. Following the initial nucleation of a product solid surface, growth and agglomeration contribute to the overall reaction rate. In actual practice, most hydrometallurgical processes involve heterogeneous reactions occurring at solid-liquid interfaces. These solid-liquid reactions are usually responsible for determining the rate of the overall reaction.

Most of the heterogeneous reactions in hydrometallurgical processes are believed to occur by the following sequence of steps (13).

1. Absorption of gaseous reactants by the solution.
2. Transport of dissolved reactants from the main body of the solution to the solid-solution interface.
3. Adsorption of reactants on the solid surfaces.
4. Reaction on the surface.
5. Desorption of the products from the surface.
6. Transport of the desorbed products into the main body of the solution.

At temperatures below 400°F, high hydrogen partial pressures, and sufficient agitation, step one is not usually rate limiting. More often the transport of dissolved reactants to the solid surface (step two) is the rate limiting step. This step may be illustrated by considering a growth model for a metal seed particle in a solution of dissolved

metal ions and hydrogen. The rate of transport of the reactants to the seed particle is determined by the rate of the species diffusing across a finite layer immediately adjacent to the seed metal surface. Within the finite diffusion layer the concentrations of the diffusing species may be represented approximately as linear functions of the layer thickness. Based on this simplified model, the rate at which each dissolved specie diffuses to the solid surface may be represented by Fick's law as:

$$\frac{dn}{dt} = \frac{DA}{\delta} (C - C_o) \qquad \text{(III-20)}$$

where n is the amount of diffusing species moving across the diffusion layer of thickness δ, in time t. D is the diffusion coefficient, A is the area of the diffusion layer or more commonly the metal surface area, C_o is the specie concentration at the metal surface and C is the bulk specie concentration.

Assuming that steps three and four are not rate limiting, the diffusing species are rapidly converted as they reach the solid surface. Consequently, the diffusion rate reaches a limiting value when C_o is zero and may be represented as:

$$\frac{dn}{dt} = \frac{DA}{\delta} C \qquad \text{(III-21)}$$

As metal ions are reduced at the seed metal surface, growth of the original seed progresses and hydrogen ions are

formed. The atom-by-atom deposition of metal presents no problem since new and more active surfaces are being created. The formation of hydrogen ions, however, if not rapidly desorbed by step five and transported from the surface by step six, creates an adversely low pH. The low pH at the solid surface can make the surface reaction of step four rate limiting.

The heterogeneous reaction of solid reactant dispersed in a solution is similarly governed by the sequence of steps previously described. In a finely dispersed solid reactant system only the diffusion of absorbed hydrogen is involved in step two. Likewise, in step three, only hydrogen is adsorbed on the reactant solid surface. The reaction of the adsorbed hydrogen on the solid reactant, in step four, is a probable rate limiting step. However, if the solid reactant is sufficiently fine, i.e., approaching atomic dimensions, this step may be exceptionally fast.

The final two steps, five and six, in a finely dispersed solid reactant heterogeneous reaction are likewise not as critical as in the growth mechanism previously described. The reduced solid reactant may, or may not, be removed from the remaining unconverted solid. In efficiently agitated systems, ancillary nucleation and attrition provide the means to separate reduced products from unreduced solid reactant.

Theoretical Aspects of Copper and Nickel Reduction

The mechanisms whereby reduction with hydrogen proceeds in copper and nickel solutions varies depending on the initial feed composition.

Copper Sulfate Acid Solutions

In general, hydrogen reduction of copper sulfate solutions with pH less than 7 may involve several reaction mechanisms. Based on the solution pH used, two of the reduction mechanisms may be isolated.

In unbuffered acid copper sulfate solutions with pH greater than approximately three, hydrolysis is a major mechanism in hydrogen reduction. Hydrolysis is the homogeneous reaction of water with solution ions at elevated temperatures and pressures resulting in the formation of precipitated basic salts. The composition and crystalline form of basic salts produced by hydrolysis varies with processing conditions. A common basic salt precipitated from copper sulfate solutions is antlerite. The hydrolysis reaction illustrating the formation of antlerite is:

$$3\ CuSO_4 + 4\ HOH \overset{T,P}{\rightleftharpoons} Cu_3SO_4(OH)_4 + 2\ H_2SO_4 \qquad \text{(III-22)}$$

During hydrogen reduction of copper sulfate systems containing hydrolysis precipitates such as antlerite, two reduction mechanisms are possible. The first involves a dissolution of the basic salt precipitate followed by

homogeneous reduction to the respective metal. The second mechanism involves the direct reduction of basic salt to cuprous oxide or metallic copper, shown for antlerite in the following reactions:

$$Cu_3SO_4(OH)_4 + \frac{3}{2} H_2 \overset{T,P}{\rightleftharpoons} \frac{3}{2} Cu_2O + H_2SO_4 + \frac{5}{2} H_2O \quad \text{(III-23)}$$

$$Cu_3SO_4(OH)_4 + 3 H_2 \overset{T,P}{\rightleftharpoons} 3 Cu^O + H_2SO_4 + 4 H_2O \quad \text{(III-24)}$$

In acid solutions with pH between three and seven, the equilibrium of the Equation III-22 hydrolysis reaction favors the formation of antlerite. An increase in the amount of sulfuric acid present, either from a parallel reduction mechanism or from an acid addition procedure, is necessary to induce the redissolution of the basic salt. The formation of acid in a parallel reduction mechanism is limited during the initial phases of reduction since most of the original solutions ions are associated with the basic salts. Consequently, the heterogeneous reduction mechanisms shown by Equations III-23 and III-24 appear probable. The results of these reactions were first encountered by Ipatieff (16) and later suggested as a possible reduction mechanism by Brown (3).

The partial reduction of antlerite to cuprous oxide, shown in Equation III-23, might be expected from a hydrogen, diffusion-limited, heterogeneous reaction. The resulting cuprous oxide product formed requires additional acid for dissolution and subsequent conversion in a homogeneous mechanism;

otherwise it would be directly reduced in the solid phase.

The total reduction of antlerite to metallic copper shown in Equation III-24, is the optimum initial reaction path. Following initial reduction via Equation III-24 it is conceivable that the acid formed from reduction functions to redissolve a portion of the precipitated basic salt. Consequently, during the later phases of hydrogen reduction the overall conversion to metallic copper may proceed by both homogeneous and heterogeneous mechanisms.

In buffered acid copper sulfate solutions with pH less than approximately three, hydrolysis is suppressed and homogeneous reduction dominates. Halpern and MacGregor (21) investigated the homogeneous reduction of cupric salts and suggested the following sequence of reactions as a probable mechanism.

$$Cu^{++} + H_2 \rightleftharpoons CuH^{+} + H^{+} \qquad \text{(III-25A)}$$

$$CuH^{+} + Cu^{++} \longrightarrow 2\ Cu^{+} + H^{+} \qquad \text{(III-25B)}$$

$$2\ Cu^{+} \longrightarrow Cu + Cu^{++} \qquad \text{(III-25C)}$$

In the Halpern mechanism, the disproportionation of cuprous ions shown in Equation III-25C is very rapid. The formation of cuprous ions shown by Equations III-25A and B, however, is normally very slow. The addition of a buffer is necessary to reduce the effective concentration of hydrogen ions in solution and maintain satisfactory rates of cuprous ion formation.

An inherent disadvantage of the Halpern mechanism lies in the reaction stoichiometry of Equation III-25C. For every mole of cuprous ions formed and reacted, only half a mole of metallic copper is produced. The remaining half mole of cupric ions produced must again be converted to cuprous ions in the rate limiting reactions of Equations III-25A and 25B. Consequently complete conversion to metallic copper by the Halpern mechanism is not theoretically possible.

Copper Sulfate Ammine Solutions

The simplified overall reaction for the hydrogen reduction of ammine-copper sulfate solutions may be summarized by two equations (7). For a free ammonia to copper feed mole ratio greater than two the reaction is:

$$Cu(NH_3)_nSO_4 + H_2 \longrightarrow Cu^{o}\downarrow + (NH_4)_2SO_4 + (n-2)\ NH_3 \quad (\text{for } n > 2) \qquad \text{(III-26)}$$

According to Equation III-26, the ammine feed contains sufficient free ammonia which, when liberated by reduction, exceeds the quantity required for the complete neutralization of acid formed during reduction. Therefore, as reduction proceeds in a batch or closed system, the unreduced feed will increase in free ammonia to copper mole ratio.

When the initial free ammonia to copper feed mole ratio is less than two, the reaction is:

$$Cu(NH_3)_nSO_4 + H_2 \longrightarrow Cu^{o}\downarrow + \frac{n}{2}\,(NH_4)_2SO_4 + (\frac{2-n}{2})\,H_2SO_4 \quad \text{(for } n < 2\text{)} \qquad \text{(III-27)}$$

In the case of Equation III-27, insufficient free ammonia is present for complete neutralization of acid produced during reduction. Consequently, as reduction proceeds in a batch or closed system the unreduced feed will decrease in free ammonia to copper mole ratio. Both reactions indicate that a free ammonia to copper mole ratio of two will theoretically neutralize all by-products of reduction as they are produced.

In reality, when the free ammonia to copper mole ratio of a soluble copper ammine complex solution is reduced below approximately three, a slurry of cupric basic salts is formed. The general formula of the precipitated basic salts is $CuSO_4 \cdot x\ Cu(OH)_2$. The predominant basic salt is a function of the free ammonia to copper mole ratio in the feed and x in the general formula usually lies between two and three.

The two phase feed slurry and subsequent intermediate reduction products complicate the detailed interpretation of the ammine-copper sulfate reduction system. However, the effects of certain variables on the reduction rate of the system provide a qualitative interpretation. For example, Mackiw (7) observed that the overall rate of reduction was favored for initial free ammonia to copper mole ratios less than two. Also the copper reduction rate was increased by the addition of fine metallic copper powder.

These observations coupled with the transient observations for the reduction of copper oxides suggests a major heterogeneous reduction mechanism is involved.

Mackiw also observed a significant increase in reduction rate with increasing addition of ammonium sulfate. One explanation of this phenomena involves the formation of a transitional ammonium radical according to:

$$NH_4^+ + \frac{1}{2} H_2 \longrightarrow NH_4\cdot + H^+ \qquad \text{(III-28)}$$

The ammonium radical $NH_4\cdot$ reduces the cupric and cuprous ammine complex in solution according to:

$$2\ Cu(NH_3)^{++} + 2NH_4\cdot \longrightarrow Cu_2(NH_3)^{++} + 2NH_4^+ + NH_3\uparrow \qquad \text{(III-29)}$$

or

$$Cu_2(NH_3)^{++} + 2\ NH_4\cdot \longrightarrow 2\ Cu^{o}\downarrow + NH_3\uparrow + 2\ NH_4^+ \qquad \text{(III-30)}$$

An alternative explanation for the beneficial effect of ammonium sulfate addition assumes that reduction takes place only from solution through a disproportionation reaction similar to

$$Cu_2(NH_3)_n^{++} \longrightarrow Cu^{o} + Cu(NH_3)_n^{++} \qquad \text{(III-31)}$$

The rate controlling step would then be the dissolution of basic salts and intermediate reduction products. In this case, ammonium sulfate increases the solubility of the various solid phases.

The latter observations concerning ammonium sulfate addition suggest the presence of a homogeneous reduction mechanism.

Nickel Sulfate Acid Solutions

According to Figure 1, nickel can be hydrogen reduced from slightly acidic solutions according to the reaction:

$$NiSO_4 + H_2 \longrightarrow Ni^o + H_2SO_4 \qquad \text{(III-32)}$$

Schaufelberger (29) experimentally confirmed the homogeneous reduction of nickel from unbuffered nickel sulfate solutions. Equilibrium conversions, however, were limited to approximately 10 percent conversion of the initial feed concentration. The pH of the terminal reduction solution in the unbuffered experiments was 2.2 which was obviously below the theoretical value of approximately 4.5 shown in Figure 1.

Addition of a buffering agent to suppress the hydrogen ions formed during reduction is an effective means of increasing conversion. Schaufelberger duplicated the unbuffered nickel reduction experiments using ammonium sulfate and acetate buffers. The resulting conversion for the reduction buffered with ammonium sulfate was approximately 50 percent to a terminal solution pH of 1.6. Ammonium acetate buffer provided essentially 100 percent conversion with a corresponding terminal solution pH of 4.1. The difference noted in buffer effectiveness is explained by the neutralization

products formed. Weakly dissociated acetic acid formed in the ammonium acetate system is obviously more effective in suppressing hydrogen ions than is the corresponding ammonium bisulfate.

Nickel Sulfate Ammine Solutions

Hydrogen reduction of ammine-nickel sulfate solutions, unlike its acid solution counterpart, is not limited by system thermodynamics. Nickel ammine hydrogen reduction, however, will not nucleate without the aid of a solid nuclei. Consequently, the nickel ammine reduction is limited by system kinetics.

The two major mechanisms of heterogeneous nickel ammine reduction are based on the use of seed nickel and nickel nucleation with a foreign catalyst. The use of seed nickel in ammoniacal nickel reduction is illustrated in the following simplified reaction:

$$Ni(NH_3)_nSO_4 + H_2 \xrightarrow[\text{seed}]{Ni^o} Ni^o + (NH_4)_2SO_4 + (n-2)NH_3 \qquad \text{(III-33)}$$

The presence of varying amounts of free ammonia in the pure feed solution of Equation III-33 does not precipitate basic salts of nickel. From Equation III-33, it is obvious that an initial reduction solution with a free ammonia to nickel mole ratio of two will not change mole ratios during reduction. Coincidentially, Bjerrum (2) calculated the thermodynamic optimum mole ratio of free ammonia to nickel to be approximately

two. Bjerrum's calculations were based on the combined potential variation of the various nickel ammine species present at various free ammonia to nickel mole ratios. The resulting maximum difference in potentials between hydrogen and a one molar solution of combined complexes occurred at a 2:1 free ammonia to nickel mole ratio.

The predominate mechanism of nickel ammine hydrogen reduction using seed nickel is growth. The critical variables describing the growth mechanism are the seed surface area and the system hydrogen partial pressure. These variables are shown in the following rate expression (24):

$$-d(Ni)^{++}/dt = k \cdot A \cdot [H_2] \qquad \text{(III-34)}$$

where A is the nickel seed surface area, $[H_2]$ is a measure of the hydrogen concentration, and k is a specific rate constant. The rate expression is observed to be independent of nickel concentration up to 85 percent reduction.

A general mechanism for the rate expression of nickel growth assumes the nickel seed to be covered with a strongly adsorbed layer of nickel ammine ions. The concentration of nickel ammine ions on the nickel seed is not affected until the bulk solution concentration falls below approximately 15 percent. Based on these assumptions the initial growth rate will be limited by the rate at which hydrogen molecules are adsorbed on the nickel seed surface. Since the hydrogen adsorption rate is proportional to both hydrogen partial pressure

and nickel seed area, the mechanism appears to satisfy the rate expression.

The other major heterogeneous mechanism of nickel ammine reduction involves heteronucleation with a foreign catalyst. Courtney and Schaufelberger (5) investigated the effectiveness of various foreign catalysts towards promoting nucleation in the nickel ammine system. The more effective catalysts studied, in order of their increasing effectiveness were ferrous sulfate, sodium sulfide, and chromous sulfate.

Common to all the effective catalysts was the formation of insoluble precipitates in the initially-catalysed, reduction feed solution and the use of vigorous agitation. In the ferrous sulfate system, after catalyst addition and before the addition of hydrogen, the formation of solid magnetite and nickel metal were observed. Based on the work of Evans and Wanklyn (35), the disproportionation of ferrous hydroxide in the presence of nickel ions forms magnetite by:

$$3\ Fe(OH)_2 \xrightarrow{NiSO_4} Fe_3O_4 + 2\ H_2O + H_2 \qquad \text{(III-35)}$$

The simultaneous liberation of nascent hydrogen shown in Equation III-35, could conceivably reduce part of the nickel ions associated with the magnetite formation. A gross discrepancy in this proposed explanation was discovered (5) when the addition of ferrous hydroxide to a nickel ammine solution failed to nucleate nickel. Likewise, the addition of ferrous sulfate at elevated reduction temperatures did not

provide rapid nucleation. Based on these observations, the effective catalytic mechanism appears to involve an intermediate species probably composed of ammonia-nickel-ferrous-hydroxy-sulfate ions.

The transient nucleation effectiveness of the proposed mixed salt involved in the ferrous sulfate nucleations makes the exact mechanism identification difficult. However, based on experimental rate data and the resulting initial parabolic reduction data, a general mechanism can be developed. This mechanism assumes the rate of reduction is directly proportional to the number of nuclei formed during catalytic nucleation. At constant hydrogen concentration this assumption agrees with the rate expression for growth given in Equation III-34. If the rate of nuclei formation is assumed constant and the two basic assumptions are mathematically combined, the following relation (22) between conversion and time follows:

$$C = Co - kt^2 \qquad \text{(III-36)}$$

where Co is the initial nickel concentration of the reduction feed, C is the reduction solution concentration at time t, and k is a combined rate constant.

The above expression does not fit the rate data obtained in the latter stages of a batch reduction. This discrepancy can be explained by agglomeration of nickel particles

which decreases the number of nuclei. Also, the growth of highly reactive nickel particles which were nucleated in the early stages of the reaction reduces the surface area, thereby reducing the overall rate of the reaction.

CHAPTER IV

DESCRIPTION OF EXPERIMENTAL EQUIPMENT

All of the previous studies and commercial applications of hydrogen reduction for recovery of metals from their aqueous solution have been conducted in batch reaction systems. The recent work of Kieswetter (17), performed in agitated, tubular, batch reactors designed for rapid heat-up and cool-down, represented a departure from the normal lengthy reduction studies. Kieswetter studied the hydrogen reduction of copper and nickel aqueous solutions down to approximately two minutes residence time and obtained results comparable to previous lengthy batch reduction studies. However, the inherent batch character of these advanced studies limited the scope of the investigation.

In this investigation, the hydrogen reduction of aqueous copper and nickel solutions was conducted in a continuous processing system. The schematic process flow diagram of the continuous hydrogen reduction system is shown in Figure 2.

The process involved the continuous charging of aqueous metal salt solutions and gaseous hydrogen through a

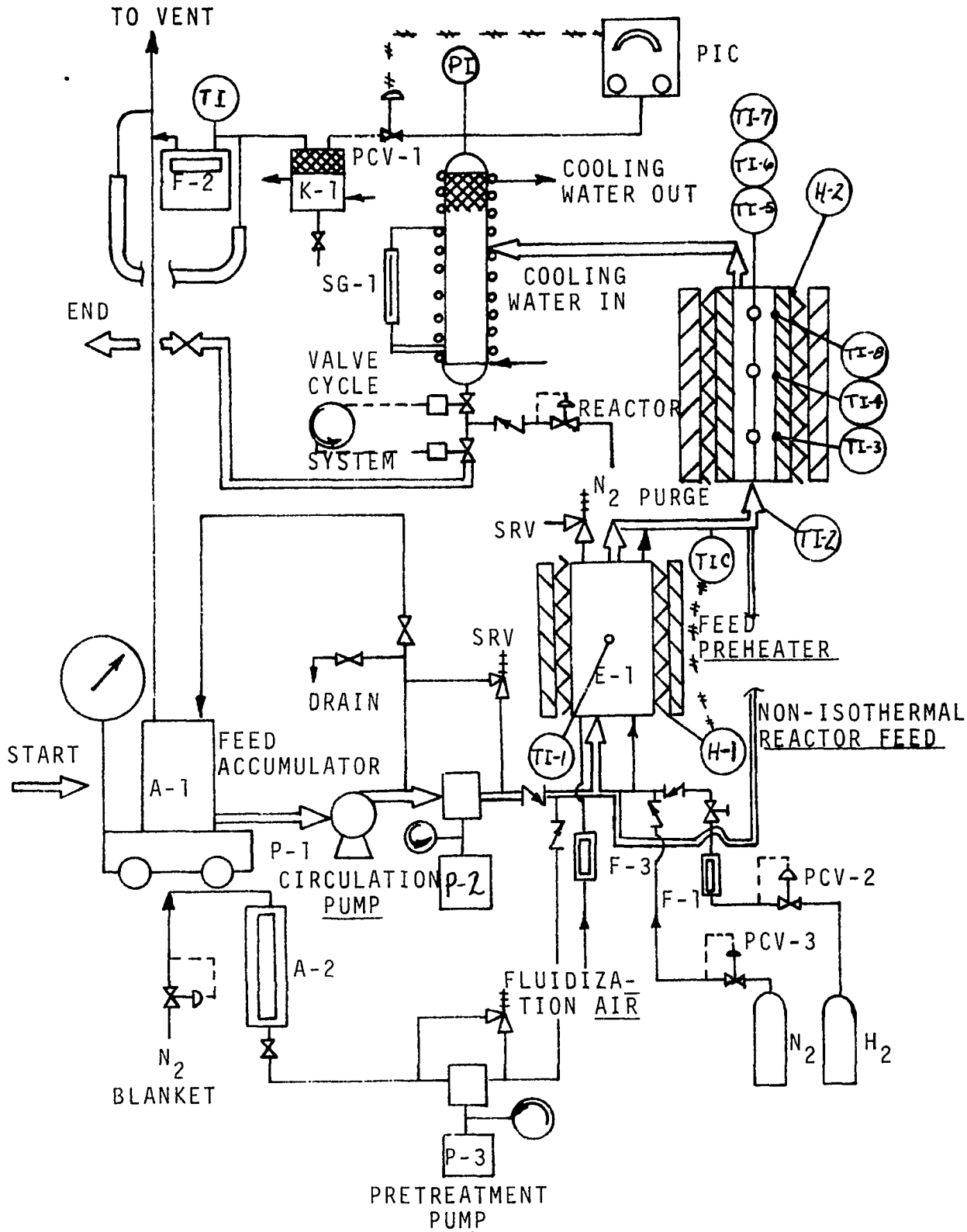

Figure 2. Schematic Diagram Continuous Hydrogen Reduction Processing System.

preheater and vertical tubular reduction reactor. The reactor products were continuously removed and separated in a high pressure separator. The product gases were throttled through a pressure control valve into a product gas cooler and knock-out pot and were measured. The liquid and solid products were continuously removed from the separator through a cycling dump valve system into a product accumulator. In the following discussion, the equipment is divided into five sections:

1. Feed system.
2. Preheater system.
3. Reactor system.
4. Product separations system.
5. Auxiliary systems.

Feed System

The major components of the feed system were the feed solution accumulator and circulation system, the high pressure solution feed pump, the calibrated sight glass pretreatment accumulator, the high pressure pretreatment pump, the high pressure gas feed system, and the high pressure hydrogen control and flow meter. The combined components of the feed system are schematically illustrated in Figure 2 and are physically shown in the photographs of Figures 3 and 4.

The feed solution accumulator (A-1) was constructed from an open top fifteen gallon (56.8 liters) steel oil drum. A threaded connection was welded into the bottom edge, and

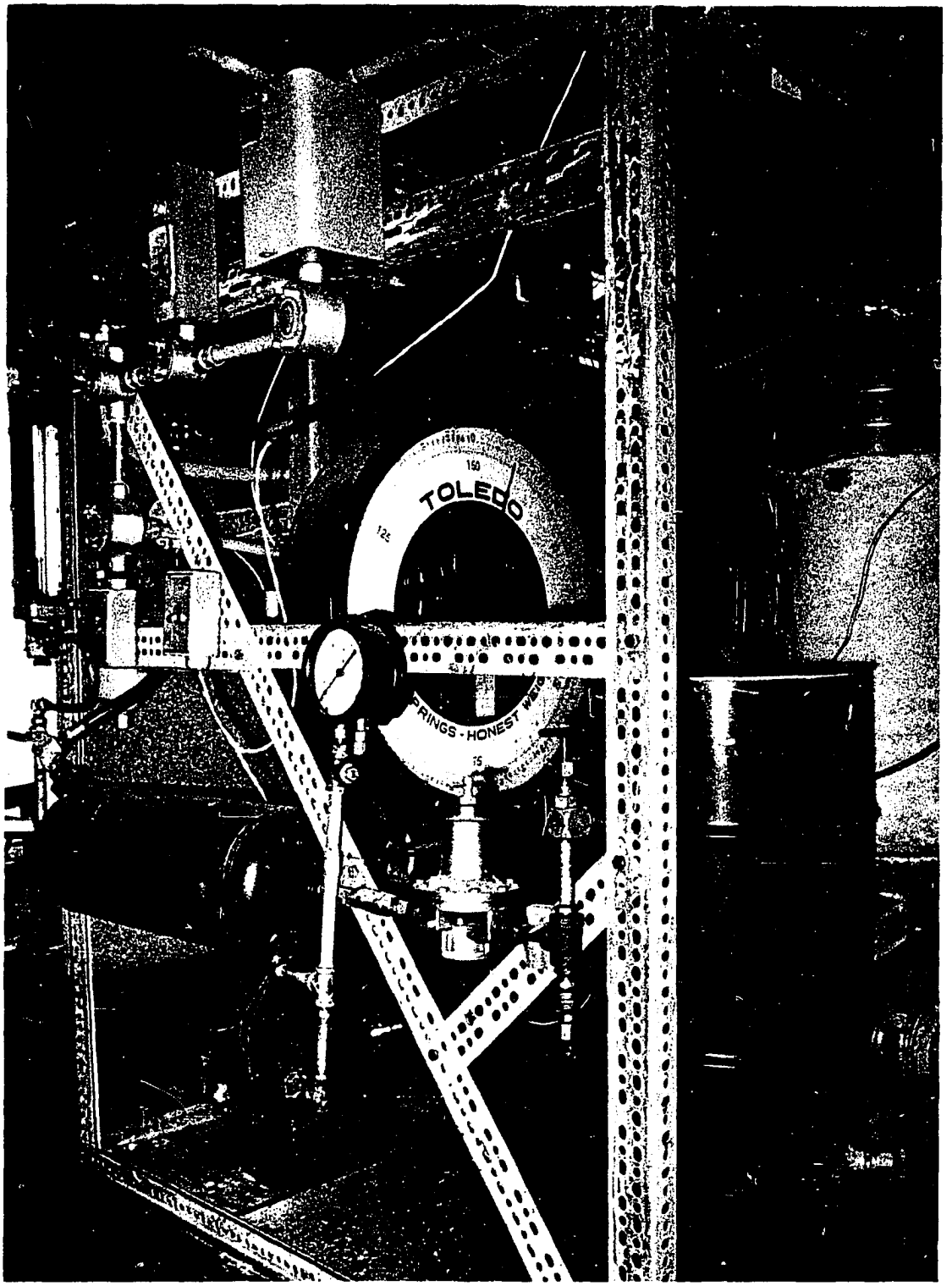

Figure 3. Feed System Accumulator.

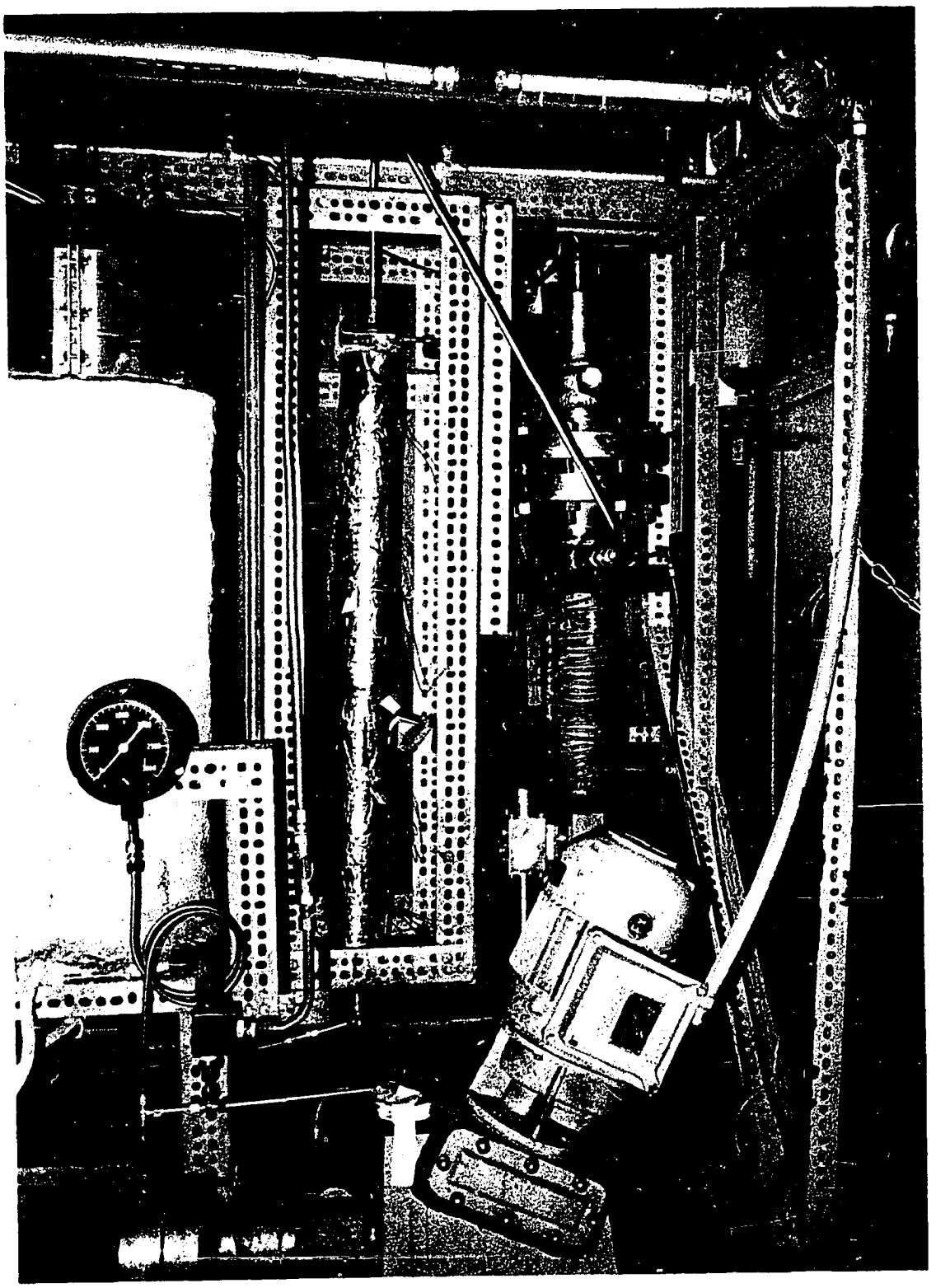

Figure 4. High Pressure Feed Pump, Reactor and Separator.

the internal drum wall was coated with epoxy paint. The feed solution accumulator was situated on a 150 pound (68.1 kilogram) Toledo platform scale graduated in 0.25 pound (113.5 gram) divisions. The Toledo scale was later replaced with a more accurate Detecto platform scale graduated in 50 gram divisions. A flexible length of 0.75 inch (1.9 cm) inside diameter tygon tubing was attached to the lower feed accumulator connection and was extended to the suction of the feed circulation pump (P-1). The feed circulation pump was a 17-gallon per minute (64 liters per minute), 0.25 horsepower Teel centrifugal pump. The cast aluminum body and impeller were thoroughly coated with epoxy paint to resist corrosion. The discharge from the centrifugal pump was branched into three streams. The largest volume stream was recycled through a section of 0.75 inch (1.9 cm) tygon tubing to the feed accumulator to insure uniform feed composition. The second discharge stream from the circulating pump served as an accumulator drain and was normally blocked off with a half inch 316 stainless steel ball valve. The last portion of the circulation pump discharge capacity was supplied to the suction of the high pressure solution feed pump through a section of 0.75 inch (1.9 cm) tygon tubing.

The high pressure solution feed pump (P-2) was an Andrea Hofer diaphram metering pump, equipped with a 5 horsepower explosion proof electric motor. All wetted surfaces of the high pressure pump were constructed from 316 stainless

steel. Maximum design operating pressure was 5000 pounds per square inch gauge (340 atmospheres). The pumping capacity could be varied from zero to 3.43 gallons per hour (13 liters per hour).

The discharge line from the high pressure pump was fabricated from 0.25 inch (0.635 cm) nominal diameter standard wall 304 stainless steel tubing. Incorporated into the discharge piping was an Anderson Greenwood, 316 stainless steel safety relief valve, pre-set to relieve at 2000 pounds per square inch gauge (137 atmospheres) pressure, and a 3000 pound per square inch gauge (205 atmospheres) Ashcroft dial pressure indicator (Figure 4).

The calibrated sight glass pretreatment accumulator (A-2) was located on the control panel; it is shown in the center lower portion of Figure 5. The steel constructed sight glass, which was rated by Jerguson Company for 600 pounds per square inch gauge (42 atmospheres) cold working pressure, had a capacity of 150 cubic centimeters (0.04 gallons). Nitrogen supplied from a nitrogen cylinder was used as blanket gas for the accumulator. A section of 0.25 inch (0.635 centimeter) nominal diameter, standard wall, 304 stainless tubing connected the sight glass accumulator to the suction of the high pressure pretreatment pump.

The high pressure pretreatment pump (P-3) was a Whitey, diaphram, laboratory feed pump, equipped with a one-third

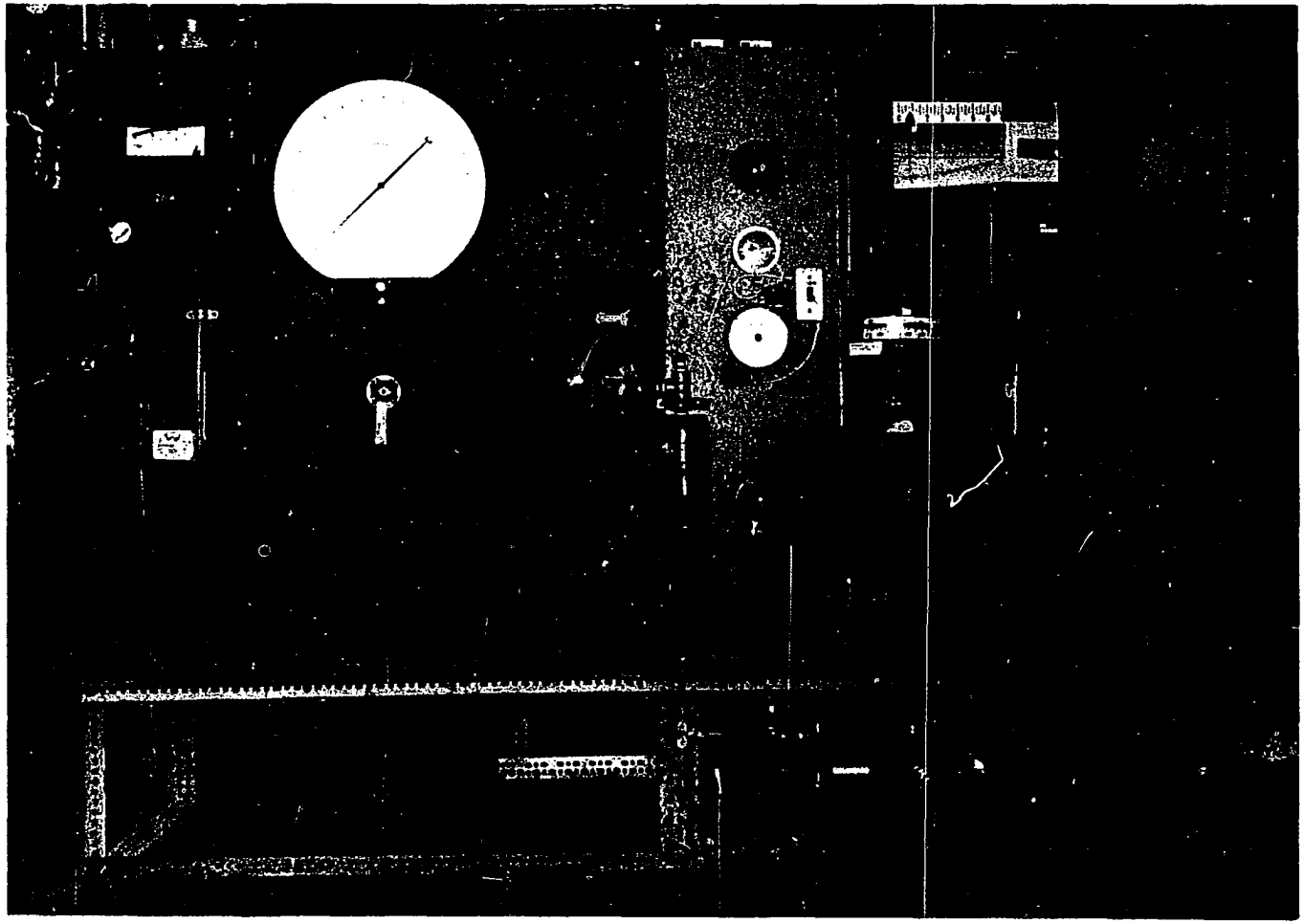

Figure 5. Continuous Hydrogen Reduction System Control Panel.

horsepower explosion proof motor. All wetted surfaces of the pump were constructed from 316 stainless steel. Maximum design operating pressure was 5000 pounds per square inch gauge (341 atmospheres). The pumping capacity could be varied from zero to 500 cubic centimeters per hour (0.13 gallons per hour). The discharge line from the pretreatment pump was fabricated from 0.25 inch (0.635 cm) nominal diameter, standard wall, 304 stainless steel tubing. An Anderson Greenwood, 316 stainless steel, safety relief valve, preset to relieve at 2000 pounds per square inch gauge (136 atmospheres) pressure, and a Nupro 316 stainless steel check valve were included in the pump discharge assembly.

The gas feed facilities included both nitrogen and hydrogen supplied from high pressure "K" cylinders equipped with Victor pressure regulators. The gas cylinders were connected through 0.25 inch (0.635 cm) nominal diameter, standard wall, 304 stainless steel tubing, containing in-line Nupro check valves, to a three-way Republic valve. The three-way valve, shown in the left center section of Figure 5, provided a choice of nitrogen, hydrogen, or no gas feed.

Nitrogen feed was usually limited to pressure testing, start-up and shut-down applications. Therefore, gas feed rate control and measurement were used only for hydrogen. The hydrogen feed rate control and measurement system was located between the supply cylinder regulator and the Nupro check valve. The hydrogen flow meter was a high pressure

armored rotometer constructed from a high pressure Strahman sight glass containing a Brooks rotometer tube and a stainless steel float. The maximum operating pressure of the hydrogen flow meter was 2850 pounds per square inch gauge (195 atmospheres) at 70°F operating temperature. The flow range of the meter at 625 pounds per square inch gauge (43.5 atmospheres) varied from 0.2 to 0.6 standard cubic feet per minute (5700 to 17,000 standard cubic centimeters per minute) hydrogen.

Hydrogen feed rate was hand controlled by a Robbins manual needle valve located on the discharge side of the armored rotometer. The Victor pressure regulator on the hydrogen cylinder provided a constant meter pressure which was at least 200 pounds per square inch (13.5 atmosphere) greater than the downstream reactor pressure. This differential pressure was used in conjunction with the hand controlled needle valve to obtain the desired hydrogen feed rates.

Preheater System

Liquid and gas feeds from the respective feed systems were separately preheated at operating pressures in an air-fluidized sand bath heater. The preheater (E-1) is illustrated in the schematic diagram of Figure 2. It is physically shown in the left background of Figure 6.

The preheater unit consisted of the preheater housing, the sand bed, electrical heating elements, two preheater coils, fluidizing air system, and a temperature measuring

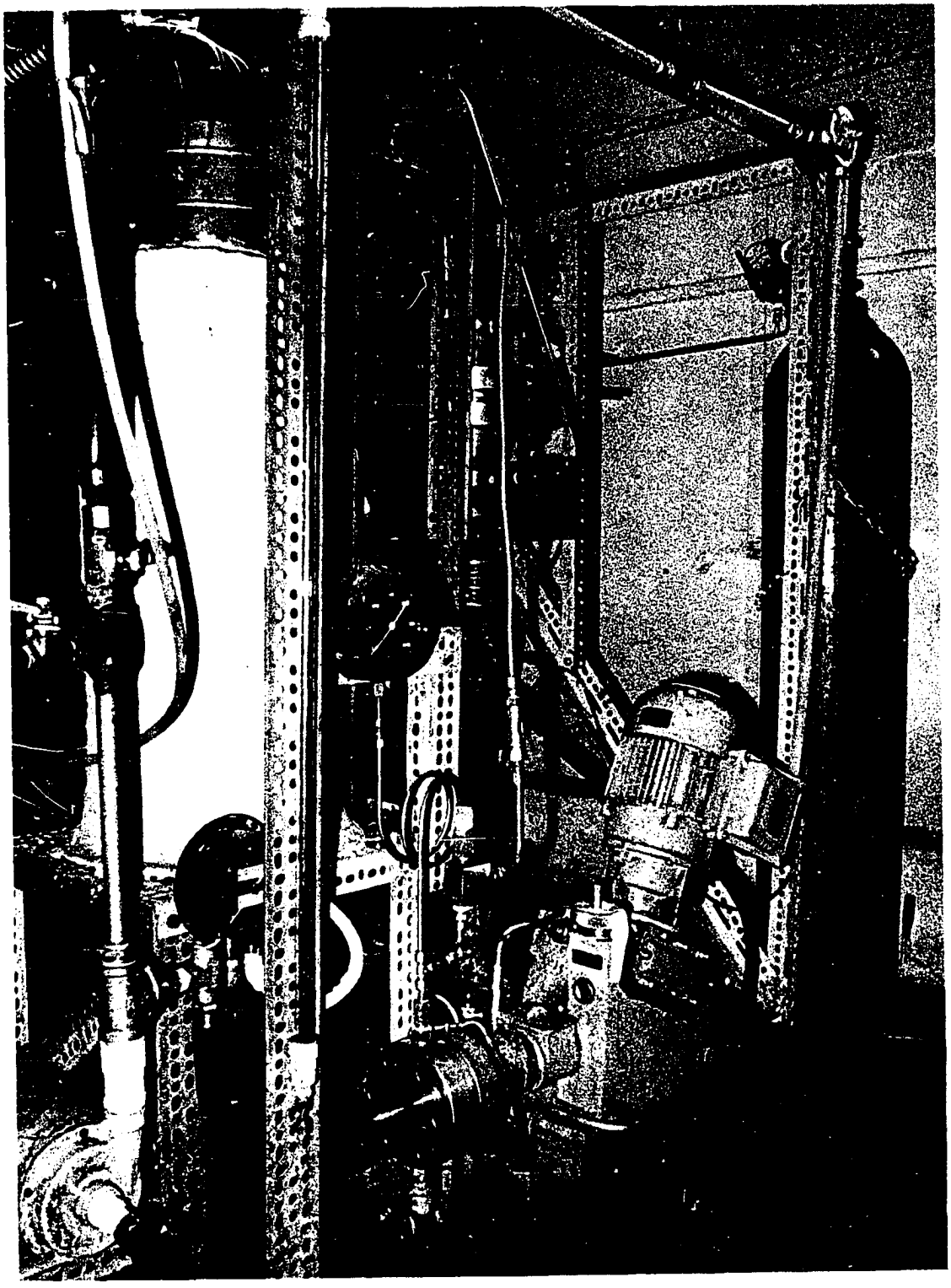

Figure 6. Feed Preheater.

and control system. The preheater housing, 3 feet (0.91 meters) long and 12 inches (30.5 cm) in outside diameter, was constructed from 0.125 inch (0.32 cm) thick rolled steel pipe. The intermediate heat transfer medium consisted of 144 pounds (65.4 kilograms) of minus 20 mesh sand. The upper 12 inches (30.5 cm) was used as a disengaging section to remove entrained sand from the air. This section was fitted with a perforated, 50-mesh screen to aid in the separation of entrained sand. A safety relief valve, preset to relieve at 10 pounds per square inch gauge (0.68 atmospheres) was installed at the top of the housing to prevent accidental pressure increases.

The two preheater coils were fabricated from 0.25-inch (0.635 cm) nominal diameter standard wall, 304 stainless steel tubing. The liquid preheater coil, 50 feet (15.2 meters) long was coiled on a 10-inch (25.4 cm) diameter. The gas preheater coil, 10 feet (3.1 meters) long, was coiled on a 4-inch (10.2 cm) diameter so that it would fit inside the liquid preheater coil. The respective process streams entered the preheater coils at the bottom of the preheater housing and exited at the top.

Air was used to fluidize and expand the sand to a working height of 24 inches (61 cm) which was sufficient to cover the preheater coils. Air was introduced through a distribution cap located in the bottom of the preheater housing, thus uniformly fluidizing the sand bed as the air moved upward through the bed. Flow rate of the air, which was manually controlled, was measured by a Brooks rotometer (F-3).

Heat was supplied by six, 700-watt chromalox strip heaters which were vertically mounted in the sand bed. Power to the strip heaters was provided by two, 220-volt single phase Powerstat variacs. The output from one variac was connected directly to three alternately spaced strip heaters, the output from the other variac was automatically controlled by a Honeywell-Brown Pyro-O-Vane temperature indicator controller (TIC). The TIC, which sensed the combined temperatures of the liquid and gas streams leaving the preheater, applied power to the three heaters as required to maintain the desired outlet temperature.

Temperatures of the preheater inlet feed, the fluidized sand bed, and preheated feed streams were continually monitored by a continuously recording 24 point Honeywell-Brown Electronik temperature recorder. The iron-constantan thermocouples for inlet feed and preheated feed streams were located in 0.25 inch (0.635 centimeter), standard wall, 304 stainless steel tubing thermowells located in Swagelok 316 stainless steel tubing tee connections. Fluidized sand bed temperatures were measured with 3 iron-constantan thermocouples spaced uniformly in a 0.25 inch (0.635 centimeter), standard wall, 304 stainless steel tubing thermowell positioned vertically in the center of the preheater.

Reactor System

The continuous hydrogen reduction reactor, shown schematically in Figure 7 and pictorially in the center

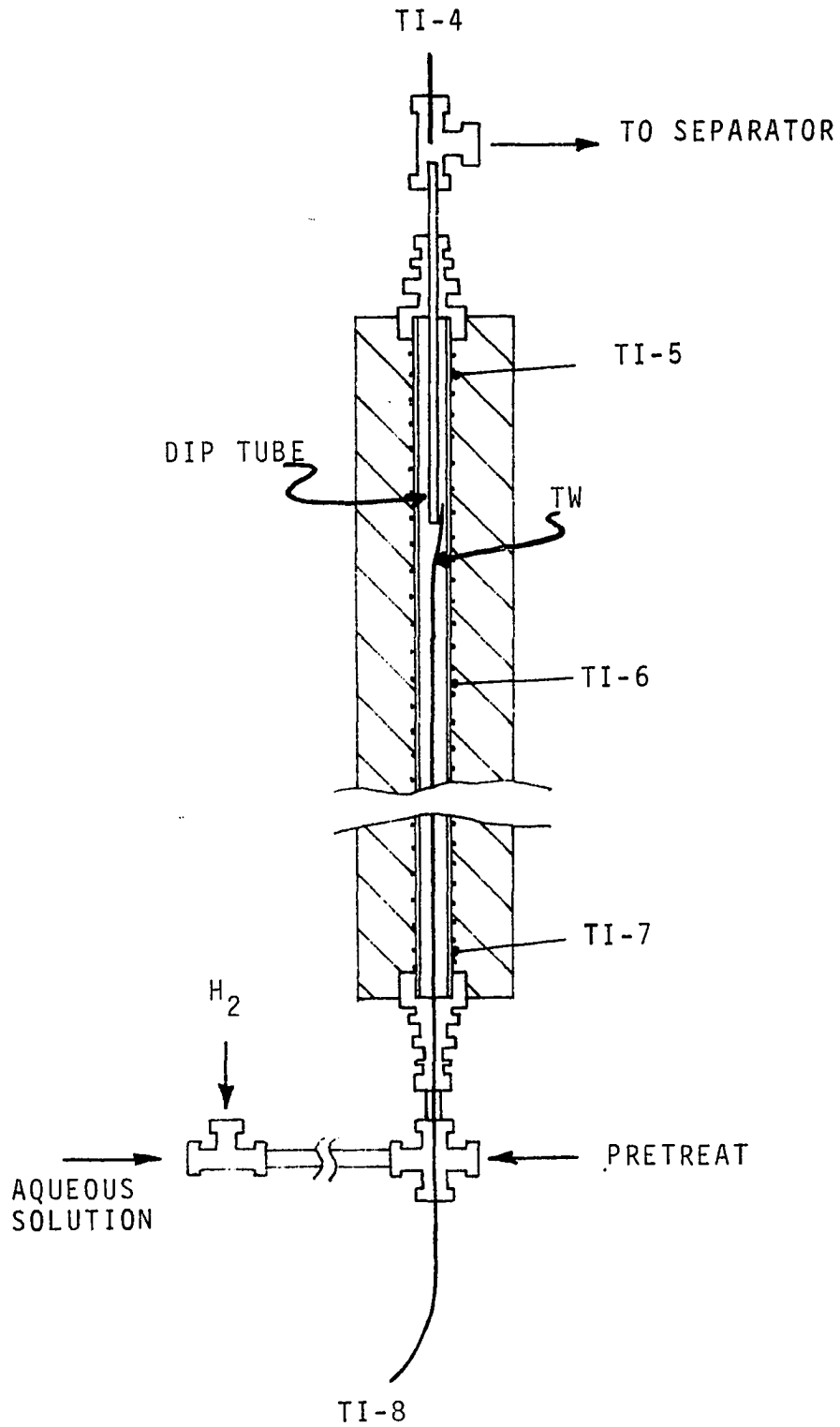

Figure 7. Continuous Hydrogen Reduction Tubular Reactor.

background of Figure 4, was a vertical tubular reactor employing three phase (solid, liquid, and gas) upward flow. The reactor was constructed from a 3-foot (91.4 centimeter) section of 0.049 inch (0.125 centimeter) wall thickness by 0.75 inch (1.9 cm) diameter 304 stainless steel tubing. The inlet and outlet reactor connections were reduced to 0.25-inch (0.635 centimeter) nominal diameter tubing by the appropriate Swagelok connections shown in Figure 7.

Combined reduction feed entered the bottom of the reactor and reduction products were discharged through a 6-inch (15.2 centimeter) long, 0.25-inch (0.635 centimeter) nominal diameter dip tube extending down from the top of the reactor. The resulting reactor liquid volume from the bottom of the reactor to the lower end of the dip tube was 180 cubic centimeters (0.0064 cubic feet).

Process heat required to maintain isothermal reactor temperatures or to provide the total system process heat in non-isothermal reactor operations, was provided by an external reactor wall heater system. The reactor wall heater was constructed by uniformly wrapping 30 feet (9.1 meters) of 20 gauge (0.081 centimeter diameter) wire around the total reactor length. A thin layer of fiber glass tape insulated the wire from the reactor wall. A heat transfer cement was applied over the wire to improve heat distribution. The reactor heaters were insulated from ambient by asbestos insulation which was 1.5 inches (3.8 cm) thick and was covered with aluminum foil.

Power to the reactor resistance wire heater was supplied by a 220-volt, single phase Powerstat variac which was manually regulated to maintain or obtain the desired reactor temperatures. The manually controlled variac is shown in the upper center section of Figure 5.

Reactor wall, feed and product process streams and internal reactor process temperatures were measured with iron-constantan thermocouples. Thermocouple output was recorded with the Honeywell-Brown Electronik temperature recorder previously described. Three wall temperature thermocouples located directly beneath the wire heater and on the reactor wall were evenly spaced over the length of the reactor. Feed and product process temperatures were measured with thermocouples located in feed and product tubing thermowells shown in Figure 7.

Internal reactor temperatures were measured by a single sliding thermocouple located in an 0.125-inch (0.318 centimeter) diameter heavy wall, 304 stainless steel thermowell. The reactor thermowell extended through the reactor inlet tubing connections and terminated approximately one inch above the reactor operating liquid level.

Product Separation System

The reduction products from the continuous hydrogen reduction reactor were discharged through a 0.25-inch (0.635 centimeter), standard wall, 304 stainless steel tube to the

product separations system. The product separations system included a high pressure liquid-solid and gas separator (S-1), a liquid-solids removal system, and a pressure control and measurement system. This system is pictorially shown in the right background of Figure 4.

The high pressure separator was constructed from a 15-inch (38 centimeter) section of 4-inch, schedule 80, 316 stainless steel pipe. The vertically positioned separator included a set of 600 pound rated ring joint flanges at the upper end and a weld cap at the lower end. The separator section below the flanges was fitted with appropriate connections for a feed inlet, a liquid level sight glass, and a liquid-solid removal system. Cooling water was circulated through thirty feet of copper tubing wrapped around the lower separator section to reduce the temperature of the accumulated liquid-solid products and consequently to reduce flashing during depressurization. The separator section above the flanges was packed with aluminum shavings to remove entrained liquids from the gas product prior to depressurizing.

The reactor products entered the separator approximately three inches below the separator flange assembly. The three phase, gas-liquid-solid products were cooled by contact with the separator walls. The liquids, with product solids, accumulated in the bottom of the separator. A Penberthy liquid level sight glass was installed on the lower separator section

to provide a visual means of monitoring the separator liquid level. A separator volume calibration is provided in Appendix C.

The accumulated separator liquid and solid products were continually removed through a cycling ball valve system located on the bottom of the high pressure separator. The cycling ball valve was composed of two pneumatically activated, 316 stainless steel ball valves connected by a short Teflon-lined section of stainless steel pipe. The valves were installed in a vertical position below the separator and were alternately opened and closed with a variable speed cam actuator. The actuator was designed to insure that only one of the two valves could be opened at a time. A typical cycle began with both valves closed. The cam actuator rotated to open the top ball valve and the section between ball valves filled with liquid and solid products. Continued rotation of the cam actuator closed the top valve and, after a short time lapse, opened the bottom ball valve. The products drained from the section between ball valves and the cycle was completed with the closing of the bottom ball valve.

The product removal section between ball valves was purged automatically with nitrogen when the lower ball valve was opened. This purging was accomplished by the use of a Grove pressure regulator and check valve combination. The pressure regulator maintained a nitrogen pressure of 20 pounds

per square inch gauge on the up-stream side of a Nupro stainless steel check valve connected to the product removal section. When the lower ball valve opened to release the captured products between ball valves, the reduced pressure allowed nitrogen to enter. As the cycle progressed and the bottom valve closed, the nitrogen pressure increased to approximately 20 pounds per square inch gauge pressure whereby the nitrogen purge was automatically stopped. The check valve in the nitrogen purge line prevented back flow of liquid and solid products during the fill cycle when full separator pressure was applied to the product removal section.

The gases removed from the top of the separator were depressurized through a Research Control pressure control valve (PCV-1). The pressure control valve maintained the desired system operating pressure through a control sequence employing a Honeywell-Brown pressure indicator controller (PIC). The pressure indicator controller sensed the high pressure separator pressure and pneumatically controlled the pressure control valve (PCV-1) to maintain the desired system pressure. The indicated pressure of the Honeywell-Brown pressure controller was supplemented by a more accurate Heise pressure indicator calibrated in one pound per square inch divisions. Both the pressure controller and pressure indicator are shown on the left side of the control panel in Figure 5.

Depressurized gas from PCV-1 was passed through a water cooled knock-out pot (K-1) to remove remaining condensables.

The resulting dry gas product was measured with a Rockwell hydrogen dry test meter and vented to the atmosphere.

Auxiliary Systems

The hazardous nature of uncontrolled hydrogen required special attention during this investigation. During each operation using hydrogen a Dayton exhaust fan 24-inches in diameter and having a 5000-cubic feet per minute capacity, was used to purge the laboratory volume once per minute. Localized hydrogen concentrations in the vicinity of the reactor and high pressure separator were continuously monitored by a Bureau of Mines combustible gas detector. All electrical motors were explosion proof; starter switches and electrical lines were sealed in conduit. Where a positive seal was not possible, nitrogen purging was utilized to prevent the accumulation of explosive gas mixtures.

Utilities required during the operations included 110-volt single phase and 220-volt three phase electricity, domestic cooling water, and compressed air at 120 pounds per square inch gauge. All of the utilities were provided by existing facilities.

CHAPTER V

EXPERIMENTAL PROCEDURES

The experimental work is divided into seven sections:

1. Feed preparation.
2. Preliminary procedure.
3. Startup procedure.
4. Run procedure.
5. Shutdown procedure.
6. Post-run procedure.
7. Problems encountered.

Feed Preparation

Synthesized copper and nickel sulfate feed solutions were prepared from reagent grade $CuSO_4.5H_2O$ and $NiSO_4.6H_2O$ obtained from the J. T. Baker Chemical Company. Distilled water was obtained from the University of Oklahoma power plant facilities.

Buffering or pretreating chemicals included ammonia, sulfuric acid, ferrous sulfate, and ammonium sulfate. Ammonia was obtained from Mallinckrodt Chemical Works in the form of reagent grade 58 weight percent ammonium hydroxide. The

approximate ammonia assay ranged from 28 to 30 weight percent. Reagent grade sulfuric acid, assaying 95 to 98 weight percent purity, was obtained from Fisher Scientific Company. Crystalline ferrous sulfate hydrate ($FeSO_4 \cdot 7H_2O$) and granular ammonium sulfate were obtained from Mallinckrodt Chemical Works.

In some operations the filtered product solutions from previous operations were used as feed for subsequent runs. New feed solutions were prepared using a Sargent analytical beam balance and a two liter graduated cylinder. The solid components were weighed to the nearest gram while distilled water was measured to the nearest 20 cubic centimeter graduation. The feed solutions were prepared and stored in 5 gallon (18.9 liter) polypropylene carboys. Prior to a run the solutions were analyzed by the appropriate "wet" analyses to confirm the actual concentrations.

Preliminary Procedure

A general systems check procedure was adopted and used prior to initiating start up procedure. The check procedure was based on operating experience and was designed to insure optimum performance during the subsequent run. The following ten step procedure was used:

1. Nitrogen and hydrogen supply cylinders were checked to insure sufficient gas volumes were available for the planned operation.

2. All utility supply sources, including domestic water, compressed air, and electricity, were activated and confirmed.
3. Oil reservoir supplies for the high pressure feed pump (P-2) and the pretreatment pump (P-3) were checked.
4. Feed accumulator reservoir (A-1) was partially filled with distilled water and accumulator circulating pump (P-1) and high pressure feed pump (P-2) operability were confirmed.
5. Pretreatment sight glass accumulator (A-3) was filled with ammonium hydroxide or sulfuric acid, and pretreatment pump (P-3) was primed and purged of air.
6. The high pressure liquid-solid removal system, including the variable-speed, cam actuator, the cycling ball valves, and the nitrogen purge, was checked to insure operability.
7. The pressure control sequence of the high pressure separator, including the Honeywell pressure indicator controller and the Research Control throttling valve, was cycled to confirm operability.
8. The Honeywell-Brown multi-point temperature recorder was activated, the recording chart paper supply was checked, and the continuity of all essential thermocouples was confirmed.
9. The Bureau of Mines combustible gas detector batteries were checked and the system was activated. The gas pilot light of the laboratory heater was shut off and the room exhaust fan was started.

10. The power to the preheater and the reactor wall heater was momentarily activated to confirm continuity of the heating elements.

When all systems satisfied the ten-step check procedure the system was ready for startup.

Startup Procedure

The startup procedure included a sequence of pressuring, establishing flows, increasing temperatures and initiating hydrogen feed. Initially, distilled water was used as feed until steady-state operating conditions were reached.

The first step of startup involved displacing the air in all pressure vessels and associated lines with distilled water. After the air was displaced, a hydrostatic pressure test was made at twice the maximum anticipated operating pressure. The hydrostatic pressure test was repeated until all leaks were traced and repaired. Following a successful hydrostatic pressure test, the liquid level in the high pressure separator was lowered through the cycling discharge ball valves until a liquid level of one-inch in the sight glass was obtained. The pressure control instrument set-point was lowered to the desired operating pressure and a nitrogen blanket was applied to maintain system pressure during the subsequent startup procedure.

After system pressures and levels were established, distilled water feed was started, and the high pressure

separator liquid removal system was activated. The high pressure feed pump rate was manually adjusted to the proposed run feed conditions based on timed, successive, accumulator (A-1) weight losses. The corresponding water removal rate from the high pressure separator was controlled by manually adjusting the cycle time of the discharge valve system to maintain a constant separator level.

The pretreatment feed pump rate was similarly adjusted to the proposed run feed pretreatment rate based on timed, successive, accumulator (A-3) level changes. The corrosive nature of unbuffered, sulfuric acid feed to the processing facilities limited the continuous operation of the pretreatment pump during startup procedure. Consequently, the pretreatment pump rate adjustments were based on a series of short tests made at fifteen minute intervals. The operational limitation of the pretreatment pump was not critical when ammonia was used as pretreatment.

When steady-state distilled water feed and removal rates were established, the preheater and reactor heater systems were activated. As the system temperatures approached the desired run conditions, nitrogen gas was replaced by hydrogen feed. The vent-gas, dry-test meter was placed in service. Hydrogen feed rate was manually controlled with a hand operated needle valve immediately downstream from the calibrated hydrogen feed rotometer.

The approach to steady-state operating conditions was closely monitored. When the proposed run temperatures,

pressures, and feed rates were reached and successive hydrogen vent gas rate checks were reproduceable, the system was ready for the run.

Run Procedures

After steady-state conditions of feed, product removal, temperature, and pressure were confirmed, run procedures were initiated. First, the distilled water in the feed accumulator (A-1) was drained, followed quickly by the addition of the process feed solution. Simultaneously with the feed solution addition, the pretreatment feed pump was started if feed pretreatment was to be used. An initial set of system operating conditions was recorded. The high pressure separator liquid-solid product receiver was replaced with an empty receiver. The initial set of operating data were recorded as zero time on the start of the run. All subsequent time references were based on this zero time.

The change from distilled water feed to ionic metal solution feed with feed pretreatment invariably involved a change in the original condition of steady-state operation. The changes most often observed involved a reduction in system operating pressure and temperature. To facilitate the rapid approach to a steady-state operation and consequently to obtain meaningful results, major changes in processing conditions were usually limited to the first fifteen minutes of the run.

System operating data, including feed rates, accumulator weights and levels, sight glass levels, pressures, temperatures, and general observations were taken at 15-minute time intervals. The data sheet for run 13 is shown in Appendix D.

Product samples were also taken at 15-minute time intervals. One minute before the regular 15-minute data period, the product receiver was replaced by a sample receiver. Two minutes later, after the operating data were taken, the sample receiver was replaced by the product receiver. The resulting two minute sample was therefore a typical sample for the set of data taken during the sampling period.

Feed composition, with the exception of a small initial dilution by distilled water at the start of the run, was essentially constant during a run. Therefore, normally only two, 50 cubic centimeter feed samples were taken during a run. One was taken during the first 15 minutes of the run, and the second was taken at the end of the run. The two feed samples were later combined to provide one composite feed sample. The feed and product sample analyses are discussed in the Analysis Procedures chapter.

The run procedures for isothermal and non-isothermal operations were essentially the same. Likewise, the run procedures for operations with and without feed pretreatment were similar. However, two exceptions to the procedure should

be noted. For non-isothermal runs, a reactor temperature profile was taken. If feed pretreatment was used, a sample of the pretreatment feed was taken at the end of the run for analysis.

The non-uniform temperature gradient over the reactor length was measured near the end of a non-isothermal operation. The normal run position of the internal reactor thermocouple was at the upper reactor liquid-gas interface. To obtain a reactor temperature profile, the thermocouple was moved downward in the reactor thermowell in two-inch intervals. The temperature at each interval was obtained and confirmed before moving to the next lower reactor position. This procedure was repeated until the thermocouple was opposite the reactor feed inlet connection. The reactor temperature profile for run 13 is shown in Appendix D.

The official end of a run, either scheduled or unscheduled, coincided with the time when process feed solution was drained from the feed accumulator and was replaced with distilled water. The pretreatment feed was also stopped at this time. Hydrogen feed was continued past the end of a run so that the system could be purged.

In the case of an unscheduled run termination, the regular operating data and product samples were taken at the time of termination. In either case, the product receiver was changed when process feed solution was replaced with distilled water feed. The disposition of accumulated

product receivers will be discussed in the following post-shutdown procedures section.

Shutdown Procedure

At the end of a run, the reactor contained approximately 200 cubic centimeters of partially converted feed, and the separator contained approximately 1500 cubic centimeters of reactor product. Consequently, in order to complete the conversion and to recover the converted run product, it was desirable to maintain operating conditions until the system was purged. Purging was accomplished by continuing distilled water and hydrogen feed in the absence of feed pretreatment.

The system was considered thoroughly purged following thirty minutes of purging operation. At this time the hydrogen was replaced with nitrogen. The system heaters were then shut off. Distilled water feed was continued until all process temperatures were below 212°F. Following termination of distilled water feed, the high pressure separator contents were drained and retained for future product recovery. The nitrogen supply to the system was blocked, and the entire system was depressurized and secured.

Post-Shutdown Procedures

These procedures included inspection of the reactor, separation of the accumulated products and preparation of synthetic feed.

Reactor Inspection

The inspection of the reduction reactor after a run was an important part of the total operation. During the initial, continuous copper reduction operations, reactor inspections were limited to qualitative inspections. The observations of some of these inspections are given in Appendix A.

Beginning with the continuous reduction of nickel, a procedure was developed to determine quantitatively the extent of product deposition in the reactor. In this procedure, the reactor was removed from the system and flushed with distilled water until all free or undeposited solids were removed. The reactor was allowed to "drip dry" over night to remove all surface water. The next day the reactor was subjected to an accurate volume determination by recording the amount of distilled water required to fill the reactor. Following the initial reactor volume determination, the reactor was disassembled for visual inspection. Samples of deposits were removed and tagged for subsequent analyses. General reactor conditions and location of major deposits were noted and recorded.

The partially cleaned reactor was reassembled and leached overnight with concentrated nitric acid. The clean reactor was then subjected to a second accurate volume determination to confirm the cleaning operation. The difference in volume between the initial "dirty" reactor and

subsequent "clean" reactor was the actual volume of reactor deposits. A typical reactor deposit following a nickel operation was 5 to 15 cubic centimeters. Based on a clean reactor volume of 180 cubic centimeters the typical nickel deposits occupied 2.8 to 8.3 volume percent of the clean reactor.

Accumulated Product Separation

Three types of accumulated product were obtained from a continuous reduction operation:

1. Accumulated product recovered during a run.
2. Accumulated product recovered during the purging operations.
3. Product recovered from the reactor following a run.

The three types of product represented different periods of operation and were usually recovered separately.

In general, the procedure for separating the products was the same. The total accumulated product or reactor product was filtered through Whatman No. 1 qualitative filter paper. The solid residues obtained from filtration were washed with distilled water and were oven-dried at 110°C temperature.

The filtrate from the separation of accumulated product recovered during a run was retained for additional processing and the filtrate from the remaining types of accumulated product were discarded.

Synthetic Feed Preparation

In the pretreatment feed operations the ammonium hydroxide or sulfuric acid feeds were combined with the corresponding feed solution streams at the reactor entrance. One reason for this procedure was based on the inability of the high pressure feed pump to handle the resulting slurries formed by pretreatment.

A sample of the pretreated feed solution entering the reactor could not be determined easily; therefore, a procedure was developed to simulate the actual reactor feed properties. In this procedure a synthetic feed or syn-feed was prepared by blending samples of pretreat solution and composite feed solution based on the actual feed ratios employed during a run. The resulting syn-feed, containing basic salt precipitates, was separated into its solid and liquid components for future analyses.

Problems Encountered

Two major problems encountered during the development of the continuous hydrogen reduction process involved:

1. Continuous, two-phase, liquid-solid removal from the high pressure separator.
2. Plugging in the preheater and reactor discharge process lines.

The initial continuous hydrogen reduction run used a single, hand-controlled, throttling valve for removing

liquid-solid products from the high pressure separator. The resulting operation was plagued with continual valve plugging caused by solids segregation at the throttling valve inlet. The corresponding liquid-level in the high pressure separator and pressure were erratic and difficult to control. Continual, and simultaneous liquid and solid removal from the high pressure separator was achieved by adopting the cycling ball valve system previously described.

The plugging of the preheater and reactor process lines was partially solved during this investigation. Initial continuous reduction runs were performed using the feed preheater and isothermal reactor configuration. Following the unscheduled shutdown of run four, the preheater coils were removed for inspection. The preheater for the feed solution was found to contain major quantities of basic salt deposits. The basic salt deposits were attributed to the hydrolysis reaction of unbuffered, copper sulfate feed solutions. Subsequent preheater plugging problems were prevented by eliminating the preheat operation and adopting the non-isothermal reactor processing configuration. By eliminating the preheater, hydrolysis problems were displaced to the tubular reactor where the presence of hydrogen during heat-up minimized the effects.

Plugging in the reactor discharge line was experienced after continuous pretreatment procedures were adopted in the copper runs. Fine particulate deposits of pure

copper were observed on the internal wall of the reactor discharge line. The resulting decrease in the process tube area created a critical plugging problem. Two consecutive modifications improved the oepration. First, the reactor discharge line was refabricated to provide the shortest and most streamline path possible. This modification was accomplished by removing restricting thermowells in the discharge line and by replacing 90 degree tubing bends with larger radius gradual bends. The resulting line plugging was reduced; however, the basic plating problem was not eliminated.

The second modification involved a replacement of the original 0.25-inch (0.635 centimeter) nominal diameter, standard wall, 304 stainless steel tubing with 0.375-inch (0.953 centimeter) nominal diameter, standard wall, 304 stainless steel tubing. Although these modifications did not eliminate the plugging problems, they did extend the operating time before terminal plugging.

CHAPTER VI

ANALYTICAL PROCEDURE

Continuous hydrogen reduction samples included liquids, solids, and liquid-solid slurries. The liquid-solid slurry samples were analyzed both in the slurry form and as separated phases. Table 4 gives a summary of the analytical techniques used for the respective phase analyses. Detailed procedures for individual analytical techniques are presented in Appendix B.

Eight different analytical techniques were used to analyze the samples. These techniques included specific gravity determination, free ammonia analysis, pH (hydrogen ion concentration) analysis, iodimetric titration, EDTA (ethylenediammetetraacetic acid) titration, x-ray diffraction analysis, particle size sieve analysis, and electron microscope scan.

Specific gravity determinations were made on actual and synthetic reduction feed solutions. The corresponding relationships between weight and volume measured at ambient conditions were used in the calculation procedures described in Chapter VII.

TABLE 4

ANALYTICAL TECHNIQUES USED FOR VARIOUS SAMPLE PHASES

Liquid-Solid Slurry	
• Specific Gravity	
• Free Ammonia Titration	
• Iodimetric Titration	
• EDTA Titration	
Liquids	**Solids**
• Specific Gravity	• X-ray Diffraction
• pH	• Sieve Analysis
• Free Ammonia Titration	• Electron Microscope
• Iodimetric Titration	• Free Ammonia Titration
• EDTA Titration	• Iodimetric Titration
	• EDTA Titration

Free ammonia analyses (the ammonia present in the complexed form) were made on samples obtained from copper and nickel ammoniacal operations. The analysis was made on all phases (liquid, solids and liquid-solid slurries) of the samples. The free ammonia analysis involved the determination of free ammonia distribution between the liquid and solid phases of the pretreated feeds as discussed in Chapter VII.

Hydrogen ion concentration (pH) analyses were made on the feed and product liquid samples. The observed reductions in pH observed between feed and product for a particular

run provided a qualitative indication of conversion.

Iodimetric titration analyses were used exclusively for copper determination. The technique did not differentiate between cuprous and cupric copper species and was therefore a measure of total copper content.

Ethylenediammetetraacetic acid (EDTA) analyses were used for nickel and total iron determination. The technique was used for analyzing all phases of the nickel and iron species.

X-ray diffraction analysis was used to analyze solid samples qualitatively. The solid samples derived from copper and nickel operations included synthetic feed precipitates, reduced product, intermediate reaction product from reactor accumulations, and various system deposits. The x-ray diffraction technique, however, was limited to absolute detection of crystalline materials; it did not provide a total qualitative analysis.

Sieve analyses were limited to particulate solid samples larger than approximately 100 grams. The smallest particle size resolved by this technique was approximately 250 mesh (0.006 centimeter or 60 micron equivalent diameter). The technique was used to analyze continuously reduced nickel powders.

The electron microscope was used for two analyses of solid samples. First, the electron bombardment of a sample provided an approximate relative elemental analysis. This

result was useful for isolating major elemental species for subsequent quantitative analysis by more accurate techniques. The second and major function of the electron microscope was to observe the physical particles under magnifications up to 24,250. Electron micrographs of nickel product samples are shown in Chapter VIII.

CHAPTER VII

METHOD OF DATA ANALYSIS

The exploratory nature of this investigation covered a wide range of processing conditions and resulted in an equally wide range of results. The purpose of this chapter is to define a common basis for the correlation of the results presented in Chapter VIII.

Reactor Residence Time

The hydrogen reduction reactor operation involved the continuous processing of a three phase (solid, liquid, and gas) mixture. At steady-state conditions an undetermined balance among phases existed. Consequently, a reactor residence time based on actual reactor conditions was not practical. Thus, a theoretical residence time, based on reactor feed solution rate measured at 70°F temperature and a reactor volume of 180 cubic centimeters, was used. The formula for calculating reactor residence time, t, is

$$t = \frac{V_R \cdot \rho}{q} \qquad \text{(VII-1)}$$

where V_R is the operating liquid volume of the reactor (180 cubic centimeters), ρ is the measured feed solution density in grams per cubic centimeter at 70°F, and q is the solution feed rate to the reactor in grams per minute.

Reaction Temperature

The reaction temperature for isothermal reduction operations was determined directly from reactor inlet and outlet temperatures. In non-isothermal reactor operations, the reaction temperature increased from the inlet temperature of the feed (about 70°F) to a maximum which occurred at the outlet of the reactor. In this case a defining reaction temperature was not directly available. For the purpose of this investigation, an integrated average reaction temperature was used to correlate data from non-isothermal operations. The integrated average reaction temperature was obtained by incrementally averaging the observed reactor temperature profile. This procedure is shown for run 13 in Appendix D.

Conversion Calculations

Feed conversions of the continuous hydrogen reduction operation were based on the liquid metal ion analyses of the separator product and the metal ion analysis of the feed. At constant feed metal ion concentration of the feed, the difference in feed and product liquid metal ion concentrations, taken as a percentage of the feed concentration, was assumed

to be the actual reduction of metal ions to metallic metal. However, the observed depletion of metal ions between feed and product was not always the same as conversion to product metal. Two cases where depletion and conversion were not synonymous were observed and are discussed below.

Dilution Effects

At the start of a continuous operation, the reactor and separator contained known quantities of distilled water. Consequently, the initial product samples were not representative of the actual product of the reaction. A correction based on the known separator volume at a given sample time was used to convert for the initial deviations in conversion. Assuming complete mixing of the contents in the separator, a mole balance of the respective metal ions in solution around the separator can be represented by:

$$\text{moles } M^{++} \text{in} = \text{moles } M^{++} \text{ accumulated} + \text{moles } M^{++} \text{out} \qquad \text{(VII-2)}$$

where M^{++} represents a specific metal ion. Incorporating flow rates, separator liquid volume and stream concentrations into Equation VII-2 gives

$$F \cdot C_R = V_L\left(\frac{dC_p}{dt}\right) + F \cdot C_p \qquad \text{(VII-3)}$$

where F is the liquid feed rate in liters per minute, C_R is the actual reactor discharge liquid metal ion concentration, V_L is the separator liquid volume, C_p is the observed separator

product liquid metal ion concentration, and t is time in minutes. Since the metal concentrations of the feed to the separator are low (less than 30 grams per liter), the difference in the densities of the feed and discharge is essentially zero; thus, the feed and discharge flow rates are essentially equal. Therefore, rearrangement of Equation VII-3 to solve for the feed concentration to the separator gives

$$C_R = \frac{V_L}{F}\left(\frac{dC_p}{dt}\right) + C_p \qquad \text{(VII-4)}$$

With the exception of the rate of change of concentration (dC_p/dt) in the separator, all other quantities in the right side of Equation VII-4 are determined directly from experimental or analytical data. The value of dC_p/dt can be obtained graphically from the lapse time for the product depletion curves which are given for each operation in Appendix A.

The correction model was applied to a hypothetical case assuming 0.1 liters per minute liquid feed, 0.5 moles per liter liquid feed concentration, a one-inch indicated separator liquid level and zero reactor conversion. The resulting graph for Equation VII-4 is shown in Figure 8. From Figure 8 it is obvious that approximately sixty minutes of operation are required before the dilution effect can be considered insignificant.

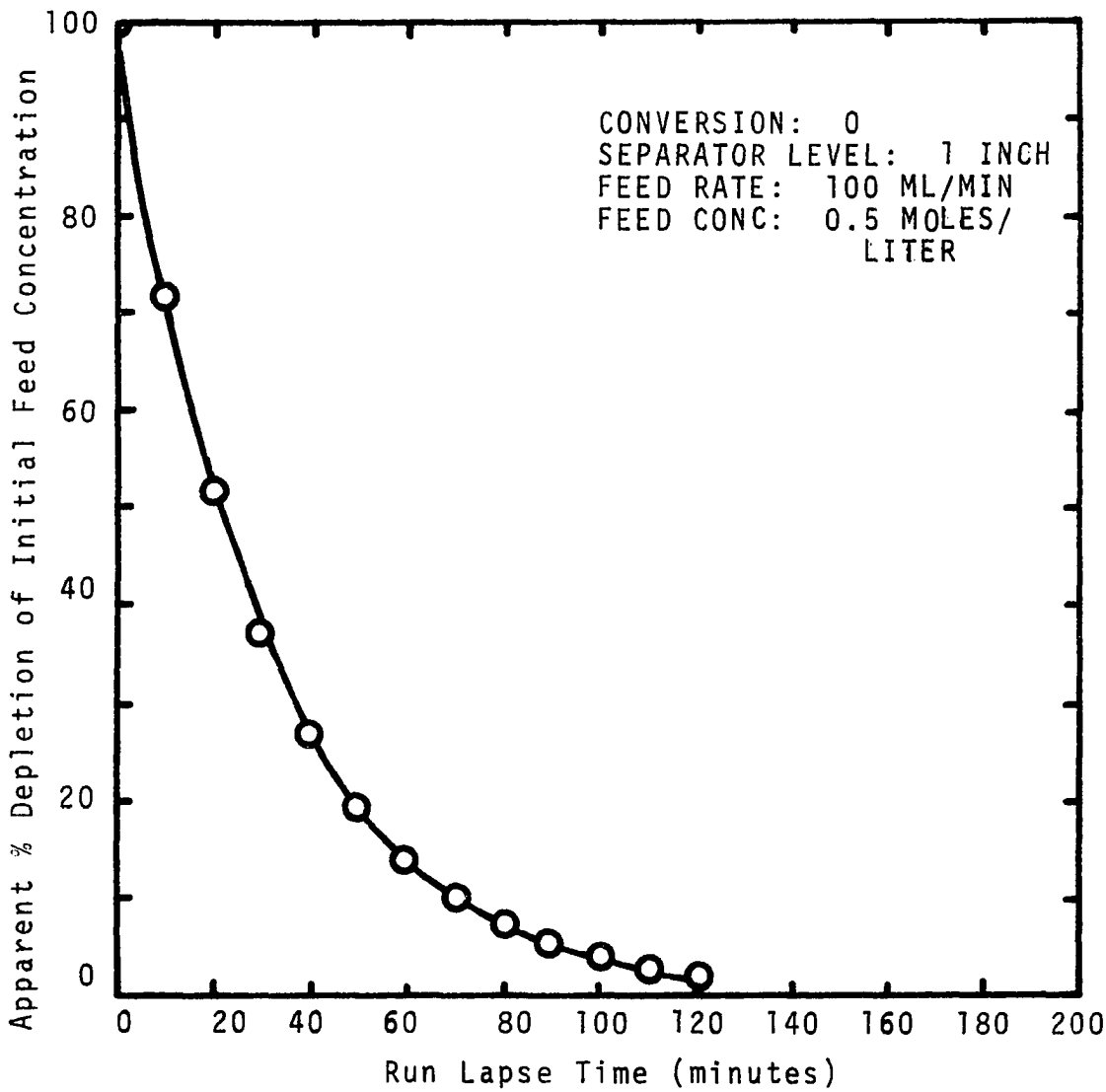

Figure 8. Dilution Effect at Start of Run.

Dilution corrections to actual operations, as shown in the graphs of Appendix A, had to be applied to product samples taken during the first thirty to forty-five minutes of the run.

Extraneous Product Formation

The formation of extraneous products, such as basic salts and metal oxides, during reduction also affected the validity of the assumed conversion basis. The effects of extraneous products were definitely observed during the continuous nickel reduction operations and during the continuous copper operation of run 13 where extraneous products appeared in the samples discharged from the separator.

Because of the wide range of conditions used in run 13, it did not merit a detailed conversion correction. However, conversion corrections for extraneous products were applied to the nickel operations.

The presence of an amorphous precipitate, containing nickel ions, in the product of the nickel operations was detected by wet analysis for nickel purity. However, results of this analysis did not differentiate between metallic nickel and ionic nickel. Consequently, a procedure to differentiate nickel ions from metallic nickel was needed. One method involved the washing of the combined metallic and amorphous solid with dilute sulfuric acid solutions. The results of these washings were inconsistent and unreliable.

A simple correction based on the nickel ion concentration of the synthetic nickel feed solutions appeared to provide the best correction procedure. In this procedure, the nickel-iron-ammonia complex formed during initial feed pretreatment was assumed to retain its initial composition during the reduction step. Consequently, the unconverted amorphous complex in the product was assumed to have the same composition as the feed complex. Data were available on the ion content of feed complexes; they are presented in the following section (Figure 11). With this assumption, the quantity of product nickel ions associated with the complex was determined analytically, with the nickel metal concentration being the difference between the concentration of the total dissolved nickel ion and the amorphous nickel. Table 5 gives the product nickel concentrations before and after correction for unconverted nickel ion complexes.

Once the concentrations of unconverted product nickel ions were determined, the actual run conversions to metallic nickel could be calculated. The corrected continuous nickel conversions are shown in the last column of Table 5.

Pretreatment Effects

The effect of continuous feed pretreatment on continuous hydrogen reduction was observed using synthetic feed samples previously discussed in Chapter V. Pretreatment resulted in the formation of varying amounts of basic salts

TABLE 5

PRODUCT NICKEL "WET" ANALYSES, ADJUSTED NICKEL CONTENT AND NICKEL CONVERSION RESULTS

Sample	Weight Percent Nickel Ion in Product	Adjusted Weight Percent Metallic Nickel in Product	Corrected Feed Nickel Conversion to Metallic Nickel
Run 15 (-250 mesh)	90.83	85	68 82 82
Run 16 (P-5 sample)	55.41	25	18
Run 17 (-200 mesh)	69.27	47	46
Run 18 (P-5 sample)	86.77	77	77

and nickel-iron complexes. The fraction of solution metal ions precipitated by pretreatment of the synthetic feed as a function of the resulting solution pH is shown in Figures 9 and 10 for copper and nickel feed solutions, respectively.

From Figures 9 and 10 it is obvious that a large portion of metal ions in the feed solution can be precipitated during pretreatment. For the ammine copper sulfate system, pretreatment with concentrated sulfuric acid to a pH of approximately 6 resulted in approximately 90 percent of the copper ions originally in solution being precipitated. The nature of the copper precipitated was discussed in Chapter III.

Pretreatment of the soluble nickel-ferrous iron system with ammonium hydroxide gave similar results to

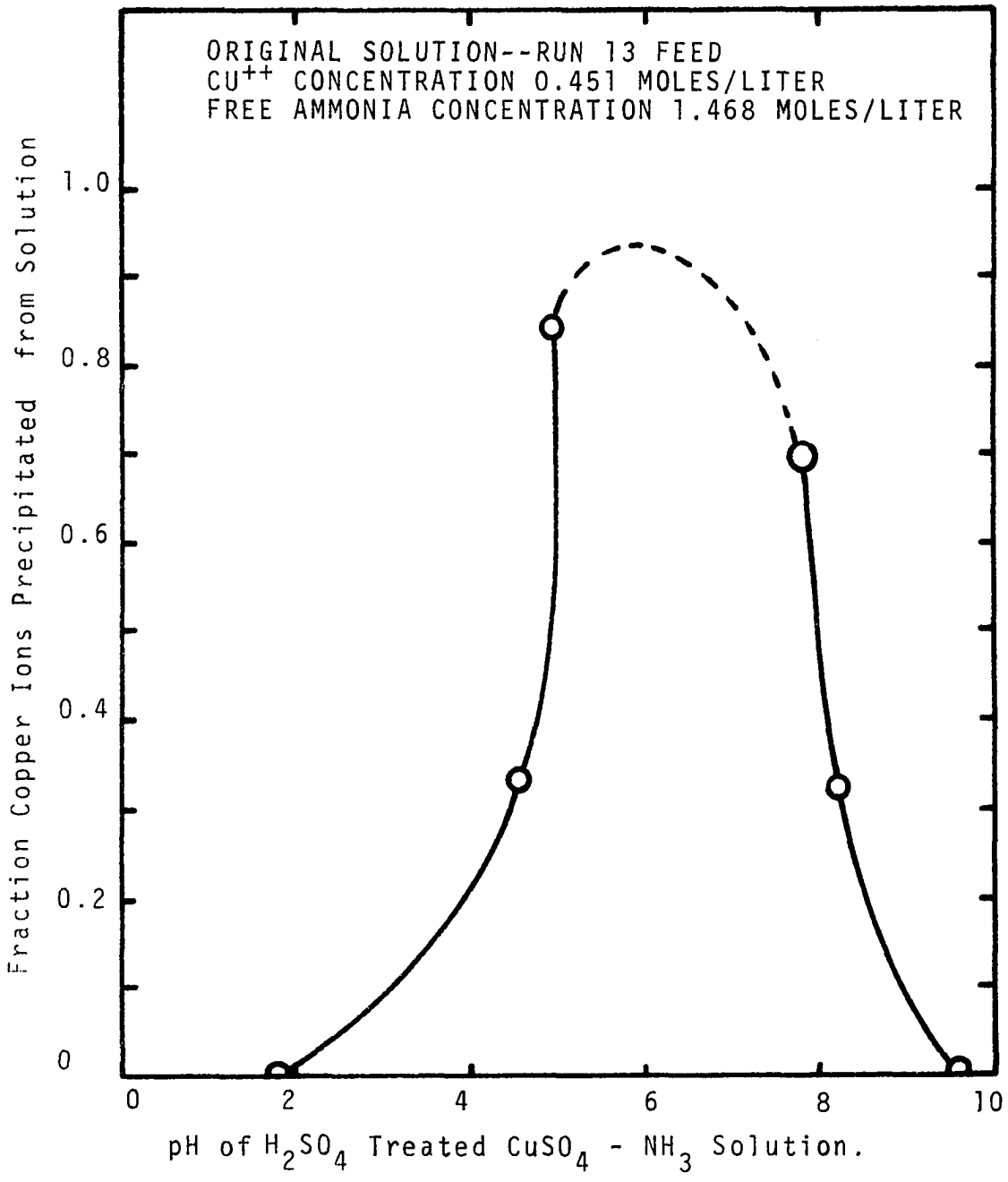

Figure 9. Fraction Original Copper Ions in Solution Precipitated by Addition of Conc. H_2SO_4 Versus pH of Resulting Solution.

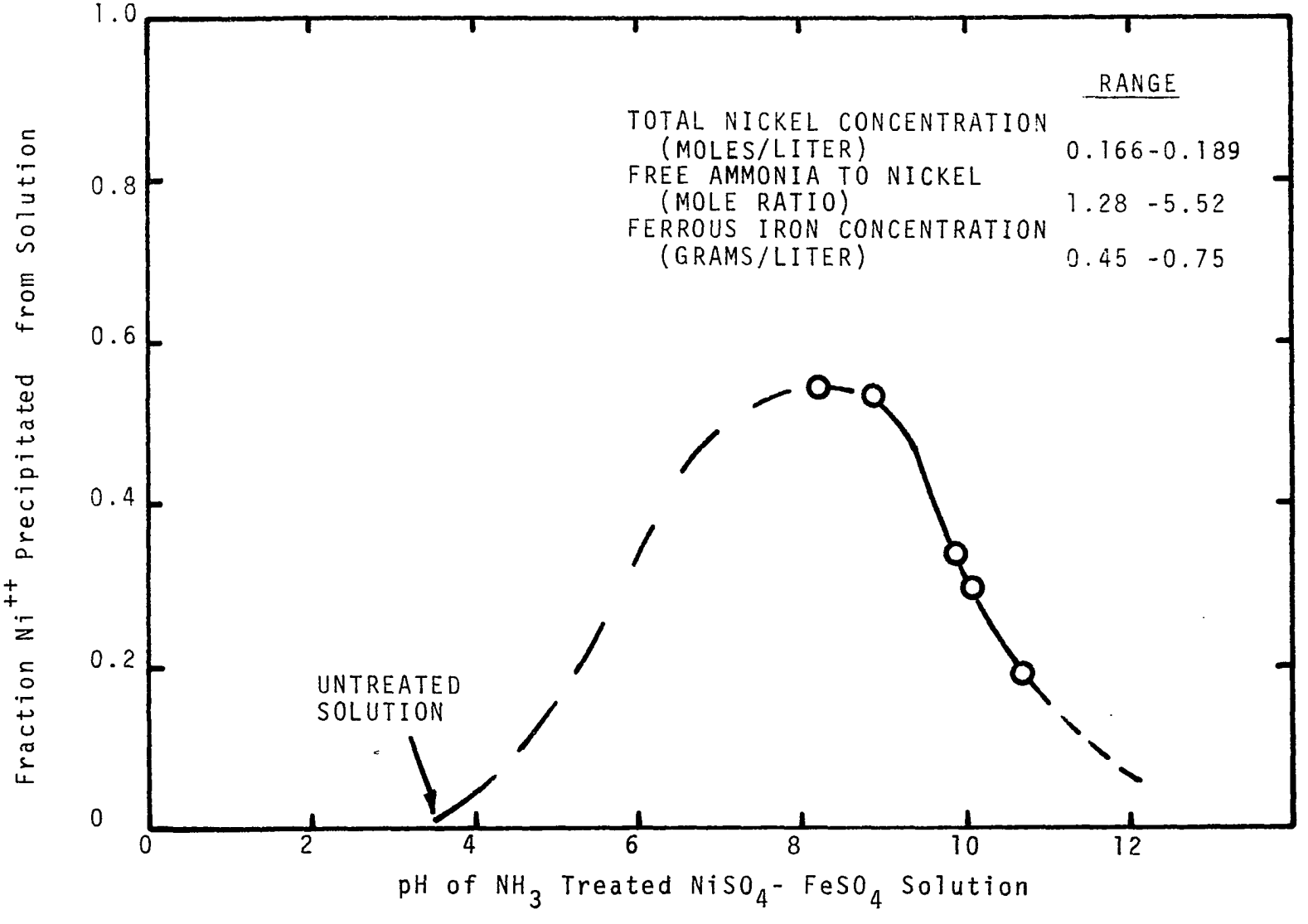

Figure 10. Fraction of Original Nickel Ions in Ferrous Sulfate Acid Solution Precipitated by Pretreatment with Ammonium Hydroxide.

those of copper solutions. The precipitate in this case was a nickel-iron-ammonia compound which precipitated approximately 50 percent of the original soluble nickel feed ions at a pH of 8.

The composition of the pretreatment nickel complex at various free ammonia to nickel feed mole ratios was analyzed. The results of these analyses are summarized in Figure 11. The corresponding solution pH values for these mole ratios begins at a pH of 8 for a mole ratio of one and increases to 10 at a mole ratio of 4. From Figure 11 it is apparent that the nickel concentration of the precipitated complex remains essentially constant over the mole ratios investigated. However, the concentration of iron in the precipitate is shown to increase with increasing ammonia to nickel mole ratio. Similarly, the free ammonia concentration (not shown) of the precipitate increases with higher mole ratio feeds. According to Figure 11, the composition of the nickel complex over the 1.0 to 2.0 free ammonia to nickel mole ratio range is

$$Ni_3(NH_3)_6Fe_{0.3}\ (X) \qquad \text{(VII-5)}$$

where X represents unidentified species. It is important to note that this mole ratio range, corresponding to a pH range of 8 to 9, correlates with the maximum amount of precipitate formed as shown in Figure 10. This spread is also the general

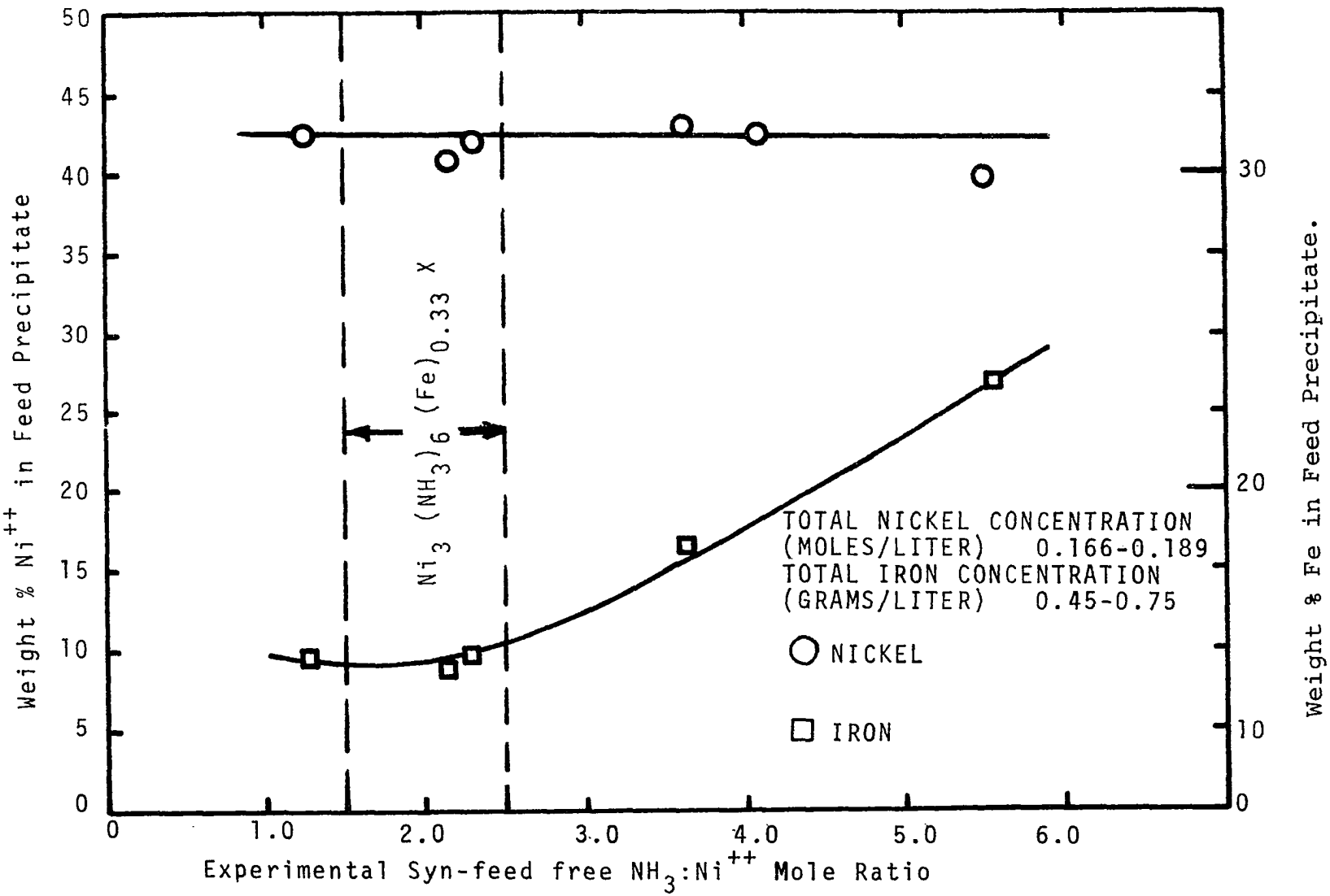

Figure 11. Nickel and Iron Composition of Synthetic Nickel Feed Precipitate.

operating range currently employed in commercial nickel hydrogen reduction operations.

Kinetics

The vertical tubular reactor used in this investigation does not strictly conform to the criteria of an ideal plug flow reactor; that is, flow of fluid must be orderly with no element of fluid overtaking any other element. However, based on several simplifying assumptions, the kinetic theory for the plug flow model was chosen to correlate the data. The assumptions used to justify application of the plug flow theory were:

1. A uniform reactor concentration profile, similar to the observed temperature profile, exists at steady-state operating conditions.
2. The hydrogen feed at steady-state reactor conditions proceeds upward in the reactor at a velocity similar to the corresponding liquid and solid species.
3. Reactor backmixing is localized and is primarily in the radial direction.

The rate constants in this investigation were calculated using the design equation (20) for ideal plug flow reactors. The nth order form of the equation is:

$$k_n = \frac{1}{tC_M^{n-1}} \int_0^{X_f} \frac{(1 + \varepsilon_M X_M)^n}{(1 - X_M)^n} dX_M \qquad \text{(VIII-6)}$$

where k_n is the rate constant, t is the mean residence time (Equation VII-1), C_M is the feed concentration of metal ions ε_M is the fractional change in system volume, X_M is the mole fraction conversion of feed metal ions and n is the order of the reaction. Considering the change in system volume, ε_M, to be negligible, Equation VII-6 simplifies to

$$k_n = \frac{1}{tC_M^{n-1}} \int_0^{X_f} (1 - X_M)^{-n} \, dX_M \qquad \text{(VII-7)}$$

The data from this investigation were analyzed by solving Equation VII-7 for the rate constant after integrating for reaction orders, zero through four. The lowest, integer order rate expression that provided a satisfactory correlation of data was the second order rate constant expression given by

$$k_2 = \frac{X_M}{tC_M(1 - X_M)} \qquad \text{(VII-8)}$$

Equation VII-8 was used in conjunction with results from Table 6 (Chapter VIII) to calculate the second order rate constants for the Arrhenius plots discussed in Chapter VIII. The corresponding activation energies were calculated using the Arrhenius equation

$$k_2 = k_o \, e^{-E_a/RT} \qquad \text{(VII-9)}$$

where k_2 is the second order rate constant calculated from

Equation VII-8, k_o is the frequency factor, E_a is the activation energy, R is the universal gas constant and T is the absolute temperature. By taking the log, Equation VII-9 gives

$$\ln k_2 = \ln k_o - \frac{E_a}{RT} \qquad \text{(VII-10)}$$

The expression for activation energy was obtained by measuring the slope of the Arrhenius curve and equating the results to the corresponding slope term in Equation VII-10 giving

$$Ea = -R \text{ (slope of Arrhenius curve)} \qquad \text{(VII-11)}$$

CHAPTER VIII

EXPERIMENTAL RESULTS AND DISCUSSION

The results discussed in this chapter were obtained from twenty-two continuous hydrogen reduction runs processing either copper or nickel aqueous feed solutions. Eighteen of the continuous runs were on copper feed solutions, of which four were derived from actual copper oxide ore leaching operations. The remaining fourteen copper runs and all of the four nickel runs used feed solutions prepared from reagent grade copper and nickel sulfate and distilled water. The following range of variables were covered:

Variable	Range	Units
pH	1.65 - 10.70	--
Pressure	305 - 611	psig
	21.7 - 42.6	atmosphere
Temperature	199 - 348	°F
Feed conc. of metal ions	0.129 - 0.486	moles/liter
Residence time	0.8 - 2.3	minutes

Table 6 summarizes the results from all runs.

TABLE 6

SUMMARY OF CONTINUOUS OPERATIONS

Run	System	Run Duration min	Feed Conc Moles/liter	Buffer or Catalyst Conc gm/l	Feed Pretreatment H_2SO_4 g/min	Feed Pretreatment NH_4OH g/min	Feed Free NH_3: Metal Ions mole ratio	Feed pH at 25°C	Feed Solu. Rate g/min	Feed H_2 Rate scfm	Reactor Pres psig	Average Reactor Temp °F	Reactor Liquid R. T. minutes	Prod Gas Rate scfm	Steady-State Depletion of Feed Conc, %
1	$CuSO_4$	63	0.435	--	--	--	0	3.85	236	--	460	292	0.8	0.93	20.9
2	$CuSO_4$	55	0.457	--	--	--	0	4.10	123	--	305	303	1.5	0.10	35.7
3	$CuSO_4$-NH_3	60	0.124	--	--	--	2.86	8.50	118	--	305	302	1.6	0.19	21.0
4	$CuSO_4$-$(NH_4)_2SO_4$	62	0.269	45	--	--	0	2.15	109	--	305	333	1.7	0.16	85.1
5	$CuSO_4$	82	0.468	--	--	--	0	3.90	113	--	485	278/328	1.7	0.13	25.0/47.9
6	$CuSO_4$-N_2	53	0.486	--	--	--	0	3.80	113	N_2	497	261	1.7	{0.14 N_2	15.8
7	$CuSO_4$-$(NH_4)_2SO_4$	55	0.480	42	--	--	0	3.75	123	--	484	265	1.7	0.24	22.3
8	$CuSO_4$-NH_3	120	0.445	--	--	--	3.80	9.10	82	--	500	275	2.3	0.26	55.5
9	$CuSO_4$-NH_3	120	0.207	--	--	--	4.60	9.06	86	--	500	323	2.1	0.29	39.6
10	$CuSO_4$-NH_3-$(NH_4)_2SO_4$	120	0.129	200	--	--	3.31	7.75	102	--	495	310	1.7	0.24	0
11	$CuSO_4$-NH_3-$(NH_4)_2SO_4$	105	{0.232 0.310	200	{yes --	--	{0.69 3.42	{5.60 7.40	122	--	505	{317 328	1.7	0.23	{88.4 6.1
12	$CuSO_4$-NH_3-H_2SO_4	75	0.175	200	2.67	--	0.34	--	132	--	495	326	1.6	0.30	65.1
13	$CuSO_4$-NH_3-H_2SO_4	186	0.451	--	{2.2, 4.8, 9.3, 10.5	--	--	{8.0, 6.2 3.3, 2.4	95	0.35	512	{348, 327 327, 333	1.9	0.30	{53.3 68.2 33.9 54.1
14	$CuSO_4$-NH_3-H_2SO_4	60	0.176	--	2.40	--	--	5.5	104	0.31	495	339	1.9	0.29	86.9

TABLE 6--Continued

Run	System	Run Duration min	Feed Conc Moles liter	Buffer or Catalyst Conc gm/l	Feed Pretreatment H_2SO_4 g/min	Feed Pretreatment NH_4OH g/min	Feed Free NH_3: Metal Ions mole ratio	Feed pH at 25°C	Feed Solu. Rate g/min	Feed H_2 Rate scfm	Reactor Pres psig	Average Reactor Temp °F	Reactor Liquid R. T. minutes	Prod Gas Rate scfm	Steady-State Depletion of Feed Conc, %
15	$NiSO_4$-NH_3-$FeSO_4$	175	0.189	0.75	--	1.76 4.89 7.43	1.28 3.60 5.52	8.2 9.9 10.7	96	0.22	477	281	1.9	0.20	85.6 72.5 98.4
16	$NiSO_4$-NH_3-$FeSO_4$	75	0.185	0.75	--	5.88	2.20	8.9	206	0.31	495	199	0.9	--	71.4
17	$NiSO_4$-NH_3-$FeSO_4$	45	0.170	0.64	--	7.08	4.10	10.1	133	0.28	498	247	1.4	0.24	100
18	$NiSO_4$-NH_3-$FeSO_4$	35	0.166	0.45	--	3.98	2.30	--	160	0.27	500	211	1.1	0.24	98.7
19	$CuSO_4$-NH_3 (Leach)	75	0.148	--	--	1.48	0.76	4.85	104	0.21	611	293	1.8	0.17	93.5
20	$CuSO_4$ (Leach)	75	0.143	--	--	--	--	1.65	98	0.21	596	287	1.9	0.18	75.0
21	$CuSO_4$-NH_3 (Leach)	43	0.143	--	--	1.30	0.82	4.80	99	0.21	611	257	1.9	0.18	87.0
22	$CuSO_4$-NH_3 (Leach)	110	0.145	--	--	1.24	0.53	--	104	0.20	547	250	1.8	0.20	84.0

The copper and nickel results were analyzed by using the analytical procedures discussed in Chapter VII. Briefly, the second order rate constants were calculated using

$$k_2 = \frac{X_M}{tC_M(1 - X_M)} \qquad \text{(VII-8)}$$

and the values for X_M, t, and C_M summarized in Table 6. The effect of temperature on rate constant was plotted in Arrhenius plots. The corresponding activation energy of the reaction was calculated by using

$$E_a = -R \text{ (slope of Arrhenius curve)} \qquad \text{(VII-11)}$$

where R is the universal gas constant.

Continuous Copper Operations

Two types of reactor operations were used to obtain the copper results: isothermal and non-isothermal. The first four copper runs were made using an isothermal reactor and the remaining fourteen copper runs used a non-isothermal reactor. Based on the results shown in Table 6 and the correlation procedures of Chapter VII, isothermal and non-isothermal reduction operations appear to be comparable.

The eighteen continuous copper runs were divided into four groups according to the feed types used and results obtained. The four groups and major contributing runs in each group were:

Group	Major Runs Involved*
I	1, 2, 5A, 5B, 6, 7
II	3, 8, 9
III	11B, 14, 19, 21, 22
IV	4, 10, 11A, 12, 13, 20

*Two sets of operating conditions were obtained from Runs 5 and 11.

Group I Runs

The feed solution pH for the runs in this group ranged from 3.75 to 4.10. The use of buffers was limited to run 7 where only 42 grams per liter of ammonium sulfate were used. As predicted in the discussions of theory in Chapter III, the presence of hydrolysis products, which included antlerite and cuprous oxide, were observed. However, except in the case of run 6, metallic copper was produced in each run. Run 6 was designed to evaluate the contribution of hydrolysis. During run 6, nitrogen feed gas was used in place of hydrogen to suppress the reduction step. The resulting depletion of feed copper ions was approximately 70 percent of the depletion observed in run 7 using hydrogen feed and otherwise comparable conditions. Consequently, based on the results of these runs, the major factor contributing to feed depletion was hydrolysis. Based on observed hydrolysis products in the preheater and reactor following these runs, the subsequent reduction of hydrolysis products to metallic copper was only partial.

An Arrhenius plot for the runs in Group I is shown in Figure 12. Corresponding activation energy calculated from the slope of the curve was 12 kilocalories per mole. This activation energy, based on the previous observations, represents the energy required to hydrolyze the initially homogeneous feed solutions of cupric ions.

Group II Runs

The runs of Group II were made with ammonium buffered feed solutions having pH values of 8.5 to 9.1. In general, hydrolysis in these runs was suppressed by the formation of soluble ammine complexes. One exception involved run 3. Feed for this run was prepared from the depleted solutions of runs 1 and 2. When ammonium hydroxide was added to this depleted solution, a precipitate of basic salt (brochantite) was formed. The subsequent products recovered during the run contained brochantite (Basic Copper (II) Sulfate) and cupric oxide. Based on the feed and product analyses, it was assumed that brochantite was an inert species during the operation. Therefore, the subsequent run calculations were based on the soluble copper ion concentrations in the feed.

The Arrhenius graph for the runs of Group II is shown in Figure 13. The corresponding activation energy calculated from the slope of the curve was 2 kilocalories per mole. Based on the recovered products, this activation energy represents the energy required for conversion of soluble

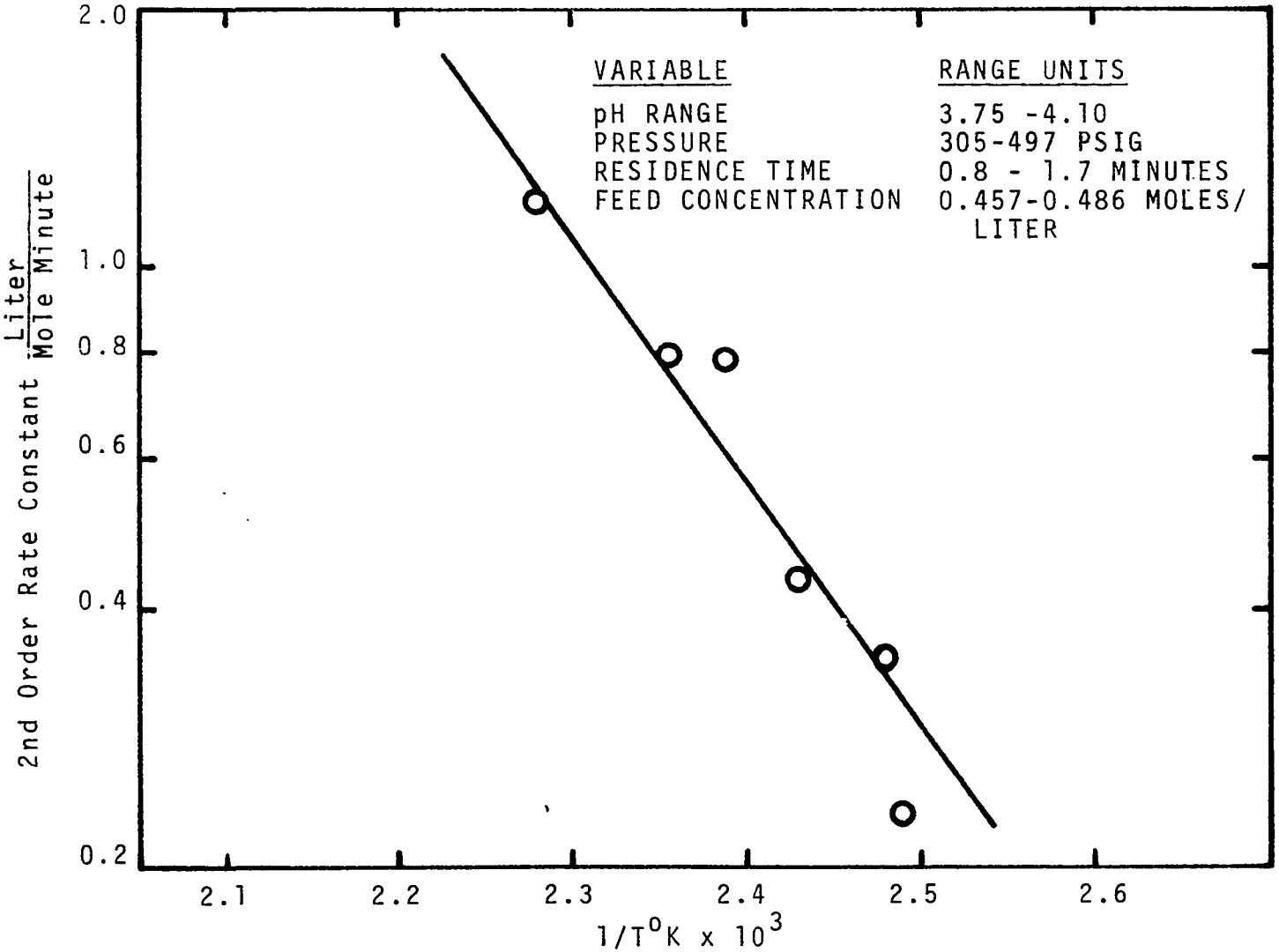

Figure 12. Arrhenius Plot-Group I Copper Runs.

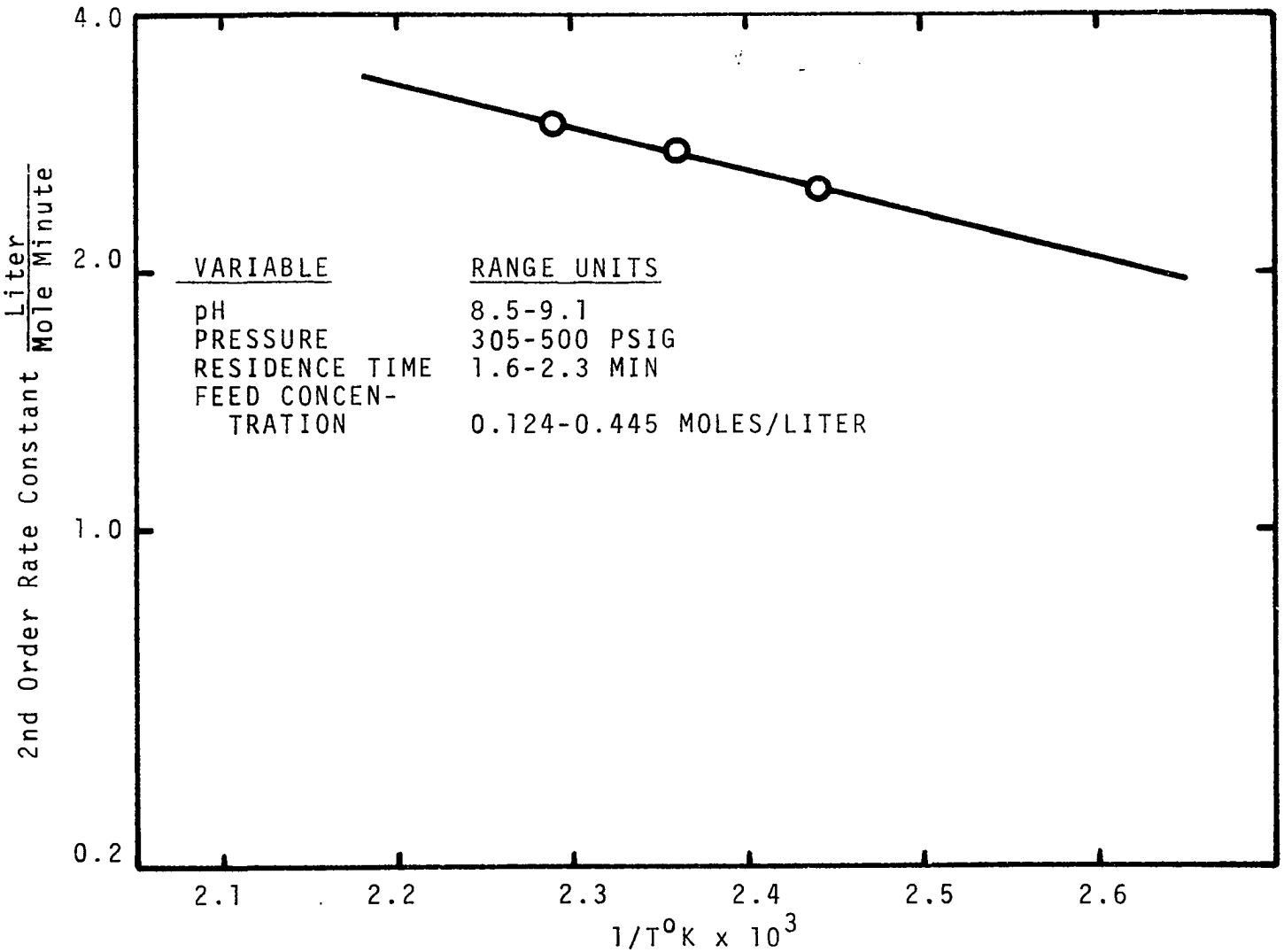

Figure 13. Arrhenius Plot-Group II Copper Runs.

cupric ammines to cupric oxides. Products recovered from these operations were composed of cupric ions; therefore, it appears that the higher (approximately 4 moles of free ammonia per mole of cupric ions) order ammines prevented the subsequent cupric ion reduction.

Group III Runs

The runs in this group included feed solutions of ammine and acid copper sulfate which were pretreated with either sulfuric acid or ammonium hydroxide. In runs 11 and 14, feed solutions of soluble copper ammines, prepared from reagent grade chemicals, were pretreated with concentrated sulfuric acid. In runs 19, 21 and 22, solutions obtained from acid-leached copper oxide ores were pretreated with 58 weight percent ammonium hydroxide. The resulting pretreated feed solutions contained approximately 0.5 moles free ammonia per mole of copper and varied in pH from 4.8 to 5.6.

These runs were characterized by high feed depletions which ranged from approximately 85 to 95 percent. The presence of hydrolysis products in the reactor following these operations was limited to thin localized deposits. Consequently, the observed feed depletions approached the actual feed conversions to metallic copper.

The quantity of metallic copper powder recovered during these runs was significantly more than that observed in the Group I runs. Copper powder quality was characterized

by fine dendritic particles easily oxidized in subsequent oven drying procedures. Concentrations of extraneous (iron, aluminum, sodium, etc.) metals in the copper powders produced from acid leach solutions was less than twenty-five hundred parts per million (0.25 weight percent). The impurities in copper powders produced from the ammine feed solutions were not analyzed since reagent grade copper sulfate crystals were used in preparing the solution.

The results of the Group III runs are correlated in the Arrhenius graphs shown in Figure 14. The activation energy calculated from the slope of the ammine feed curve was 11 kilocalories per mole, and the corresponding activation energy for the acid leach feed was 13 kilocalories per mole. The 2 kilocalorie difference in activation energies observed between acid and ammonia feed pretreatment is within experimental accuracy of the acid pretreatment procedures used. The five-fold increase in rate constant, for ammonia feed pretreatment, however, is a significant difference. Two explanations for the observed increase in rate constant for ammonia feed pretreatment are offered. First, the pretreatment of copper ammine feed solution with acid produces more by-product ammonium sulfate than the ammonium hydroxide pretreatment of acid feed solution. For example, the neutralization of a 0.1 mole per liter solution of tetrammine copper sulfate solution with concentrated sulfuric acid produces 0.2 moles per liter of ammonium sulfate. The corresponding neutralization

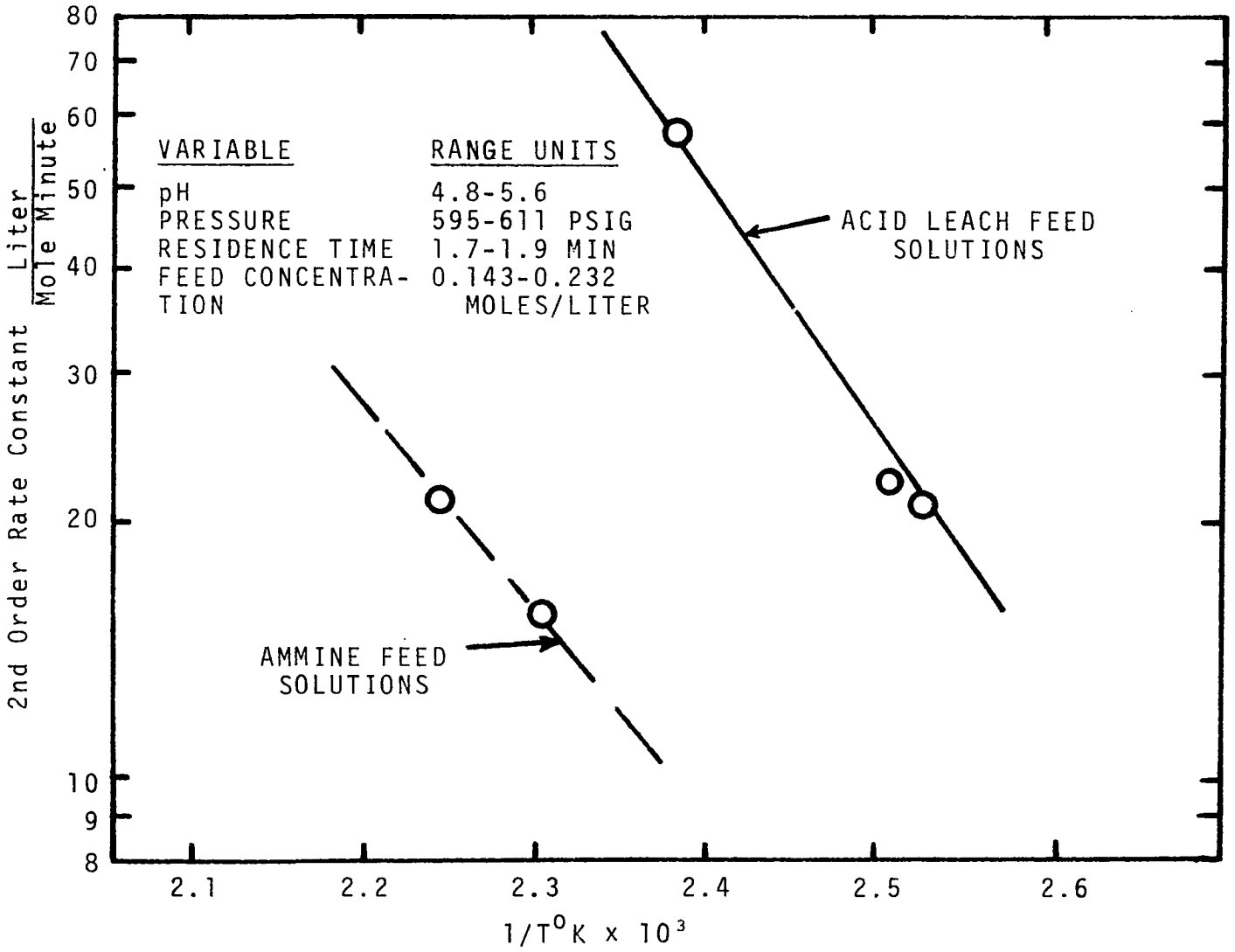

Figure 14. Arrhenius Plot-Group III Copper Runs

of a 0.1 mole per liter solution of copper sulfate with pH of 2 (0.005 moles per liter sulfuric acid) using ammonium hydroxide, produced 0.005 moles per liter ammonium sulfate. Therefore, for this example, approximately forty times more ammonium sulfate is produced in the sulfuric acid pretreatment procedure than in the ammonium hydroxide pretreatment.

The presence of ammonium sulfate, in limited quantities, enhances the reduction rate of copper from ammine solutions; however, as was discussed in Chapter III, excess concentrations of ammonium sulfate retard the reduction rate. Consequently, the observed differences in rate constants for acid and ammonia pretreatment could reflect the good and bad aspects of ammonium sulfate buffering.

The second explanation for the observed differences in the rate constants is attributed to the feed solution properties. The acid-leached copper oxide ore contained various species of soluble metallic and non-metallic ions. The presence of these extraneous ions during reduction could conceivably account for a catalytic effect similar to that noted in nickel reduction.

Group IV Runs

The runs in this group did not correspond to the conditions and results of the previous three groups. Three out of the six runs in this group were plagues with operating difficulties and consequently did not reach steady-state

operations. These operations included runs 4, 12 and 13. Run 4 was an isothermal operation using an ammonium sulfate, buffered feed recovered from previous operations, runs 1 and 2. The pH of the feed solution was 2.15 and the corresponding feed depletion was approximately 85 percent. The run was terminated after 62 minutes operation because of a plugged liquid preheat coil. The uncertainty involved in determining the exact time of plugging invalidated the encouraging results of this operation.

Runs 12 and 13 were characterized by unsteady-state operations incurred during the development of acid feed pretreatment operations. Erratic acid pretreatment of feed solutions buffered with ammonium hydroxide resulted in sporadic production of metallic copper. Consequently, the results obtained were qualitative and not suitable for subsequent correlations.

Runs 10 and 11A processed soluble copper ammine feed solutions which were buffered with 200 grams per liter ammonium sulfate. The resulting zero and 6 percent depletions observed for runs 10 and 11A, respectively, were initially confusing. However, in light of the earlier discussions involving ammonium sulfate buffering, the results of these runs are not surprising. Consequently, runs 10 and 11A substantiated the detrimental effects of excessive ammonium sulfate buffering on copper ammine reduction.

Run 20 processed unbuffered and untreated acid leach solution with a pH of 1.65. Since the resulting solution of depleted product was very acidic (approximately 1.0 pH) severe corrosion problems were encountered in the high temperature portion of the non-isothermal reactor. The run was characterized by a slow approach to steady-state depletion, shown in Appendix A, and the presence of metallic copper deposits in the reactor. The presence of basic salts were not detected during the run; consequently, the mechanism of reduction appeared to be homogeneous.

Continuous Nickel Operations

Four data points were obtained from four continuous nickel runs under non-isothermal reactor conditions. The nickel operations were restricted to hydrogen reduction from ammine solutions because the thermodynamics are more favorable for nickel reduction (as noted in Chapter III). However, nickel reduction from ammine solution are characterized by a very slow homonucleation of the metallic nickel. This difficult homonucleation of nickel from nickel ammine solutions was eliminated by using an acid feed solution of ferrous-nickel sulfate. The feed solution was pretreated with an ammonium hydroxide solution to form a precipitate complex of ferrous-nickel-ammonia-sulfate. This precipitate then acts as a heteronucleating catalyst during the subsequent hydrogen reduction step.

Continuous nickel operations were conducted over a wide range of ammonium hydroxide pretreatment rates, residence times, and reaction temperatures. However, the corresponding variations in feed concentrations, feed hydrogen rates, and reaction pressures were comparable in all operations. The operations are summarized in Table 6, and run details are described in Appendix A.

The results and significance of the operation are summarized below.

Run 15

Ammonium hydroxide pretreatment rates during the first nickel reduction run were varied to provide 1.28, 3.60, and 5.52 free ammonia to nickel mole feed ratios. The remaining system variables were maintained at relatively constant values. In traversing from a free ammonia to nickel mole feed ratio of 1.28 to 5.52, a decrease in feed depletion was observed at the 3.6 mole ratio operation. However, following the depletion correction procedure, discussed in Chapter VII, the 3.6 mole ratio conversion was similar to the conversion calculated for the initial 1.28 feed free ammonia to nickel operation. The maximum depletion of nickel in the feed, approximately 98 percent with a corresponding conversion to metallic nickel of approximately 82 percent, was obtained at the highest ammonia to nickel feed ratio. However, another factor, besides ammonia to nickel feed ratio, may be

associated with the observed high conversion value. This factor involves the reactor accumulations of nickel powder experienced throughout the run.

The solution feed rates for run 15 were based on feed rates used in previous copper operations; however, the difference in density between metallic copper and nickel were not considered. Consequently, the more dense nickel particles formed during reduction were not effectively removed from the reactor. The resulting concentration of nickel powder in the reactor increased with operating time, reaching a maximum at the end of the run. Therefore, the higher conversion obtained near the end of this run is more likely attributed to the increased nickel surface area available at this time. This observation was confirmed in later operation where effective removal of reactor products resulted in lower nickel conversions.

The products continuously recovered during run 15 included a depleted solution of soluble nickel ammine, metallic nickel, and an amorphous precipitate. The precipitate, analyzed by x-ray diffraction, was found to contain ferrosoferric oxide (magnetite), thus confirming the finding of Wanklyn (35).

Approximately 80 percent of the product nickel produced during the run was recovered from the reactor following the run. The x-ray analysis of this powder product indicated

100 percent metallic nickel; however, the analytical technique did not detect the presence of amorphous constituents. Subsequent purity corrections, based on the methods discussed in Chapter VII and shown in Table 5, revealed the product powder contained approximately 85 percent metallic nickel. The remaining 15 percent was an unconverted amorphous complex which was discussed in Chapter VII (Figure 11).

Additional analyses were performed on the nickel product recovered. Two of these analyses included a sieve analysis and an electron microscope analysis. The sieve analysis was made on approximately 100 grams of nickel powder recovered from the reactor. The corresponding sieve analysis is shown in Figure 15 with a comparison curve for nickel product produced by Sherritt Gordon Mines, Ltd., in batch hydrogen reduction operations. The difference in product between the operations is obvious. Rather than containing a narrow size range, similar to the Sherritt Gordon product, the product from this continuous hydrogen reduction run contained a broad spectrum of particle sizes. The reason is based on the physical, particle bonding effect associated with filtering and oven drying the product. During this procedure the particles of nickel were physically agglomerated together and during subsequent sieve analyses were not completely separated into single particles. This phenomenon was substantiated by an electron microscope scan of the minus

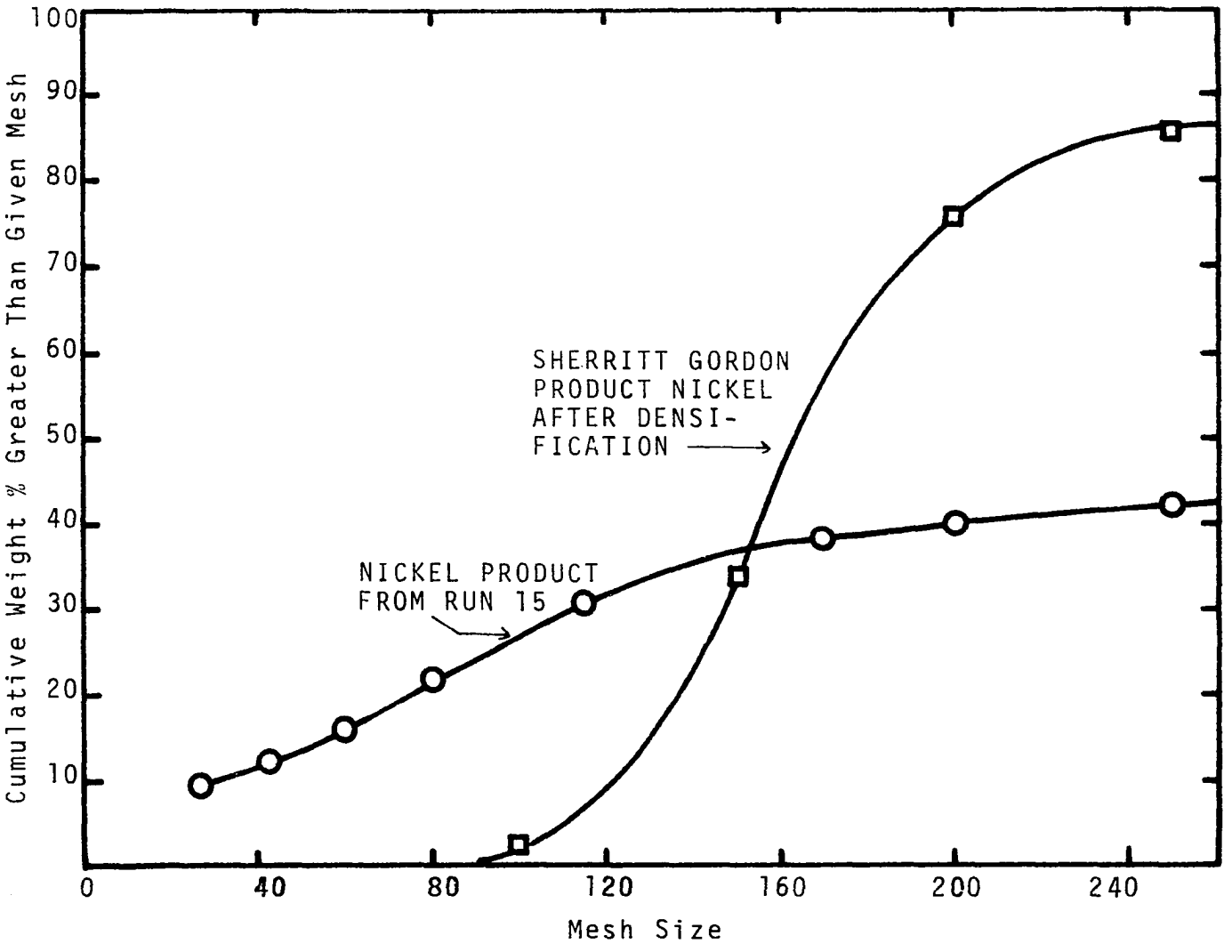

Figure 15. Nickel Product Sieve Analyses.

250 mesh fraction of the sieve analysis. The resulting micrograph, shown in Figure 16, reveals the sub-micron particle size of the continuously produced nickel powder. Based on the electron microscope analysis and assuming the larger mesh sizes are composed of similar sized particles, continued sieving should break up the agglomerates and shift the curve for nickel product recovered in run 15 to the right. The final distribution curve should have a shape similar to the Sherritt Gordon distribution curve.

Run 16

The objective of run 16 was to reduce nickel continuously at a 2.2 free ammonia to nickel feed mole ratio without accumulating reactor nickel. Accumulation was prevented by increasing the solution feed rate and therefore increasing the upward velocity in the reactor. The resulting operation at the greater feed rate was severely hampered by the heating capacity of the non-isothermal reactor heater. The resulting depletion of feed concentration was approximately 70 percent; the corresponding conversion to metallic nickel was approximately 20 percent.

Analysis, by x-ray diffraction, of the product recovered during the run revealed the presence of metallic nickel; however, the diffraction pattern did not provide the peak resolution obtained in the product analysis of run 15. subsequent product analysis of run 16, using the electron

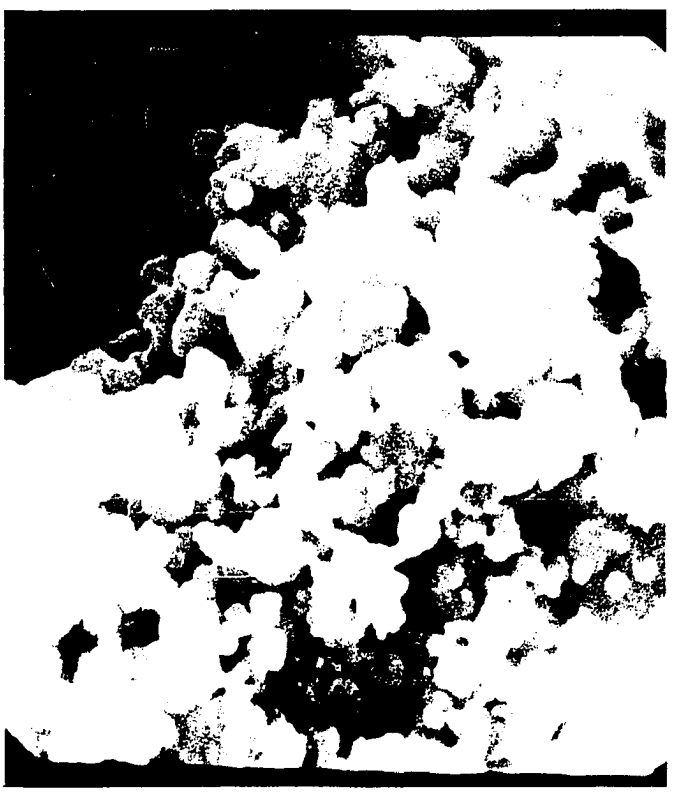

Figure 16. Electron Micrograph of Run 15 Minus 250 Mesh Nickel Product x 14,000.

microscope, revealed clouds of sub-micron particles as shown in Figure 17, which were undefined at magnifications of 24,250. The ultrafine product contained approximately 55 percent total nickel and only approximately 25 percent metallic nickel as shown in Table 5. The exceptionally low conversion and resulting nickel product purity can be attributed to the low reaction temperature (199°F) and short reactor residence time (0.9 minutes).

Inspection of the reactor at the end of the run revealed approximately 5 cubic centimeters of reactor deposit and essentially no free reactor solids. Consequently, based on the original objective, the run was a success.

Run 17

The objectives of run 17 were to increase feed conversion to metallic nickel and simultaneously to limit reactor accumulations of nickel product. To accomplish these objectives the free ammonia to nickel mole ratio of the feed was increased to 4.1 and the feed solution rate was reduced to 133 grams per minute. The resulting reaction temperature increased to 247°F. The residence time increased to 1.4 minutes.

As expected, the depletion of feed concentration increased to approximately 100 percent and the corresponding calculated feed conversion to metallic nickel increased to approximately 45 percent. The resulting product nickel purity,



Figure 17. Electron Micrograph of Run 16 Product Nickel x 24,250.

shown in Table 5, increased to approximately 45 percent.

Following run 17 the reactor deposits, which were determined experimentally by the procedure outlined in Chapter V, were found to be less than 5 cubic centimeters.

Run 18

Run 18 was the last continuous nickel reduction operation in this investigation. The objective of the run was to increase the conversion to metallic nickel. To accomplish this objective, a lower feed solution mole ratio of free ammonia to nickel in the feed was used. The 2.3 mole ratio of free ammonia to nickel chosen was based on the results obtained during the initial phase of run 15, when reactor nickel accumulations were minimal.

Although this run showed considerable promise, it had to be terminated due to a plug in the reactor discharge line approximately 30 minutes after initiation of the feed solution. Since steady-state operations were not achieved, the results were not suitable for subsequent correlations. However, the limited results obtained before plugging were encouraging. At the time of termination, feed depletion was approixmately 100 percent and calculated conversion to metallic nickel was approximately 75 percent. Product nickel analyzed approximately 75 percent metallic nickel with the balance being nickel complexes.

Reactor free and deposited solids, following the run, were experimentally determined to be approximately 15 cubic centimeters. The increased reactor accumulation can be attributed to the straining effect provided by the partially plugged reactor dip tube.

Correlation of Nickel Results

Four data points from the first three continuous nickel reduction operations are correlated in the Arrhenius plot shown in Figure 18. The corresponding activation energy, calculated from the slope of the curve, is 10 kilocalories per mole. This value of activation energy agrees within half a kilocalorie with data obtained in previous batch nickel reduction studies (24).

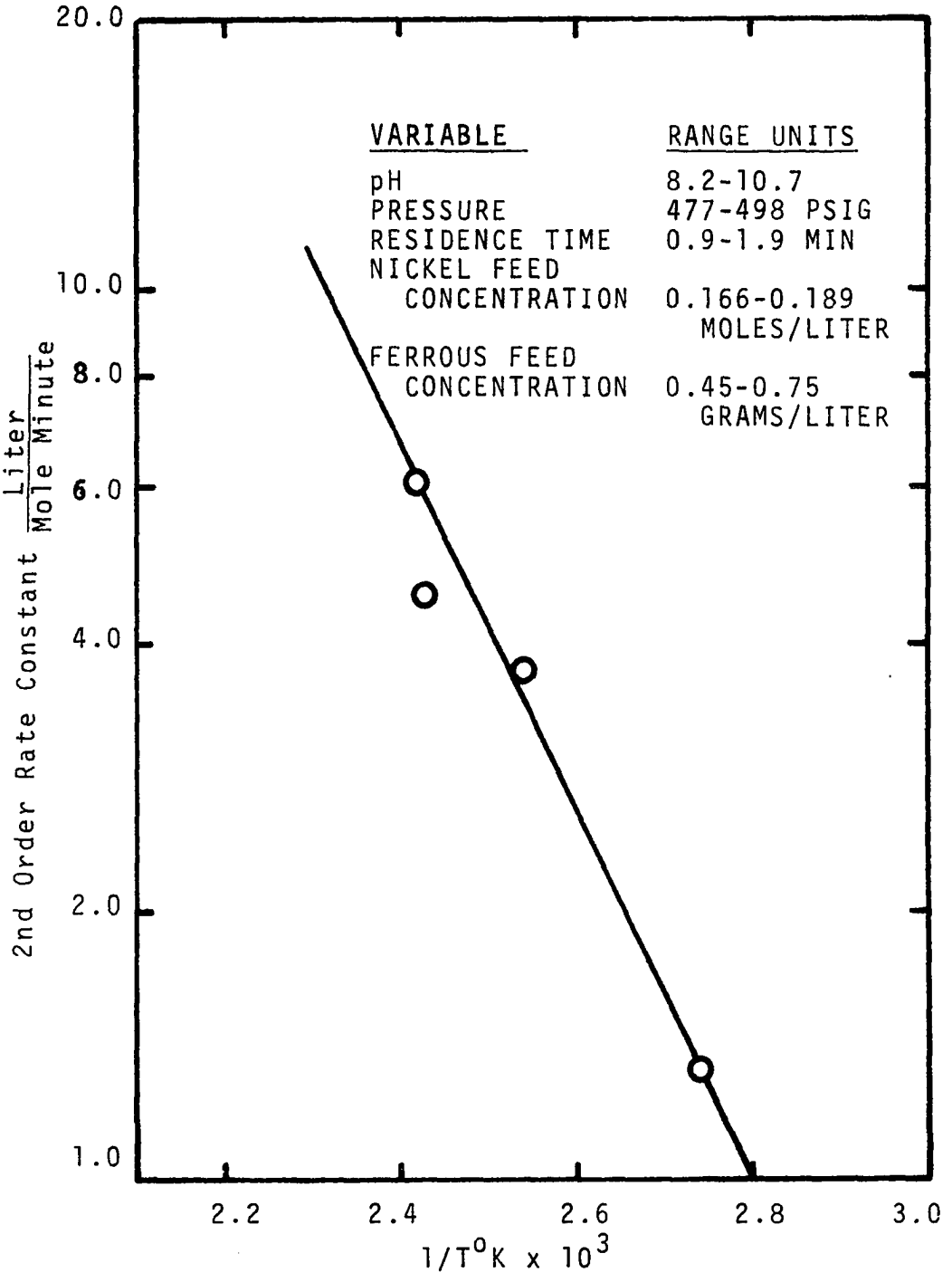

Figure 18. Arrhenius Plot-Nickel Runs.

CHAPTER IX

CONCLUSIONS

The results of this investigation demonstrate that continuous hydrogen reduction of aqueous solutions containing copper or nickel ions is feasible. Although copper and nickel can be reduced from homogeneous solutions, more effective reductions are obtainable via a heterogeneous mechanism according to this investigation.

Metallic copper was continuously recovered from acid solutions of copper sulfate having a pH greater than approximately 3 through the reduction of intermediate copper basic salts. The basic salts of copper are formed naturally through a hydrolysis mechanism or are induced by pretreatment. Sulfuric acid pretreatment of ammine copper sulfate solutions, and ammonium hydroxide pretreatment of acid copper sulfate solutions having a pH less than approximately 3, increase the resulting feed depletion rates by factors of 20 to 80. The more effective procedure is ammonium hydroxide pretreatment of acid solutions. The activation energy for the hydrolysis formation reaction is 12 $\pm$ 2 kilocalories per mole. The rate limiting step for copper reduction by the proposed

heterogeneous mechanism is the reduction of the intermediate basic salts. No previous data on activation energies for the heterogeneous reductions of copper have been published.

Metallic nickel was continuously reduced from ammine solutions catalyzed by the addition of ferrous sulfate. The heterogeneous mechanism involved the formation of an intermediate precipitate containing ammonia, nickel ions, and ferrous ions. An intermediate form of this precipitate heteronucleates metallic nickel which provides active growth sites for subsequent nickel reduction from solution. The calculated activation energy for nickel reduction is 10 kilocalories per mole which agrees within half a kilocalorie with published values obtained from batch experiments.

The agreement obtained between calculated and published activation energies for nickel reduction should lend credibility to the experimental procedures and methods of analysis used in this study.

The results derived from this preliminary, continuous, hydrogen reduction study indicate that additional work must be performed to establish the feasibility of extended continuous operations. Continuous operations, on the order of eight or more hours, would be required for a comprehensive process evaluation.

NOMENCLATURE

a	chemical activity
A	solid particle surface area
A-	symbol for accumulator vessel
C	bulk solution concentration of metal ions
C_m	feed solution metal ion concentration
C_o	concentration of metal ions at solid surface
Co	initial feed concentration of metal ions
C_P	concentrations of metal ions in separator product
C_R	concentration of metal ions in reactor discharge
Cu^+	symbol for cuprous ion
Cu^{++}	symbol for cupric ion
Cu^o	symbol for metallic copper
cc	cubic centimeters
cm	centimeters
D	diffusion coefficient
E	electrode potential, volts
E_a	reaction activation energy, kilocalories/mole
E^o	electrode reference potential at standard state
e^-	symbol for electron
F	Faraday equivalent, 96,496 coulombs
F	feed solution rate, liters/minute

F- symbol for flow meter

Fe symbol for iron

G Gibbs molal free energy

H_2 gaseous hydrogen

H^+ hydrogen ion in solution

K equilibrium constant in terms of activity

k_x dissociation constant for ammine complex with x moles ammonia per mole metal ions

k_o frequency factor in Arrhenius equation

k_n nth order reaction rate constant

K- symbol for knock out vessel

M^o symbol for metallic metal

M^{++} symbol for divalent metal ion

N_2 gaseous nitrogen

N_i^{++} symbol for ionic nickel

N_i^o symbol for metallic nickel

n number of electrons transferred per mole of metal ion reduced

NH_3 free ammonia molecule

NH_4^+ ammonium ion

P pressure, psig

P- symbol for pump

P_{H_2} hydrogen partial pressure

PCV symbol for pressure control valve

PIC symbol for pressure indicator controller

PI symbol for pressure indicator

pH	measure of hydrogen ion concentration
psig	pounds per square inch pressure gauge
q	solution feed rate, grams/minute
R	universal gas constant, 1.987 calories/gram-mole^{o}K
SRV	symbol for safety relief valve
T	absolute temperature, ^{o}K
TI	symbol for thermocouple
TIC	symbol for temperature indicator controller
t	general, time
t	specific, reactor liquid residence time, minutes
V_L	liquid volume in high pressure separator, cc
V_R	liquid volume in reactor, 180cc
X_f	mole fraction conversion or depletion at reactor exit
X_M	mole fraction conversion or depletion along reactor length
X	symbol for unidentified specie in nickel feed complex precipitate

Greek Letters

ε	fraction volume change during reaction
ρ	density of feed solution, grams/cc

BIBLIOGRAPHY

1. Beketov, N. N. (1859), Compt. rend., Vol. 48, p. 442.

2. Bjerrum, J. "The Tendency of Metal Ions Toward Complex Formation." Chemical Review, 46 (1950):381-401.

3. Brown, R. L. "Steady State Crystallization from Solutions of Metal Salts under Hydrogen Atmospheres at Elevated Temperatures and Pressures." M.S. Thesis. University of Oklahoma, Norman, Oklahoma, 1965.

4. Conner, H. S. "Equilibrium Thermodynamics of Copper Displacement from Copper Salt Solutions Under Hydrogen Atmospheres at Elevated Temperatures and Pressures." M.S. Thesis. University of Oklahoma, Norman, Oklahoma, 1965.

5. Courtney, W. G., and Schaufelberger, F. A. "Observations on the Kinetics of the Reduction of $NiSO_4$ in Aqueous Solutions." Physical Chemistry of Process Metallurgy. New York: Interscience Publishers, 1961.

6. Dobrokhotov, G. N. "Reduction of Metals in Solution with Hydrogen Under Pressure." Tsuet. Metally, Musk, 2, No. 2, 27-33.

7. Evans, D. J. I. "Production of Metals by Gaseous Reduction from Solution--Process and Chemistry." Advances in Extractive Metallurgy. Essex, England: Elsevier Publishing Co., Ltd., 1968.

8. Evans, D. J. I., Romanchuk, S., and Mackiw, V. N. "Production of Copper Powder by Hydrogen Reduction Techniques." The Canadian Mining and Metallurgical Bul., 591 (1961):530-538.

9. Evans, D. J. I., Romanchuk, S., and Mackiw, V. N. "Treatment of Copper-Zinc Concentrates by Pressure Hydrometallurgy." The Canadian Mining and Metallurgical Bulletin, 628 (1964):857-866.

10. Forward, F. A. "Hydro Metallurgy--Its Scope and Limitations." Chemical Engineering Process. (1958):41-46.

24. Meddings, B., and Mackiw, V. N. "The Gaseous Reduction of Metals from Aqueous Solutions." Unit Processes in Hydrometallurgy, Vol. 24. New York: Gordon and Breach, Science Publishers, Inc., 1963.

25. Mellor, J. W. "A Comprehensive Treatise on Inorganic and Theoretical Chemistry." Longmans, Green and Co., London (1922).

26. Peters, E., and Halpern, J. "Homogeneous Catalytic Activation of Molecular Hydrogen by Cupric Perchlorate." Journal of Physical Chemistry, 59 (1955):793-796.

27. Pierce, W. C., Sawyer, D. T., and Haenisch, E. L. Quantitative Analysis. 4th ed. New York: John Wiley and Sons, Inc., 1960.

28. Psnnjak, E., and Tunell, G. (1929). The System Cupric Oxide-Sulphur Trioxide-Water: American Journal of Science, 5th Series, Vol. 18, pp. 1-34.

29. Schaufelberger, F. A. "Precipitation of Metal from Salt Solution by Reduction with Hydrogen." Journal of Metals, 8 (1956):695-704.

30. Sliepcevich, C. M., and Brown, R. L. "Extractive Metallurgy: Recovery of Metals by Gaseous Reduction from Solutions." Unpublished Research Proposal. University of Oklahoma Research Institute, Norman, Oklahoma, 1972.

31. Sobol, S. I., and Kononov, A. V. Autoclave Technology of Producing Copper Powders. Tsuet. Metally, Mosk, 38, No. 1, 1965, 22-26.

32. Tammann, G., and Nernst, W. (1892). Z Physik. Chem., 9:1.

33. Von Hahn, E. A., and Peters, E. "Role of Copper (I) in the Kinetics of Hydrogen Reduction of Aqueous Cupric Sulfate Solutions." The Journal of Physical Chemistry, 69, 2 (1965):547-552.

34. Wadsworth, M. E., and Kaneko, T. M. The Catalytic Reduction of Cobret from Ammoniacal Cobret Sulfate Solution. J. Phys. Chem. 60, April 1956, 457-62.

35. Wanklyn, J. N. and Burns, U. R. "Evolution of Hydrogen from Ferrous Hydroxide." Nature, 4105, July 1948.

11. Guenther, W. B. Quantitative Chemistry: Measurements and Equilibrium. 1st ed. Massachusetts: Addison-Wesley Publishing Company, 1968.

12. Habashi, F. Principles of Extractive Metallurgy, Vol. II. New York: Gordon and Breach, Science Publishers, Inc., 1970.

13. Halpern, J. "Some Aspects of the Physical Chemistry of Hydrometallurgy." Journal of Metals. 1957:280-289.

14. Homer, J. University Engineers, Inc., Norman, Oklahoma. Private Communication, June, 1972.

15. Ipatieff, V. N. (1946). The Life of a Chemist: Stanford University Press, California and Oxford University Press, London, pp. 123-477.

16. Ipatieff, V. N. "Early Work on the Displacement of Metals and Metal Oxides." Journal of Chemical Education. pp 110-115 (March, 1953).

17. Kieswetter, O. "Reduction of Curpic and Nickelous Ions from Aqueous Copper and Nickel Sulfate Solutions by Hydrogen." Ph.D. Thesis. University of Oklahoma, Norman, Oklahoma, 1973.

18. Kothari, R. H. "Precipitation of Metals from Their Salt Solutions by Hydrogen." M.S. Thesis. University of Oklahoma, Norman, Oklahoma, 1971.

19. Kunda, W., and Evans, D. J. I. "Hydrogen Reduction of Copper to Powder from the Ammine Carbonate System." Modern Developments in Powder Metallurgy, Vol. IV. New York: Plenum Press, 1971.

20. Levenspiel, O. Chemical Reaction Engineering. 5th ed. New York: John Wiley and Sons, Inc., 1967.

21. MacGregor, E. R., and Halpern, J. "The Reduction of Cupric Salts in Aqueous Perchlorate and Sulfate Solutions by Molecular Hydrogen." Trans. Met. Soc. A.I.M.E., 212 (1958):244-247.

22. Mackiw, V. N., Lin, W. C., and Kunda, W. "Reduction of Nickel by Hydrogen from Ammoniacal Nickel Sulfate Solutions." Journal of Metals, 9,6(1957):786-793.

23. Meddings, B., and Evans, D. J. J. "The Changing Role of Hydrometallurgy." The Canadian Mining and Metallurgical Bulletin. 1971:48-57.

24. Meddings, B., and Mackiw, V. N. "The Gaseous Reduction of Metals from Aqueous Solutions." Unit Processes in Hydrometallurgy, Vol. 24. New York: Gordon and Breach, Science Publishers, Inc., 1963.

25. Mellor, J. W. "A Comprehensive Treatise on Inorganic and Theoretical Chemistry." Longmans, Green and Co., London (1922).

26. Peters, E., and Halpern, J. "Homogeneous Catalytic Activation of Molecular Hydrogen by Cupric Perchlorate." Journal of Physical Chemistry, 59 (1955):793-796.

27. Pierce, W. C., Sawyer, D. T., and Haenisch, E. L. Quantitative Analysis. 4th ed. New York: John Wiley and Sons, Inc., 1960.

28. Psnnjak, E., and Tunell, G. (1929). The System Cupric Oxide-Sulphur Trioxide-Water: American Journal of Science, 5th Series, Vol. 18, pp. 1-34.

29. Schaufelberger, F. A. "Precipitation of Metal from Salt Solution by Reduction with Hydrogen." Journal of Metals, 8 (1956):695-704.

30. Sliepcevich, C. M., and Brown, R. L. "Extractive Metallurgy: Recovery of Metals by Gaseous Reduction from Solutions." Unpublished Research Proposal. University of Oklahoma Research Institute, Norman, Oklahoma, 1972.

31. Sobol, S. I., and Kononov, A. V. Autoclave Technology of Producing Copper Powders. Tsuet. Metally, Mosk, 38, No. 1, 1965, 22-26.

32. Tammann, G., and Nernst, W. (1892). Z Physik. Chem., 9:1.

33. Von Hahn, E. A., and Peters, E. "Role of Copper (I) in the Kinetics of Hydrogen Reduction of Aqueous Cupric Sulfate Solutions." The Journal of Physical Chemistry, 69, 2 (1965):547-552.

34. Wadsworth, M. E., and Kaneko, T. M. The Catalytic Reduction of Cobret from Ammoniacal Cobret Sulfate Solution. J. Phys. Chem. 60, April 1956, 457-62.

35. Wanklyn, J. N. and Burns, U. R. "Evolution of Hydrogen from Ferrous Hydroxide." Nature, 4105, July 1948.

APPENDICES

APPENDIX A

Run Observations and Lapse Time Versus Depletion Plots

Run 1 Observations and Notes

1. Isothermal reactor.
2. No feed buffering.
3. High pressure separator liquid level manually controlled with throttling gate valve.
4. Copper powder immediately separated from depleted solution contained 5 micron minus particles and analysed 100% copper by X-ray diffraction.
5. Copper powder left in depleted solution oxidized rapidly to curpous oxide.
6. Unsatisfactory high pressure separator liquid level control.
7. Refer to Figure 19 for lapse time versus depletion plot.

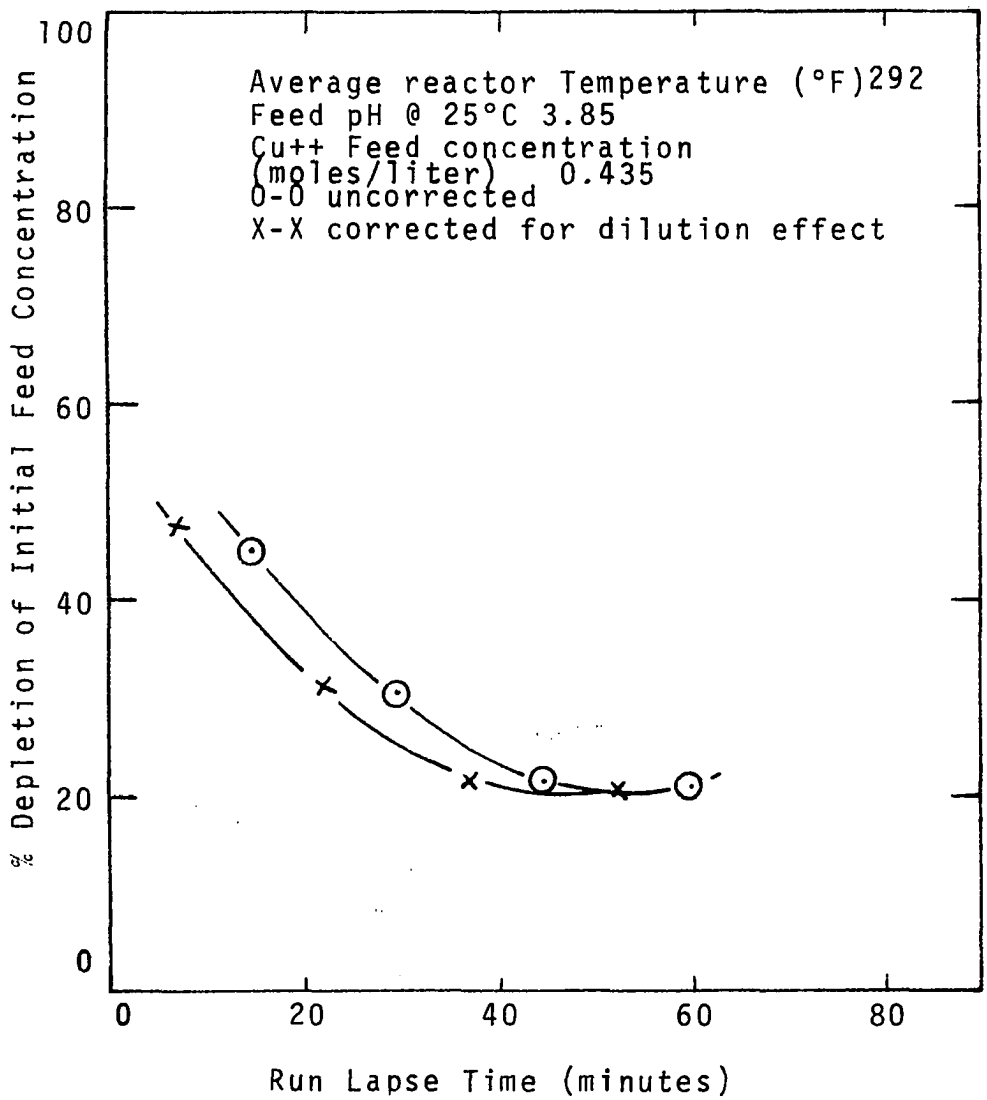

Figure 19. Lapse Time versus Depletion (Run 1)

Run 2 Observations and Notes

1. Isothermal reactor.
2. No feed buffering.
3. Solution feed rate approximately half of Run 1 feed rate.
4. High Pressure liquid control valve replaced with cycling ball valve system.
5. Copper powder produced analysed 100% metallic copper by X-ray diffraction.
6. Copper particle size increased to 10-20 micron size range.
7. Product copper recovery did not correspond with disappearance of feed copper ions.
8. Refer to Figure 20 for lapse time versus depletion plot.

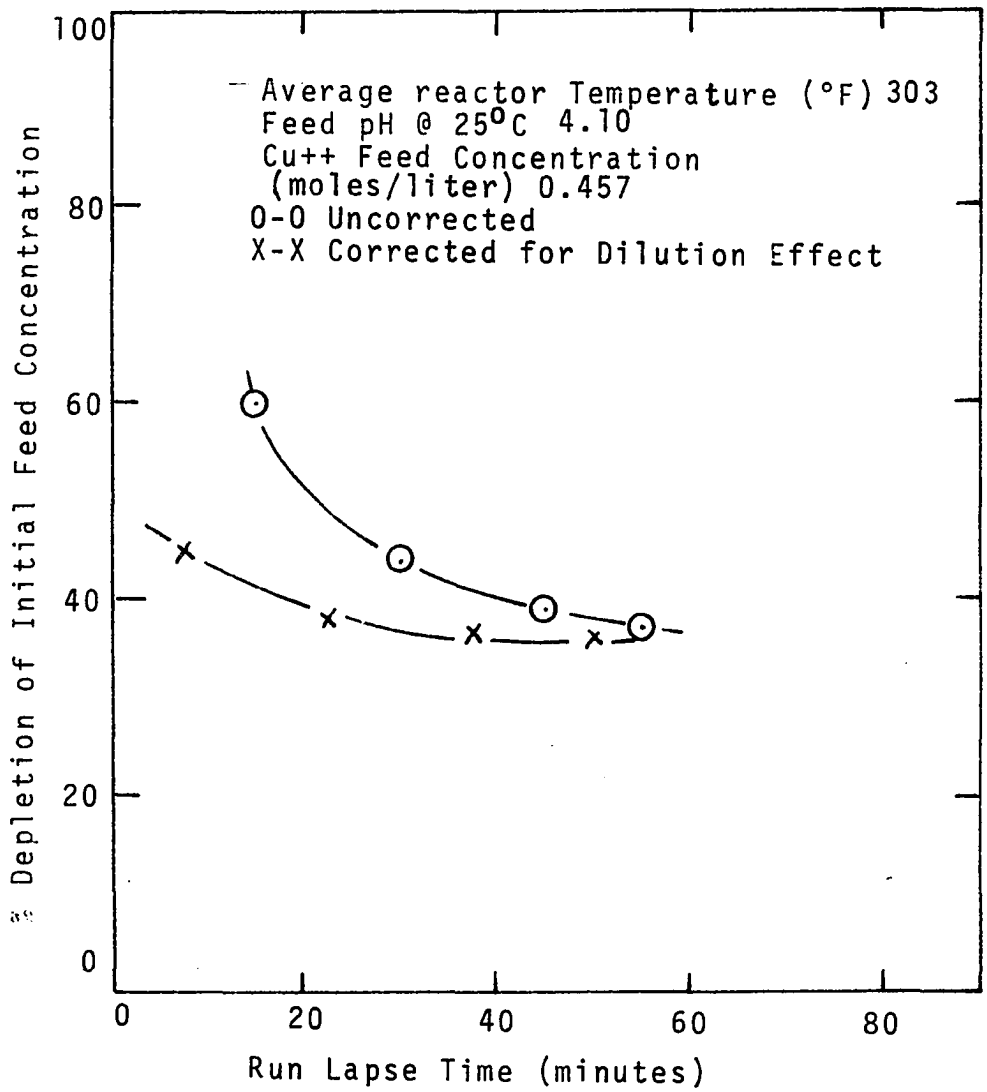

Figure 20. Lapse Time versus Depletion (Run 2)

Run 3 Observations and Notes

1. Isothermal reactor.
2. Ammonium hydroxide treatment of depleted solution from Runs 1 and 2 resulted in precipitation of approximately 55 percent of original solution copper ions.
3. Precipitate formed in feed solution contained brochantite.
4. Products recovered from run included brochantite and cupric oxide.
5. Copper depletion calculations based on soluble feed and product copper analyses.
6. Refer to Figure 21 for lapse time versus depletion plot.

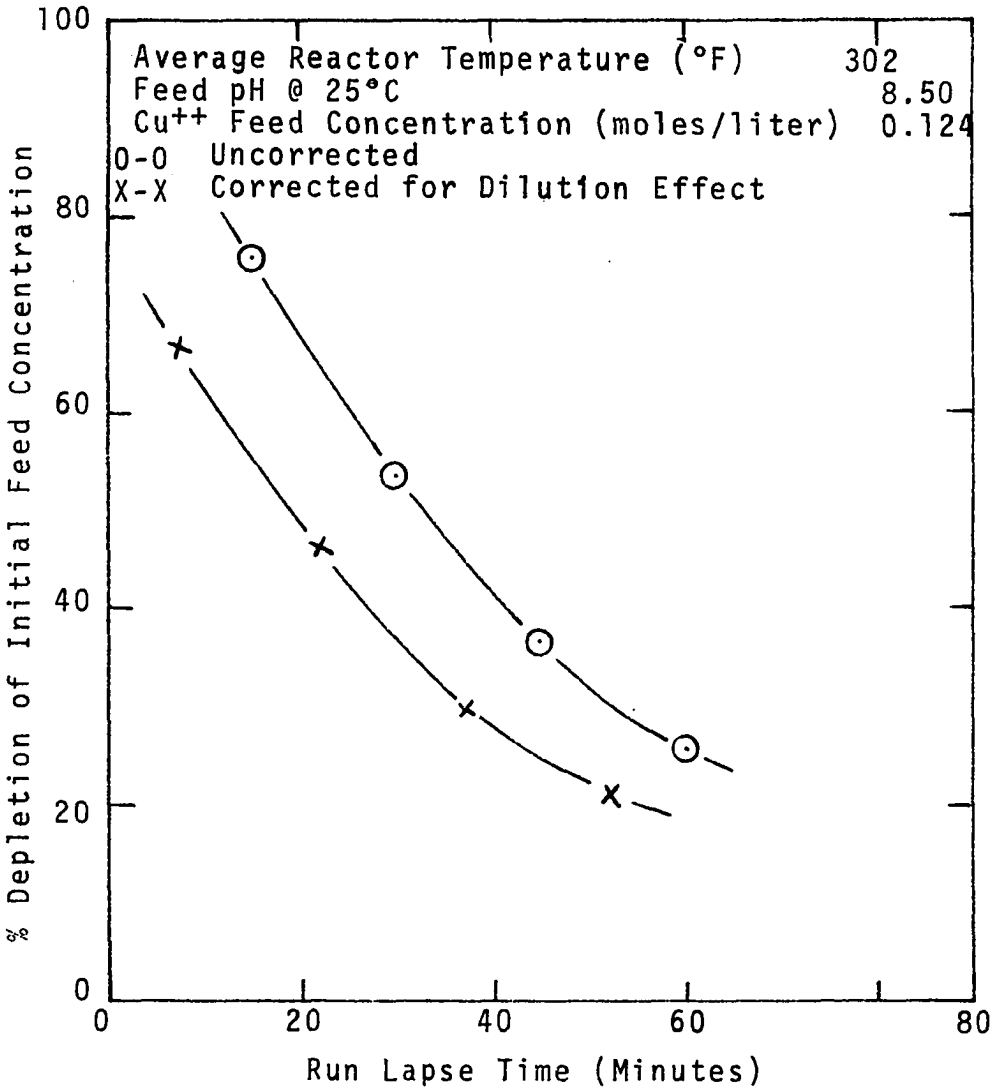

Figure 21. Lapse Time versus Depletion (Run 3).

Run 4 Observations and Notes

1. Isothermal reactor.
2. Ammonium sulfate buffering of depleted solution from Runs 1 and 2. (45 grams/liter).
3. Processing temperature increased to approximately 330°F.
4. Run provided high feed depletions to a metallic copper product.
5. Run was terminated at 62 minutes due to a plugged preheater coil.
6. Second half (25 feet) of liquid preheat coil was deposited with antlerite and other basic salts.
7. Reactor was inspected and found to be relatively free of deposits.
8. Uncertainty of exact time of plugging makes run results debatable.
9. Refer to Figure 22 for lapse time versus depletion plot.

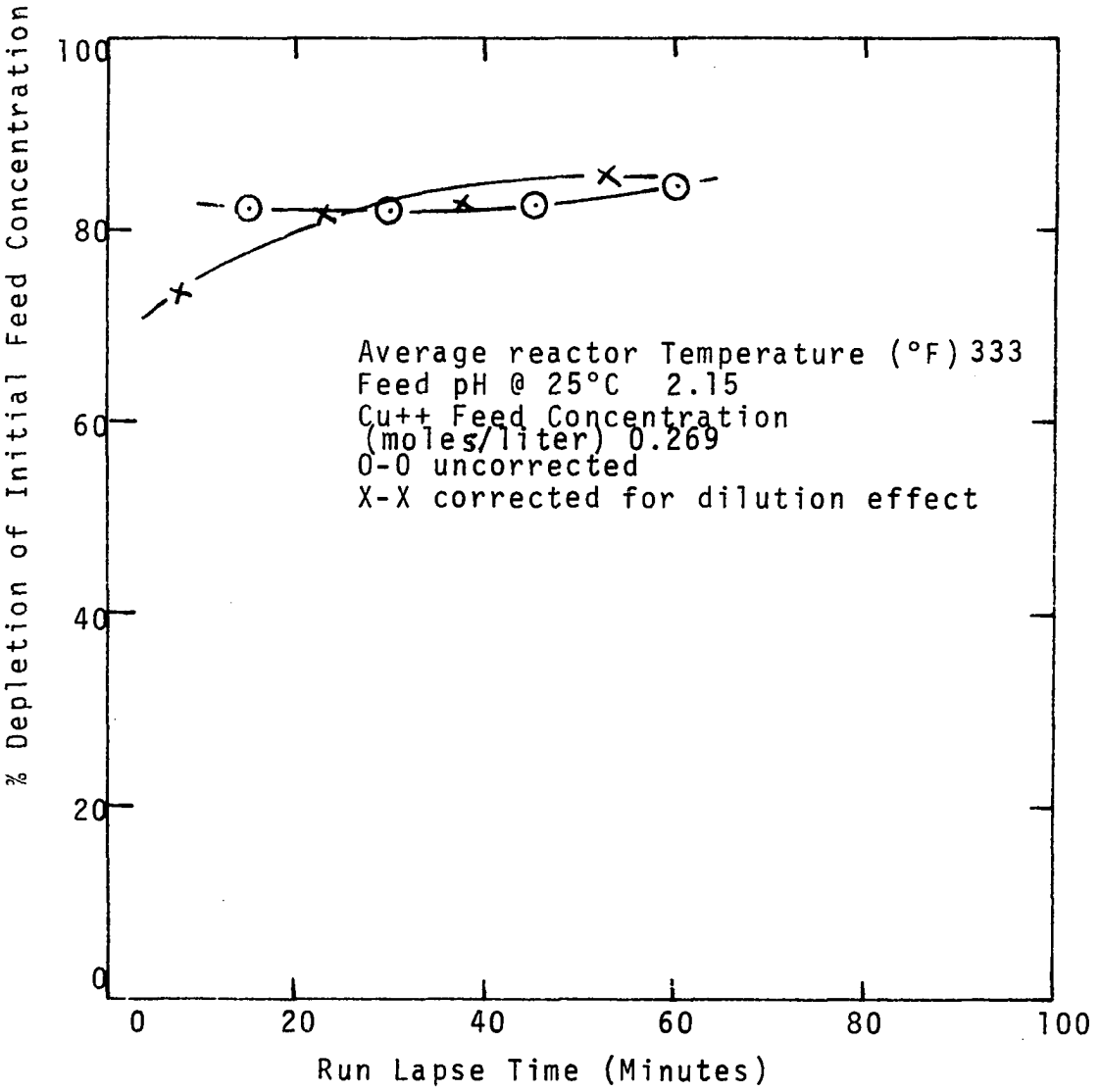

Figure 22. Lapse Time versus Depletion (Run 4)

Run 5 Observations and Notes

1. First non-isothermal reactor operation.
2. No buffering agents used.
3. Two sets of operating data at two different temperatures were obtained.
4. Product copper recovered analyzed 100% pure copper metal.
5. Reactor dip tube was found to be partially plugged with fine particulate copper.
6. Reactor inspection revealed six inches of antlerite basic salt deposit midway between inlet and exit.
7. Refer to Figure 23 for lapse time versus depletion plot.

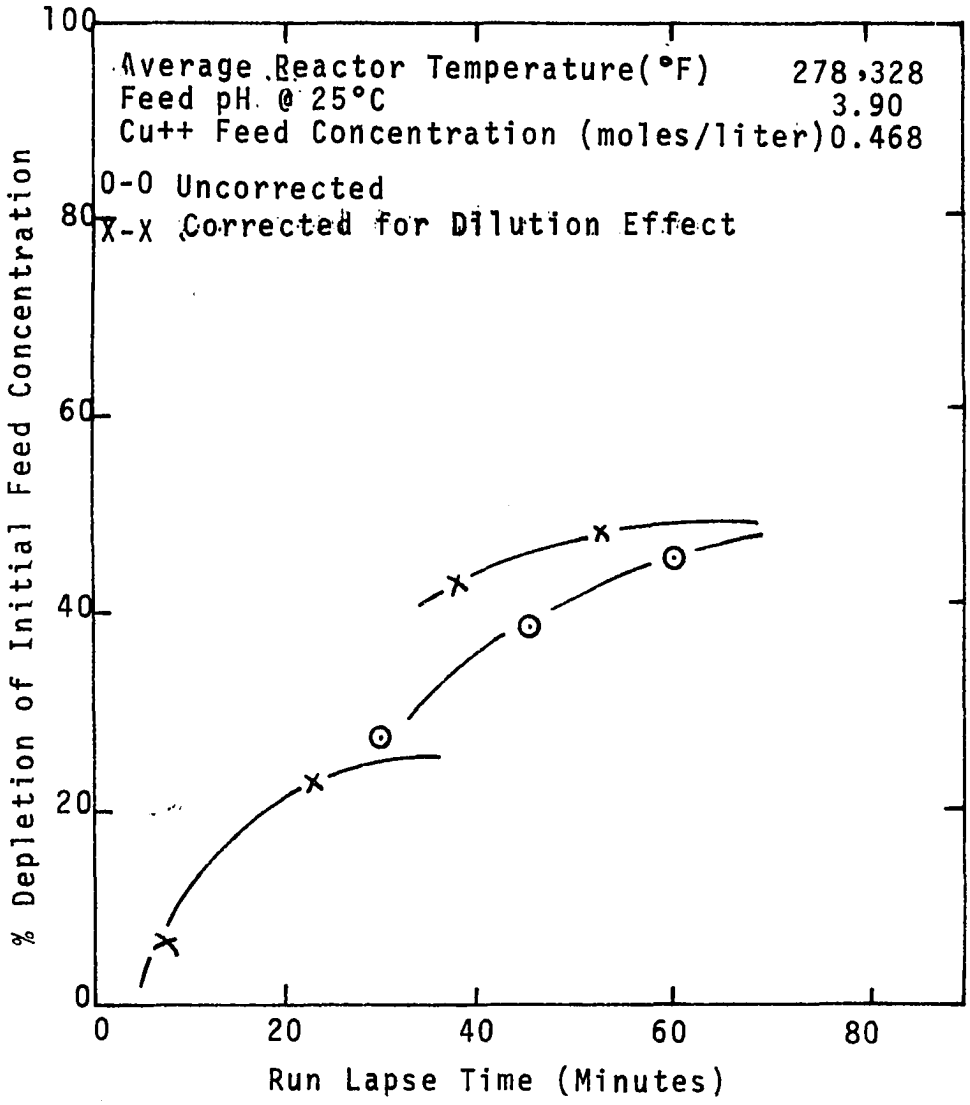

Figure 23. Lapse Time Versus Depletion (Run 5).

Run 6 Observations and Notes

1. Non-isothermal reactor.
2. Hydrolysis test run using unbuffered copper sulfate feed solution.
3. Hydrogen feed gas replaced with nitrogen gas feed.
4. Run terminated at 53 minutes because of antlerite plug in reactor discharge dip tube.
5. Reactor inspection following run revealed antlerite deposit on upper internal walls of reactor. Deposit equivalent to approximate 17 cubic centimeter volume.
6. Refer to Figure 24 for lapse time versus depletion plot.

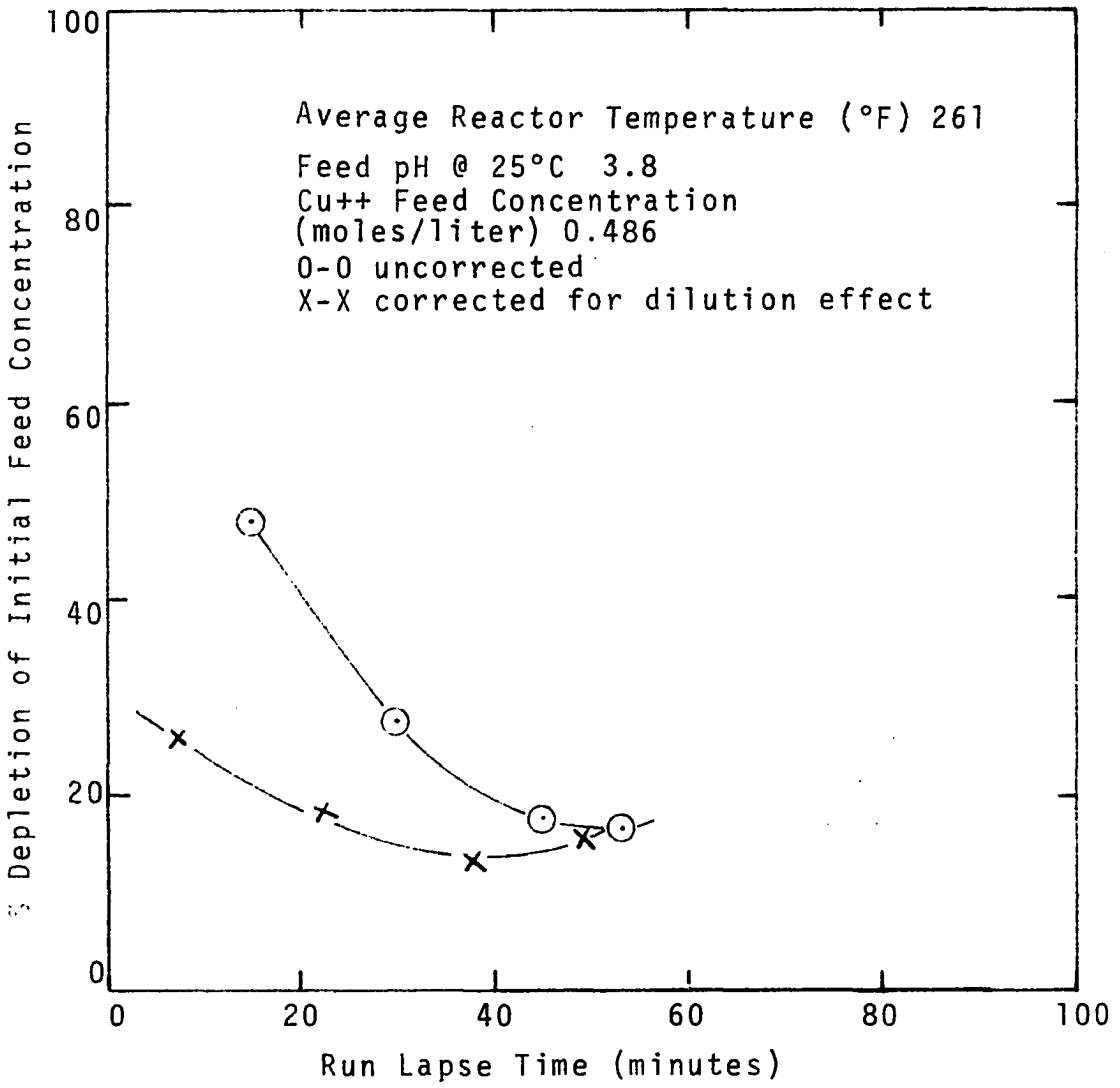

Figure 24. Lapse Time versus Depletion (Run 6)

Run 7 Observations and Notes

1. Non-isothermal reactor.
2. Internal reactor process thermowell installed in reactor.
3. Feed solution prepared from copper sulfate crystals and buffered with 42 grams ammonium sulfate per liter to repeat previous Run 4 feed conditions.
4. Run was terminated at 55 minutes because of plugging reactor discharge line.
5. Reactor inspection following run revealed wall deposits of metallic copper and cuprous oxide sheets.
6. Reactor thermowell was deposited with cuprous oxide at its lower end and antlerite at its upper end.
7. Refer to Figure 25 for lapse time versus depletion plot.

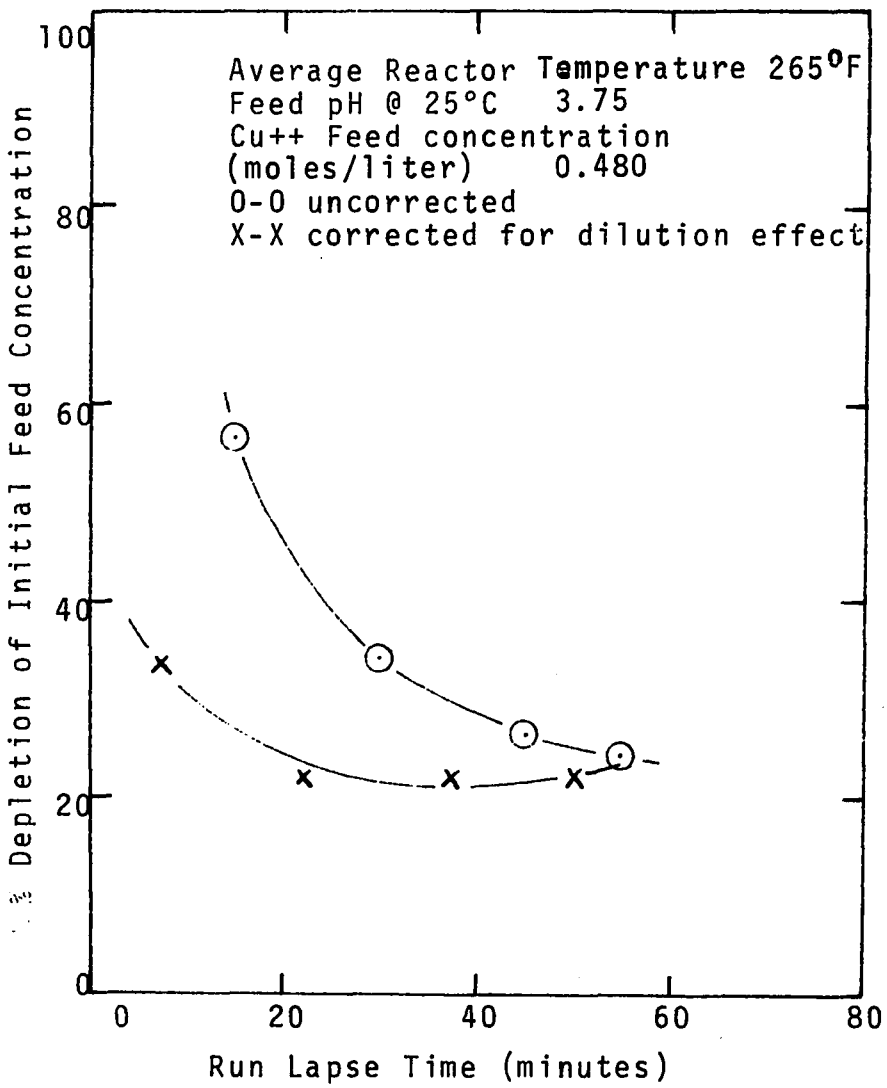

Figure 25. Lapse Time versus Depletion (Run 7)

Filmed as received

without page(s) 148 .

UNIVERSITY MICROFILMS.

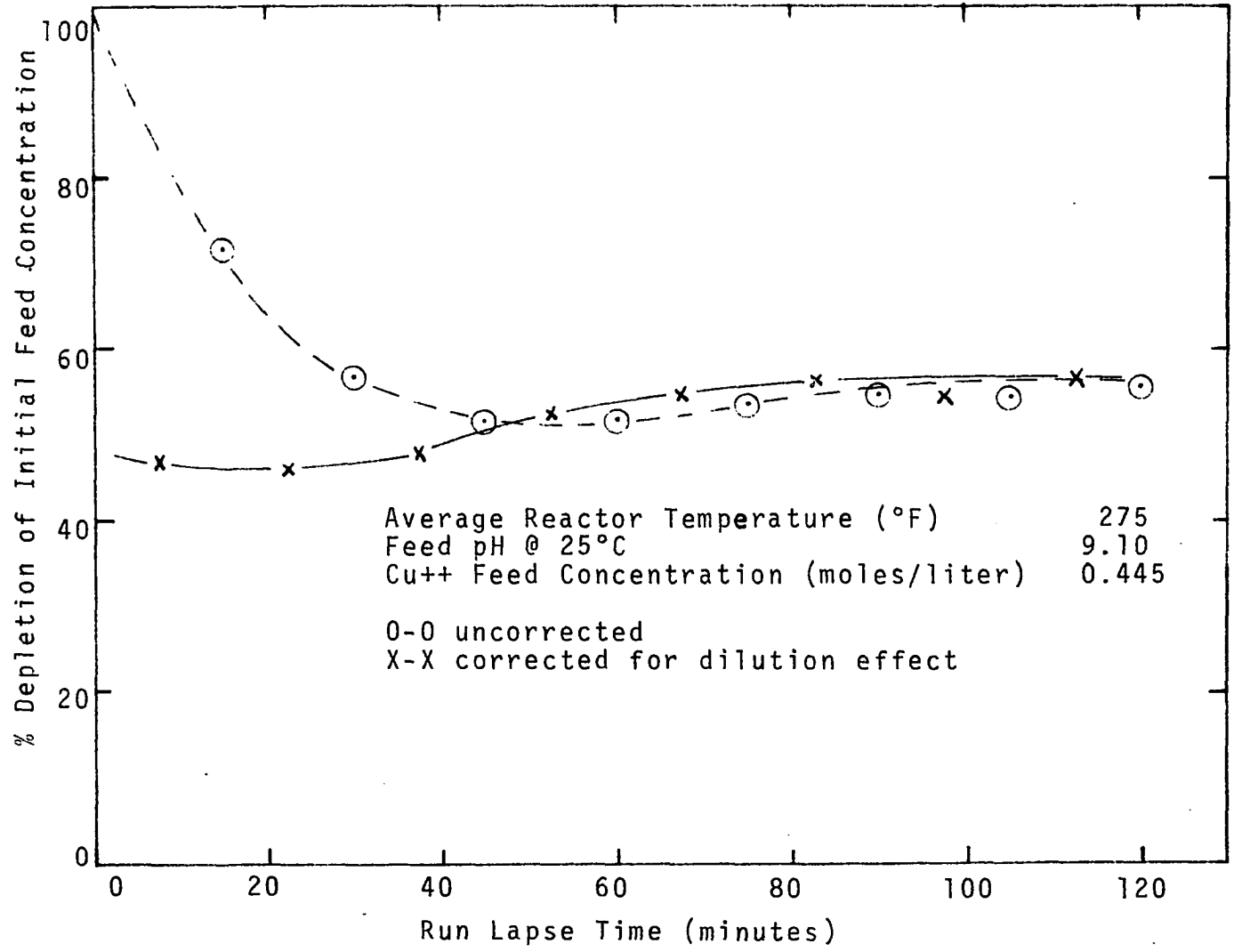

Figure 26. Lapse Time versus Depletion (Run 8)

Run 9 Observations and Notes

1. Non-isothermal reactor.
2. Feed solution was depleted product solution from Run 8 treated with ammonium hydroxide.
3. Smooth operation and run was terminated as scheduled.
4. Product formed during run analyzed 100% cupric oxide
5. Refer to Figure 27 for lapse time versus depletion plot.

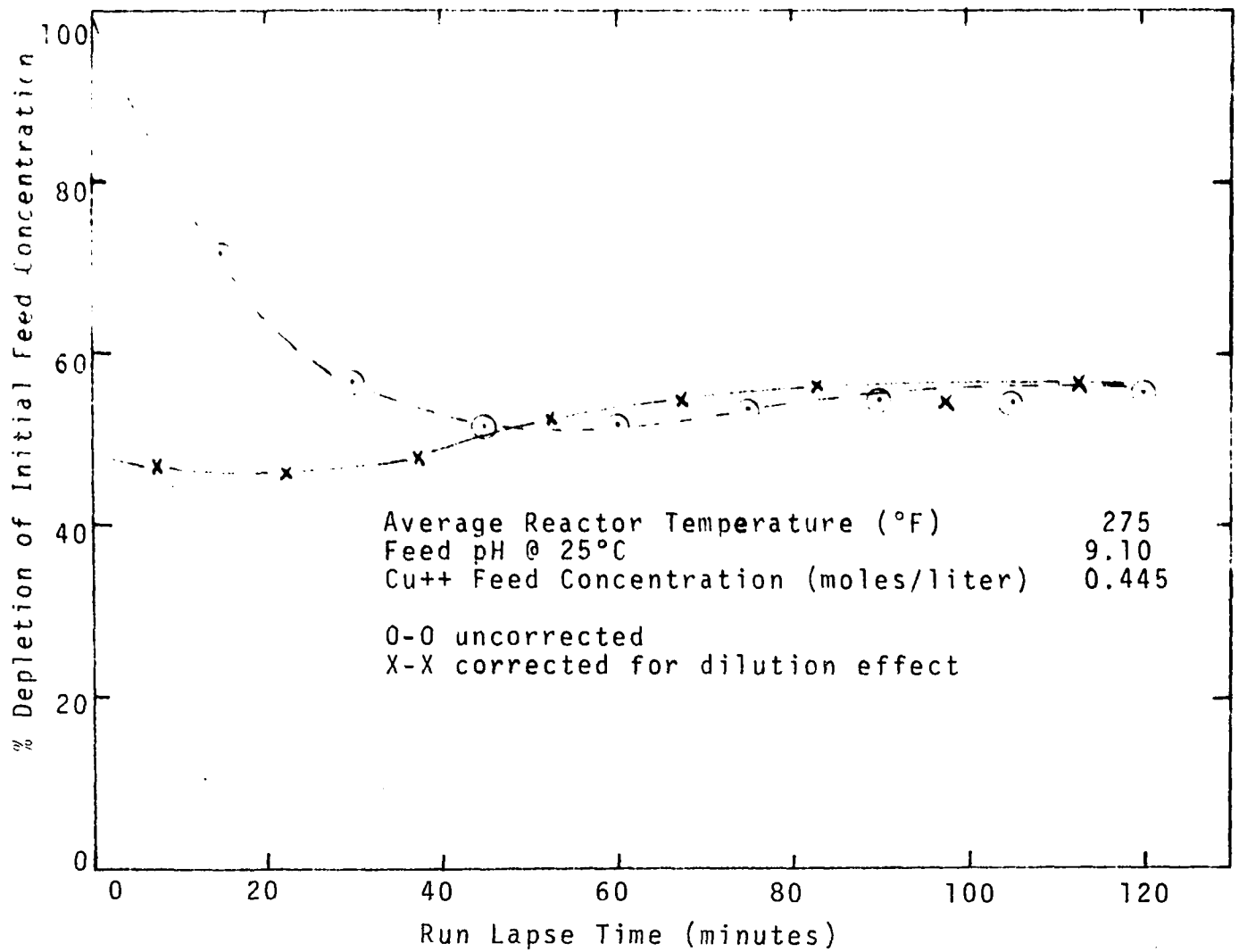

Figure 26. Lapse Time versus Depletion (Run 8)

Run 9 Observations and Notes

1. Non-isothermal reactor.
2. Feed solution was depleted product solution from Run 8 treated with ammonium hydroxide.
3. Smooth operation and run was terminated as scheduled.
4. Product formed during [illegible]zed 100% cupric oxide
5. Refer to Figure 2[illegible]rsus depletion plot.

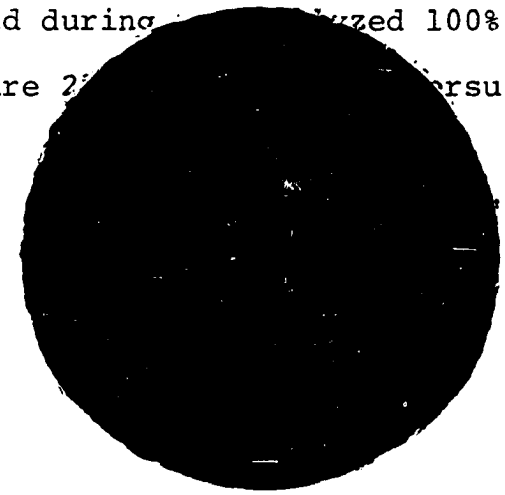

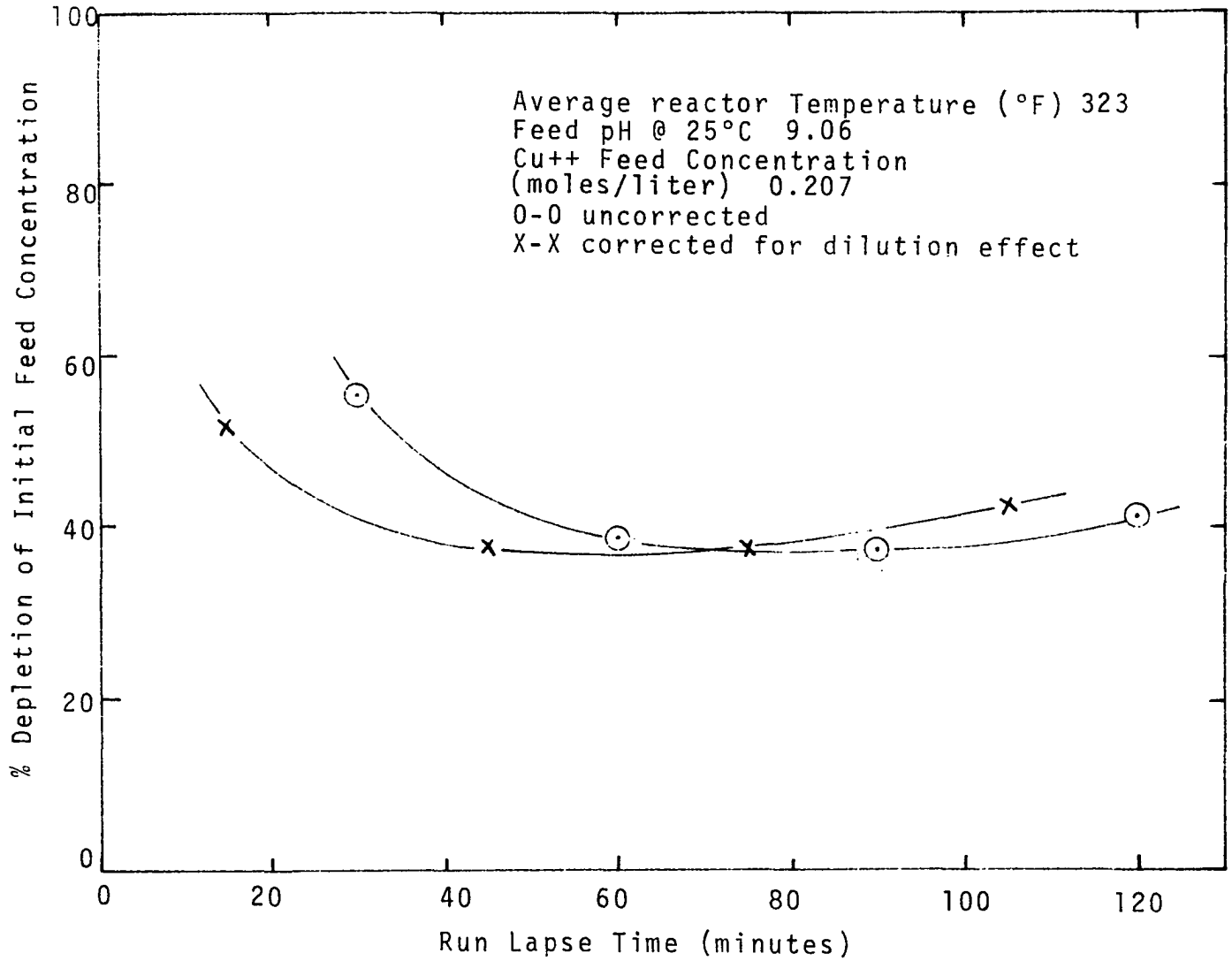

Figure 27. Lapse Time versus Depletion (Run 9)

Run 10 Observations and Notes

1. Non-isothermal reactor.
2. Feed solution was prepared from depleted solutions from runs 3, 4, and 9 and treated with ammonium hydroxide and buffered with an additional 200 grams/liter ammonium sulfate.
3. Smooth operation and run was terminated as scheduled.
4. Small amount of product solids recovered analyzed 100% ammonium sulfate.
5. No conversion to metallic copper, oxides, or basic salts were observed.
6. Analysis of feed and product solutions confirmed zero feed depletion.
7. Lapse time versus depletion correlations were not necessary.

Run 11 Observations and Notes

1. Non-isothermal reactor.
2. Repeat operation of Run 10 with freshly prepared copper sulfate-ammonium hydroxide solution containing 200 grams per liter ammonium sulfate buffer.
3. Following the first 60 minutes of operation, depletion of initial feed concentration was approximately 5 percent. Product solution did not contain solids of any type.
4. At 83 minutes lapse time, 100 cc of concentrated sulfuric acid was added to the approximately 4500 grams of feed solution remaining in the feed accumulator.
5. Resulting neutralization of feed solution formed a very finely dispersed precipitate of basic salts.
6. Depletion increased to approximately 90 percent and fine 100% purity metallic copper product was produced after the neutralization.
7. Lapse time versus depletion plot for Run 11 is given in Figure 28.

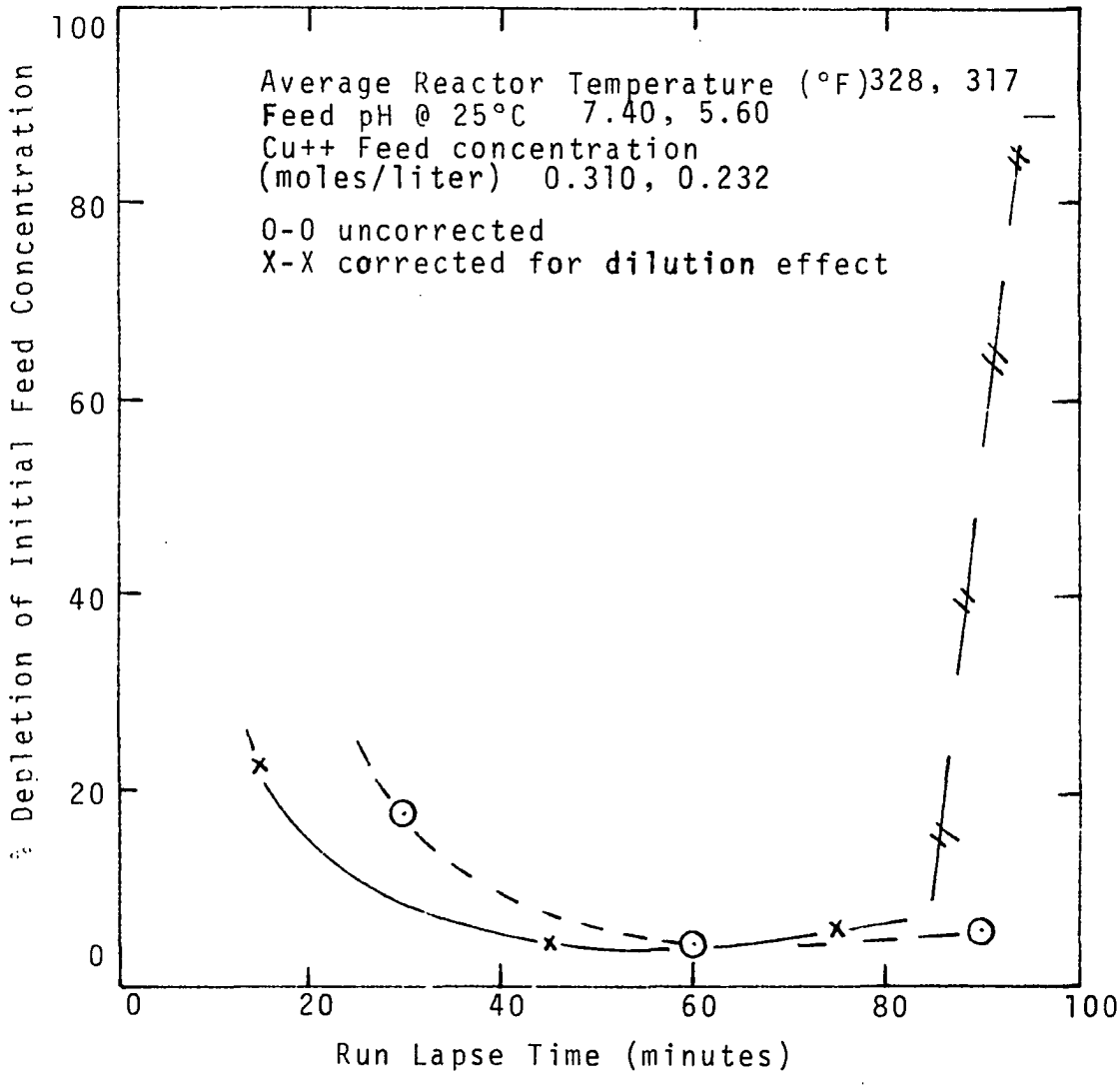

Figure 28. Lapse Time versus Depletion (Run 11)

Run 12 Observations and Notes

1. Non-isothermal reactor.
2. Feed solution for run was obtained from filtered depleted solution recovered during initial phase of Run 11.
3. Objective of run was to neutralize ammine feed solution downstream of high pressure feed pump and thus insure all precipitate formed during neutralization was charged to the reactor.
4. Acid feed system using a nitrogen pressured acid feed accumulator with a manual acid throttling valve was installed.
5. Resulting acid feed rate control was unsatisfactory. Period of operation between 30 and 60 minutes lapse time provided desired ammonia to copper feed ratio and resulted in high purity metallic copper product.
6. Reactor inspection following run did not reveal any free or deposited solids.
7. Lapse time versus depletion plot for Run 12 is given in Figure 29.

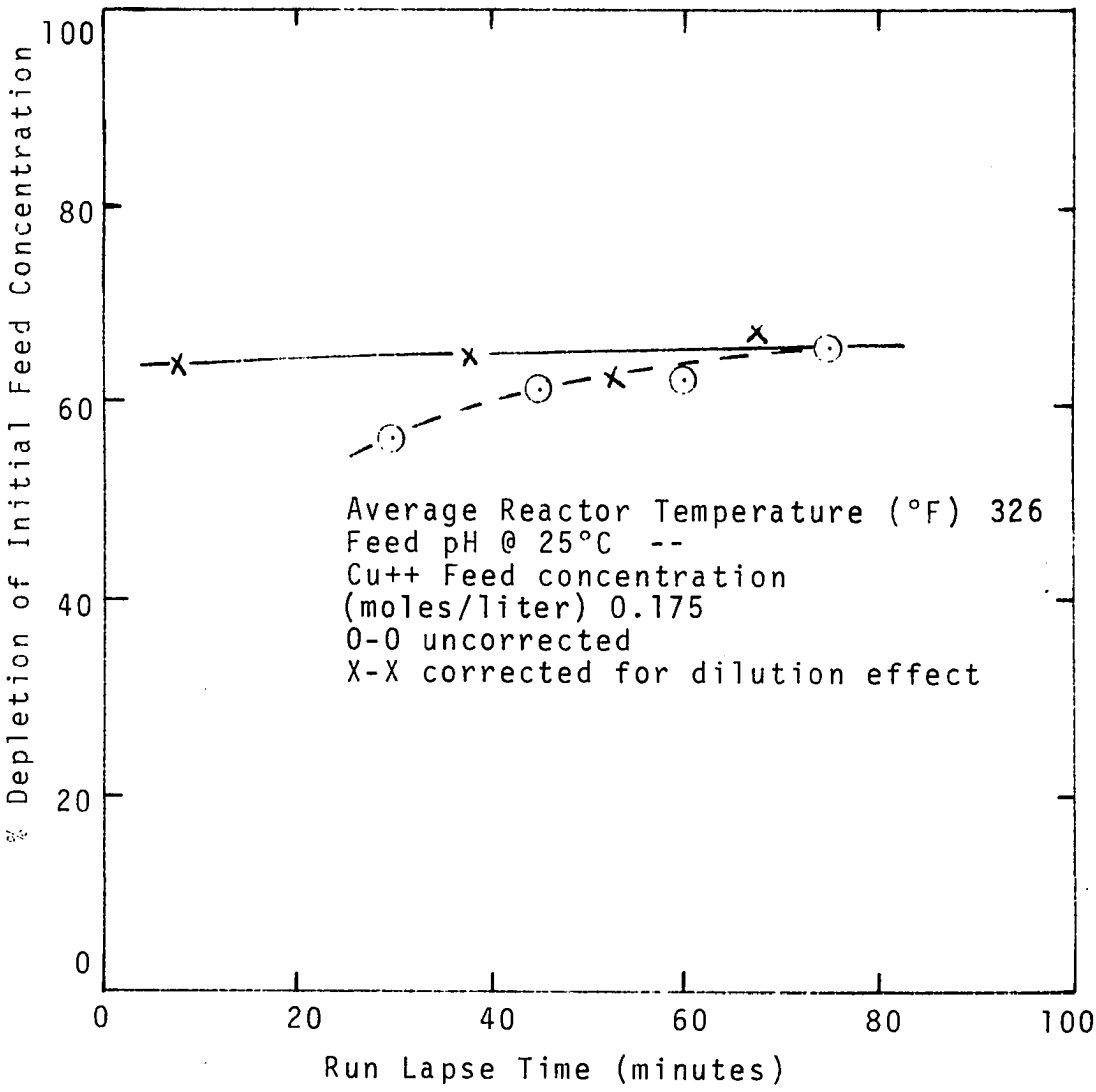

Figure 29. Lapse Time versus Depletion (Run 12)

Run 13 Observations and Notes

1. Non-isothermal reactor.
2. Feed neutralization and pretreatment procedure initiated in Run 11 and pursued in Run 12 was used.
3. Improved acid feed system using laboratory, diaphram feed pump was installed prior to run.
4. Fresh ammine-copper sulfate feed solution prepared.
5. Acid feed rate control was satisfactory, however, acid feed rates were changed too rapidly and steady-state operations were not established.
6. Intermediate products recovered included oxides, basic salts of copper and metallic copper.
7. Lapse time versus depletion plot for Run 13 is given in Figure 30.
8. Data obtained during run and reactor temperature profile are given in Appendix D.

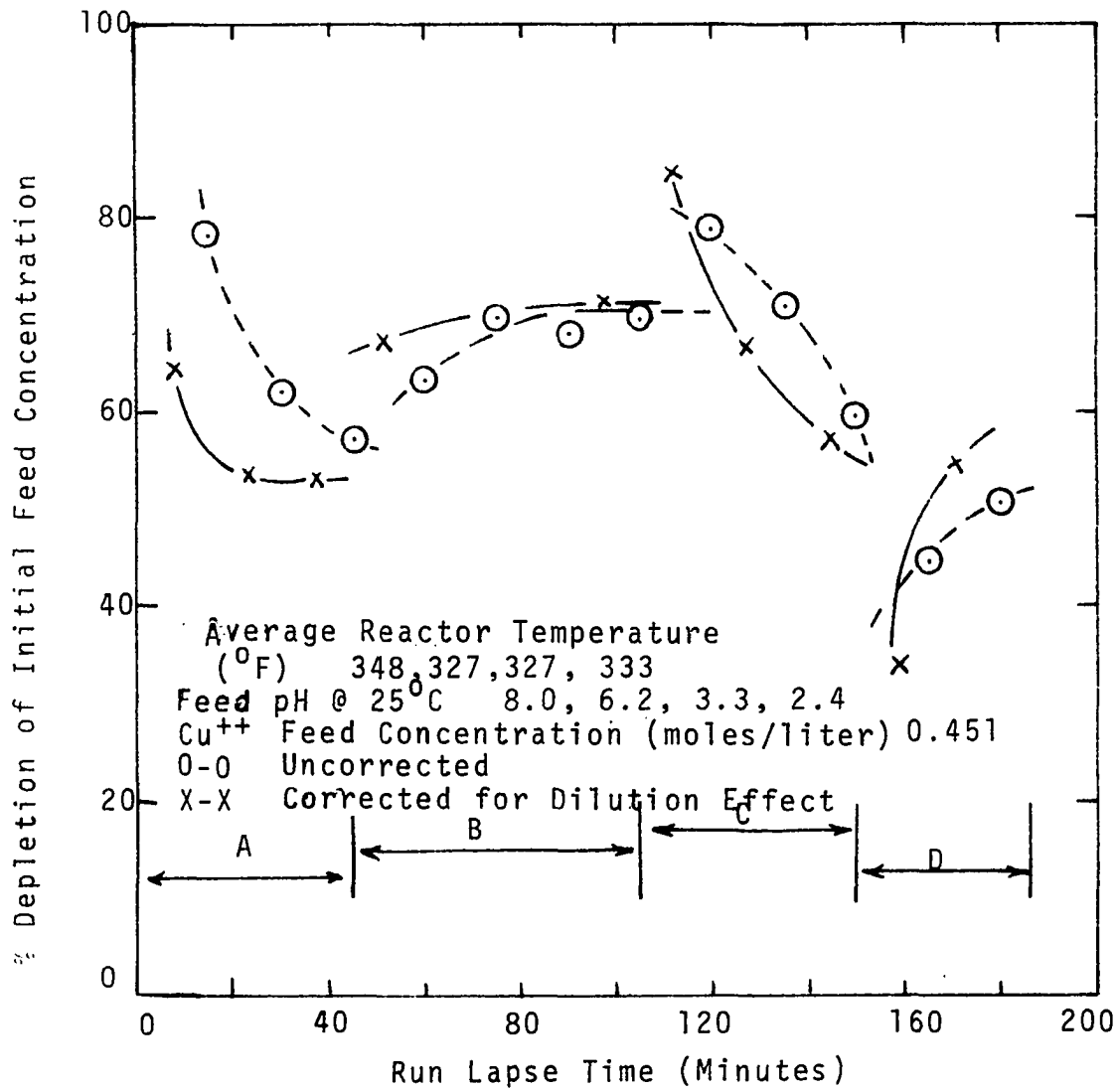

Figure 30. Lapse Time versus Depletion (Run 13).

Run 14 Observations and Notes

1. Non-isothermal reactor.
2. Feed solution was obtained by filtering depleted product solution from Run 13. Ammonium hydroxide was added to depleted solution to increase effective ammonia to copper mole ratio to approximately 4.
3. Excellent control of acid feed rate was maintained during first 60 minutes of operation.
4. After 60 minutes operation, electrical problems with the acid feed pump forced termination of the run.
5. Product copper sample recovered at 30 minutes lapse time analyzed 100 percent metallic copper. Sixty minute product sample and accumulated run product analyzed the following day contained cuprous oxide and metallic copper.
6. Lapse time versus depletion plot is given in Figure 31.

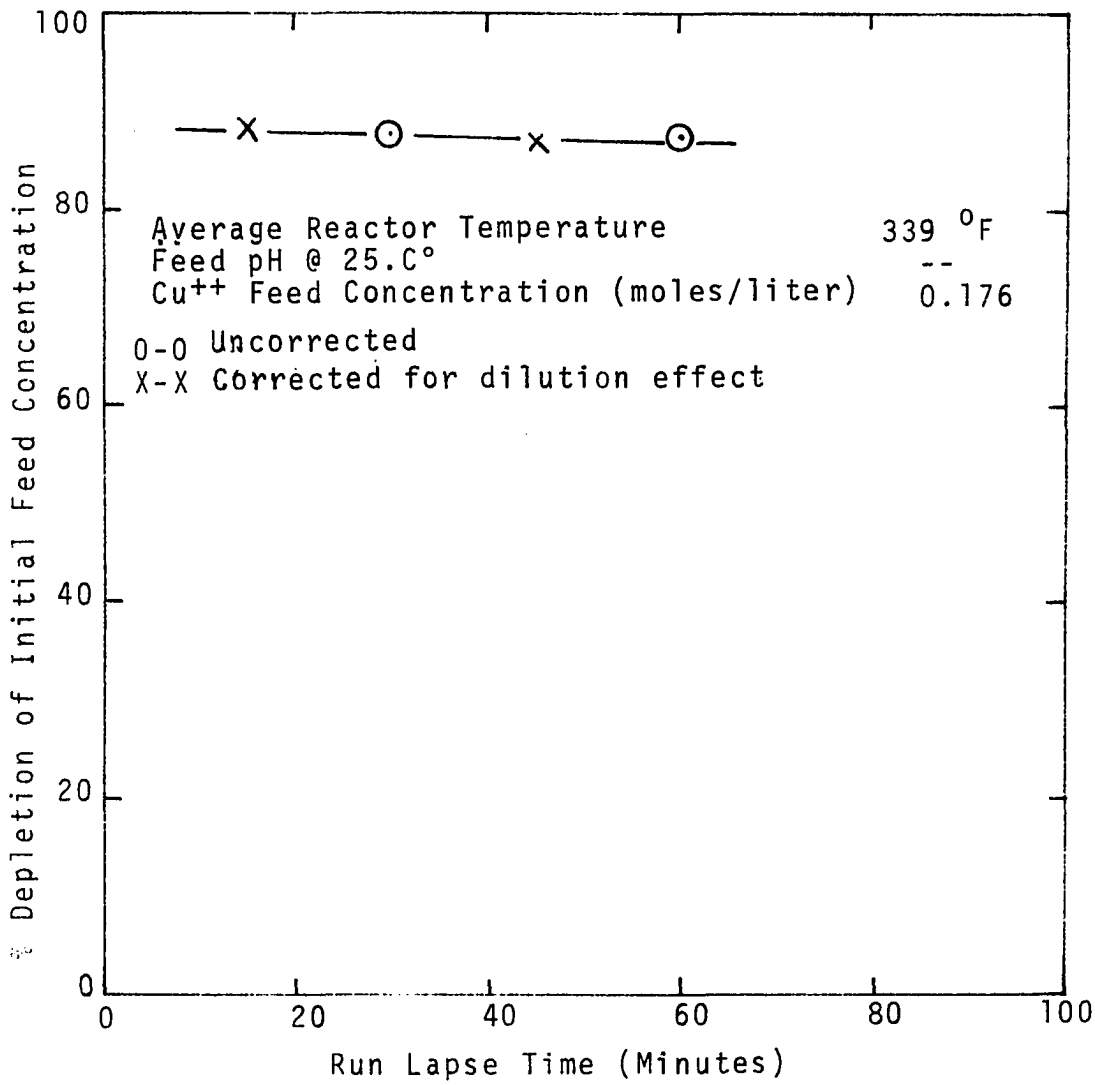

Figure 31. Lapse Time versus Depletion (Run 14).

Run 15 Observations and Notes

1. First non-isothermal continuous nickel reduction run.
2. Feed solution was prepared by adding ferrous sulfate to distilled water solution of nickel sulfate. This combination of feeds did not form a precipitate.
3. Addition of ammonia to the nickel-ferrous sulfate solution forms a precipitate.
4. Ammonium hydroxide was added using the acid pretreatment pump and accumulator system.
5. Objective of run was to explore wide range of ammonia to nickel mole feed ratios.
6. Improved apparent feed depletions were observed at the highest ammonia to nickel mole feed ratio.
7. The reactor upward velocity used in previous copper operations was insufficient to remove nickel produced during this run. Therefore, approximately 80 percent of nickel produced during the run stayed in the reactor.
8. Reactor inspection following the run revealed limited surface deposits with the majority of the contents being in the form of powder.
9. Reactor nickel recovered from the run was subjected to particle size analysis described in Chapter VIII.
10. Lapse time versus depletion plot is given in Figure 32.

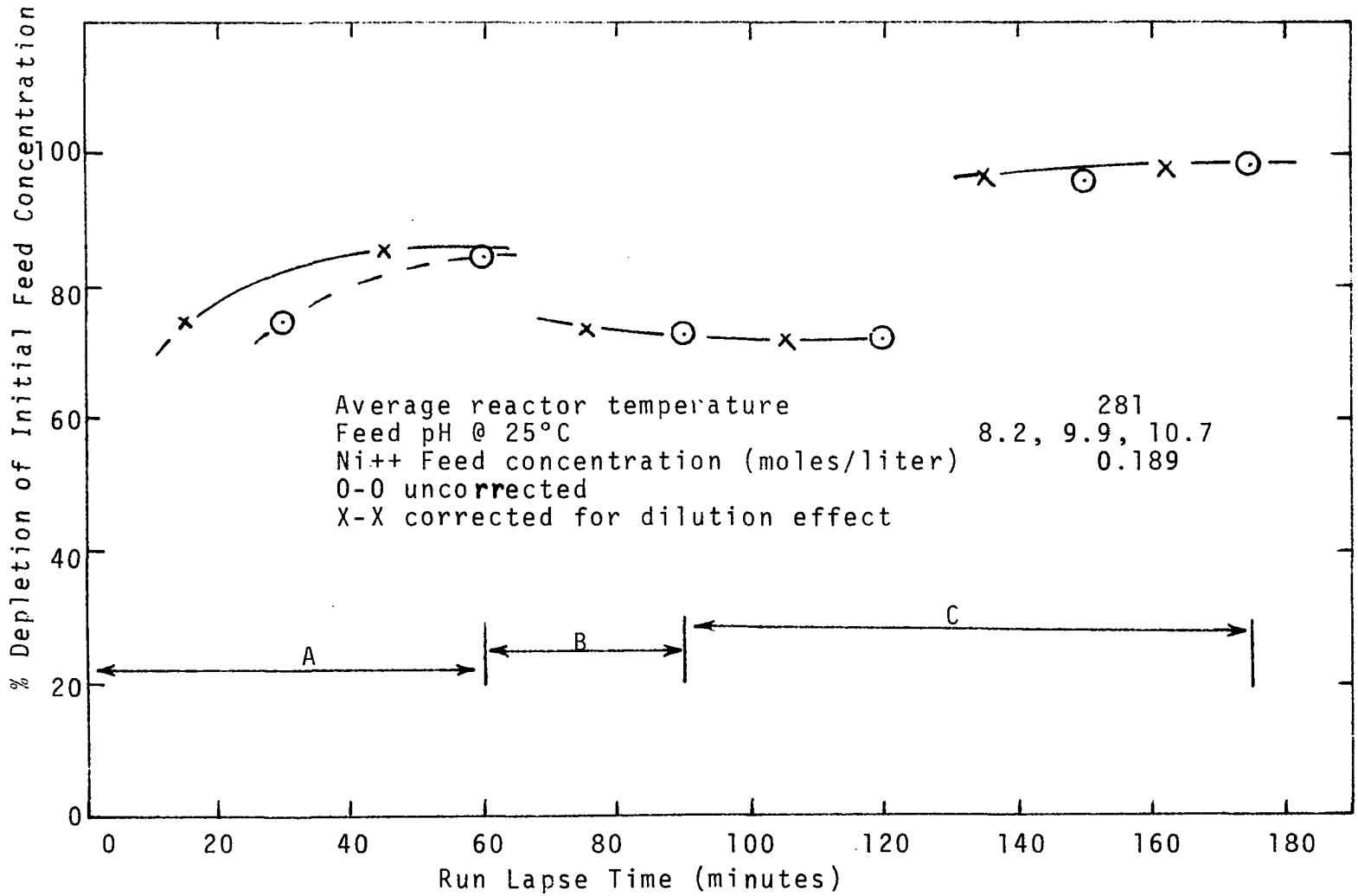

Figure 32. Lapse Time versus Depletion (Run 15)

Run 16 Observations and Notes

1. Non-isothermal reactor.
2. Feed solution similar to previous Run 15.
3. Feed rates approximately doubled to provide sufficient upward reactor velocity to prevent accumulation of product in reactor.
4. Corresponding average reaction temperature during run was below 200°F.
5. Vent gas dry-test meter was inoperative during this run.
6. Approximately 70 percent feed depletion was obtained and nickel product recovered from the separator analyzed, by X-ray diffraction, 100 percent metallic nickel.
7. Product nickel recovered appeared to be a very fine colloidal suspension. Details of product analyses are given in Chapter VII.
8. Reactor deposits following run were determined to be approximately 5 cc.
9. Lapse time versus depletion plot is given in Figure 33.

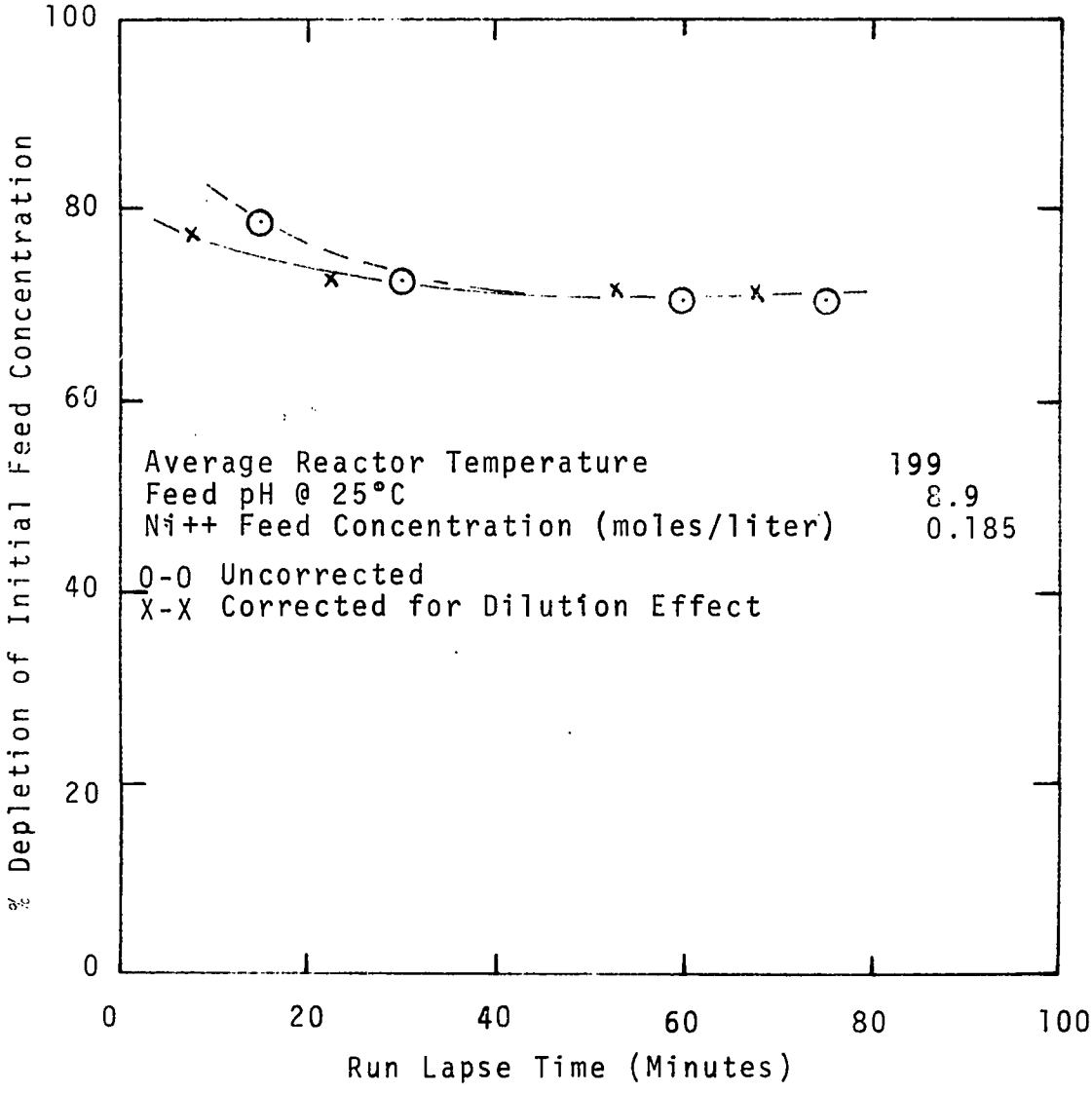

Figure 33. Lapse Time versus Depletion (Run 16).

Run 17 Observations and Notes

1. Non-isothermal reactor.
2. Similar feed solution composition was used in Runs 15 and 16.
3. Ammonium hydroxide pretreatment rate increased to obtain higher depletion rates.
4. Feed solution rate reduced to obtain higher reaction temperature.
5. Resulting depletion of feed nickel concentration was approximately 100 percent. Actual conversion (to metallic nickel) after correction was approximately 45 percent.
6. Reactor product accumulations were greater than in previous Run 16 but less than during Run 15.
7. Reactor inspection following run revealed partially plugged discharge line and less than 5 cc actual reactor deposits.
8. Lapse time versus depletion plot is given in Figure 34.

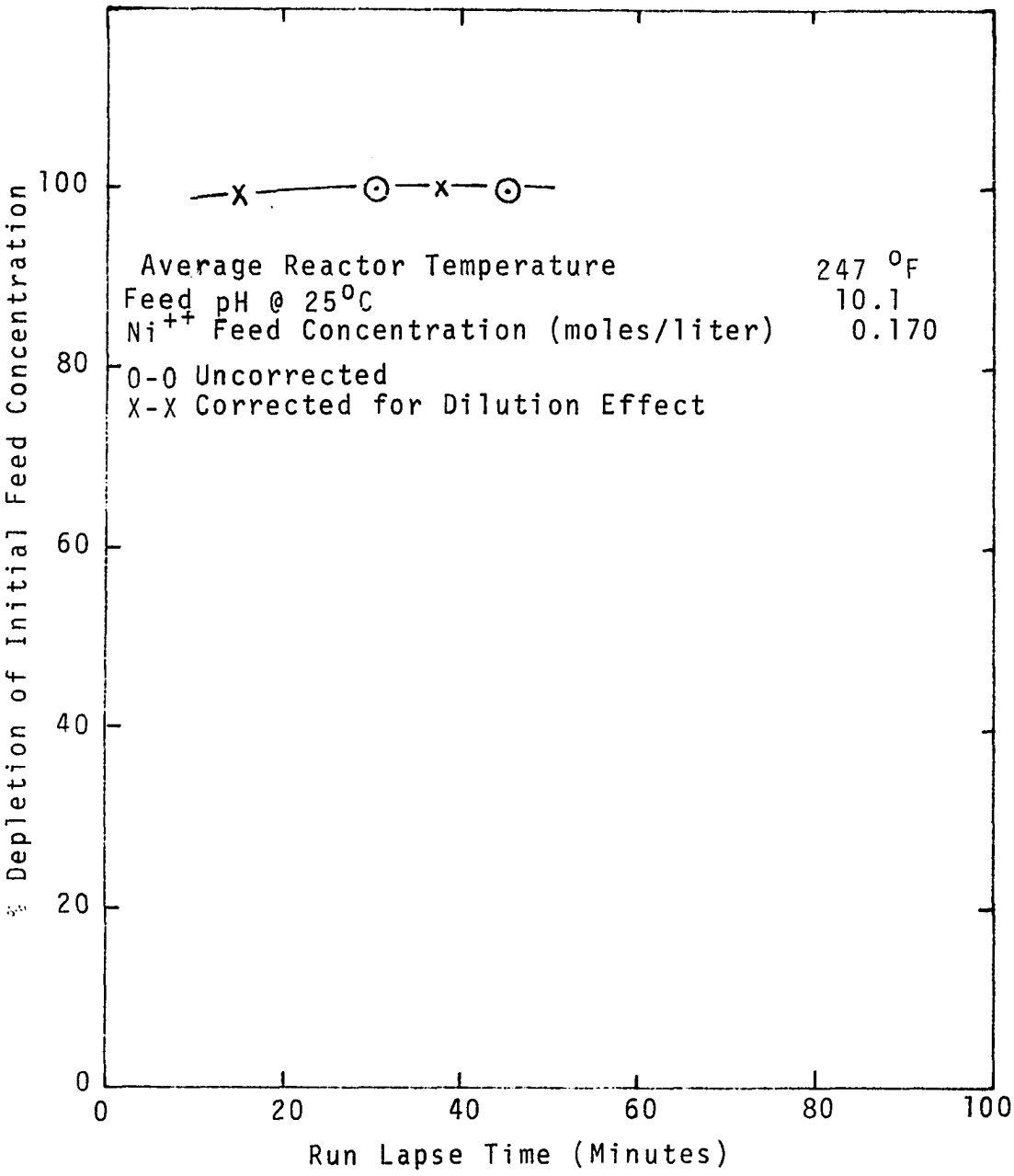

Figure 34. Lapse Time versus Depletion (Run 17).

Run 18 Observations and Notes

1. Non-isothermal reactor.
2. Similar feed solution composition was used in Runs 15, 16, and 17.
3. Intermediate solution feed rate between that used in Runs 16 and 17 was chosen to optimize feed depletion and minimize reactor product accumulation.
4. Reactor discharge plugging was observed after approximately 30 minutes lapse time and forced termination of the run after 42 minutes operation.
5. High feed depletions were obtained and very limited reactor accumulations were observed following the run.
6. Measured reactor deposits were approximately 15 cc.
7. Lapse time versus depletion plot is given in Figure 35.

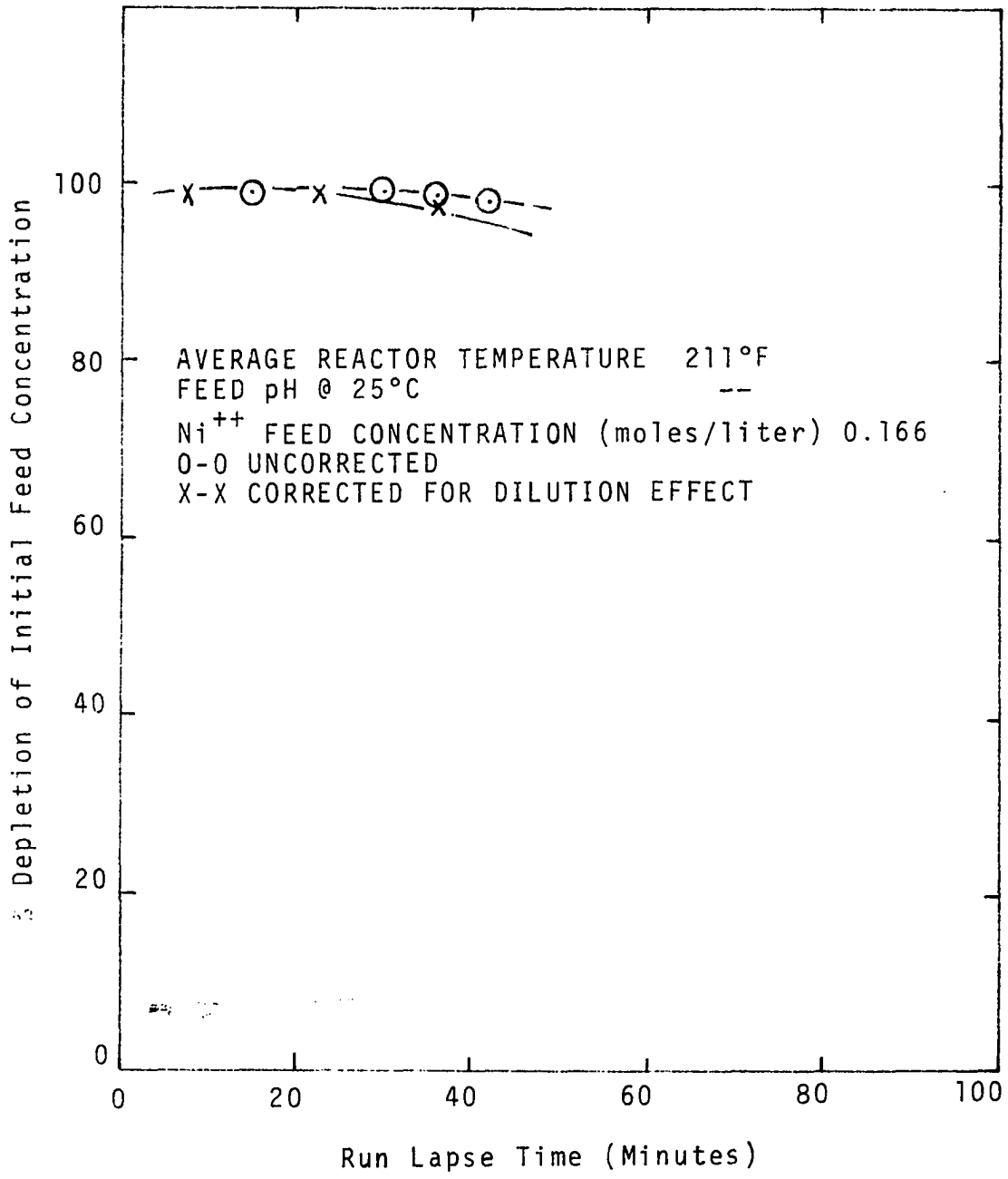

Figure 35. Lapse Time versus Depletion (Run 18)

Run 19 Observations and Notes

1. Non-isothermal reactor.
2. Feed solution of copper sulfate was obtained from the acid leach of an oxide ore and contained soluble iron, aluminum and magnesium ions.
3. The pH of the solution from acid leaching was 1.65.
4. Continuous reduction feed for Run 19 was continuously pretreated with ammonium hydroxide to increase the resulting feed pH to approximately 5.
5. The resulting 75 minute operation provided a steady-state feed depletion of approximately 95 percent.
6. Product copper recovered immediately following the run and analyzed by X-ray diffraction contained only metallic copper.
7. Comparison of solution iron concentration in the feed and in the steady-state depleted product solution revealed essentially all iron remained in solution.
8. Copper product left in depleted solution overnight rapidly oxidized to cuprous oxide.
9. Reactor inspection following run revealed loose granular deposits of cuprous oxide on the upper reactor walls and process thermowell.
10. Total reactor contents, including loose solids and deposited solids, were experimentally determined to be approximately 40 cc.

Run 19 Observations and Notes (continued)

11. Overall material balance for the operation, including reactor solids recovered, was 97.9 weight percent of the original feed weight.

12. Lapse time versus depletion plot is given in Figure 36.

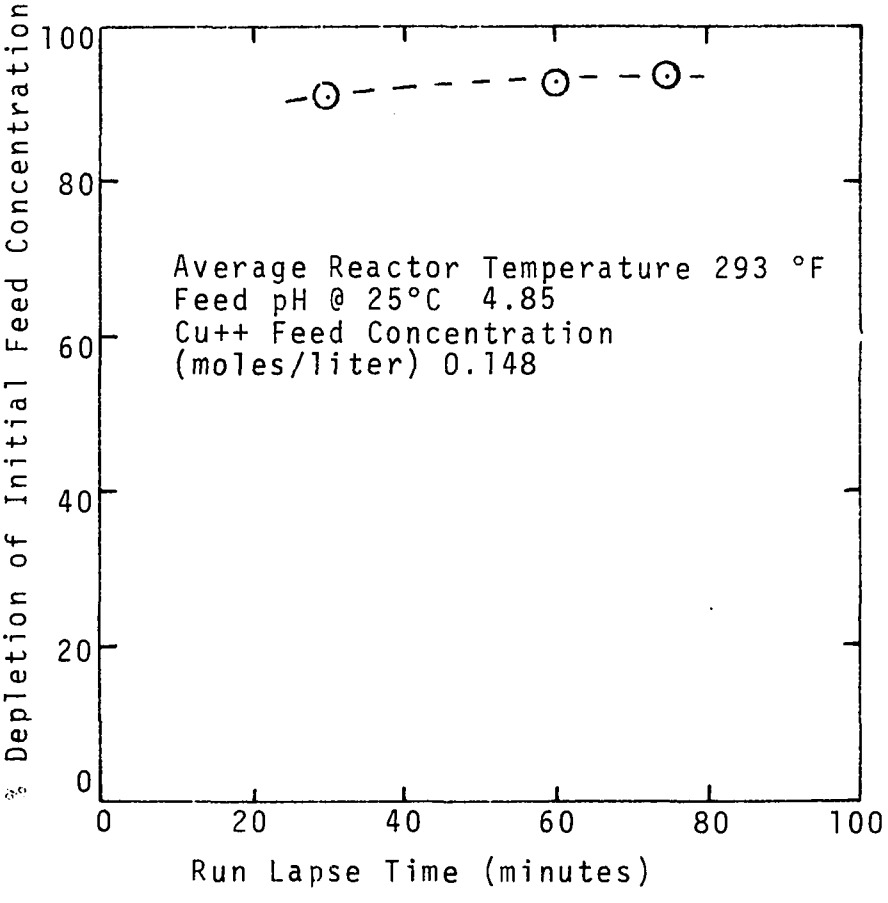

Figure 36. Lapse Time versus Depletion (Run 19)

Run 20 Observations and Notes

1. Non-isothermal reactor.
2. Same acid leach feed solution used in previous Run 19.
3. Ammonium hydroxide feed solution pretreatment was not used.
4. The resulting 75 minute continuous run did not reach steady-state operation. Feed depletion was approximately 75 percent when the run was ended.
5. Pressure increase was observed near the end of the run.
6. Reactor inspection following the run revealed severe corrosion near the top of the reactor process thermowell. The reactor walls in the same location also appeared to be corroded.
7. Reactor and thermowell deposits included wall deposits of metallic copper and copper oxides.
8. The total reactor deposits following the run were determined to be approximately 25 cc.
9. Reactor discharge dip-tube was observed to be partially plugged with metallic copper.
10. Overall material balance for the operation, including reactor solids recovered, was 99.5 weight percent of the original feed weight.
11. Lapse time versus depletion plot is given in Figure 37.

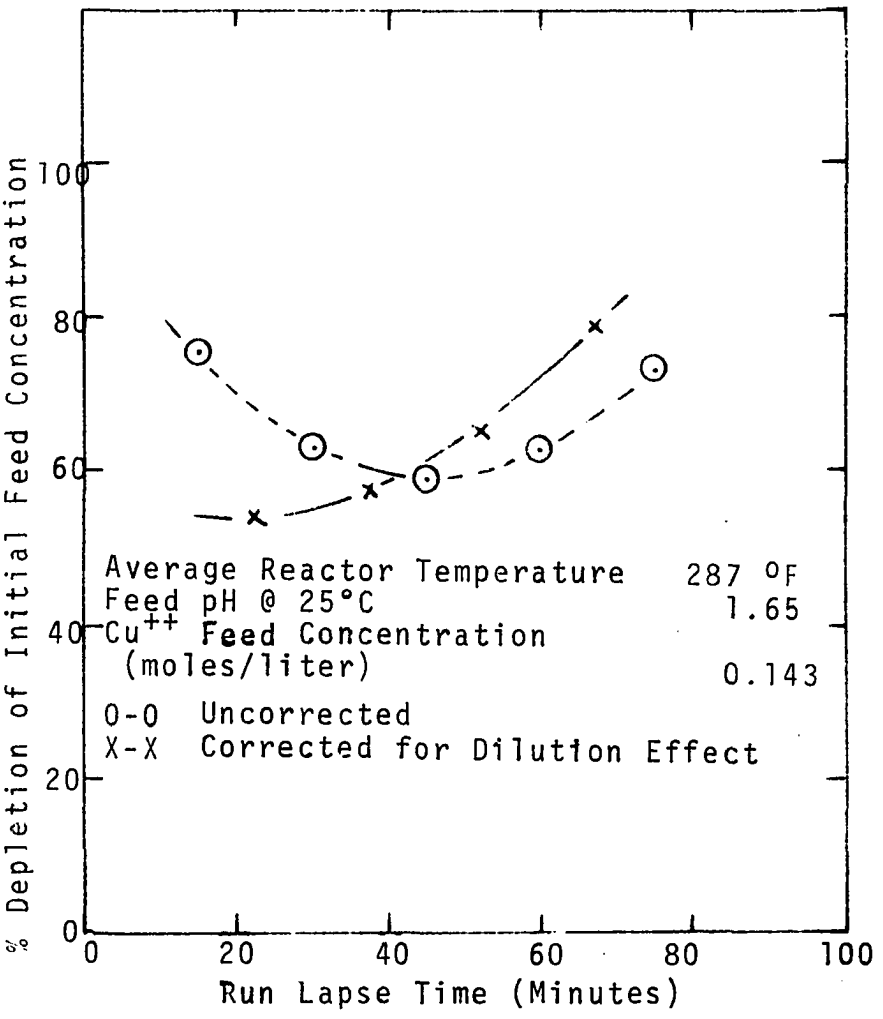

Figure 37. Lapse Time versus Depletion (Run 20).

Run 21 Observations and Notes

1. Non-isothermal reactor.
2. Same acid leach feed solution used in prior two runs.
3. Ammonium hydroxide pretreatment, similar to Run 19 was used to increase the reactor feed solution pH to approximately 5.
4. Run was terminated after 43 minutes operation due to a plugging reactor discharge line.
5. Initial feed depletion at the time of plugging was approximately 90 percent.
6. Reactor inspection following the run revealed cuprous oxide granular deposits similar to those observed during Run 19.
7. All reactor solids were recovered using a burrett cleaning brush and nitric acid cleaning was not necessary.
8. Total reactor solids occupied approximately 15 cc of the original 180 cc clean reactor volume.
9. Overall material balance for the operation, including reactor solids recovered, was 98.5 weight percent of the original feed.
10. Lapse time versus depletion plot is given in Figure 38.

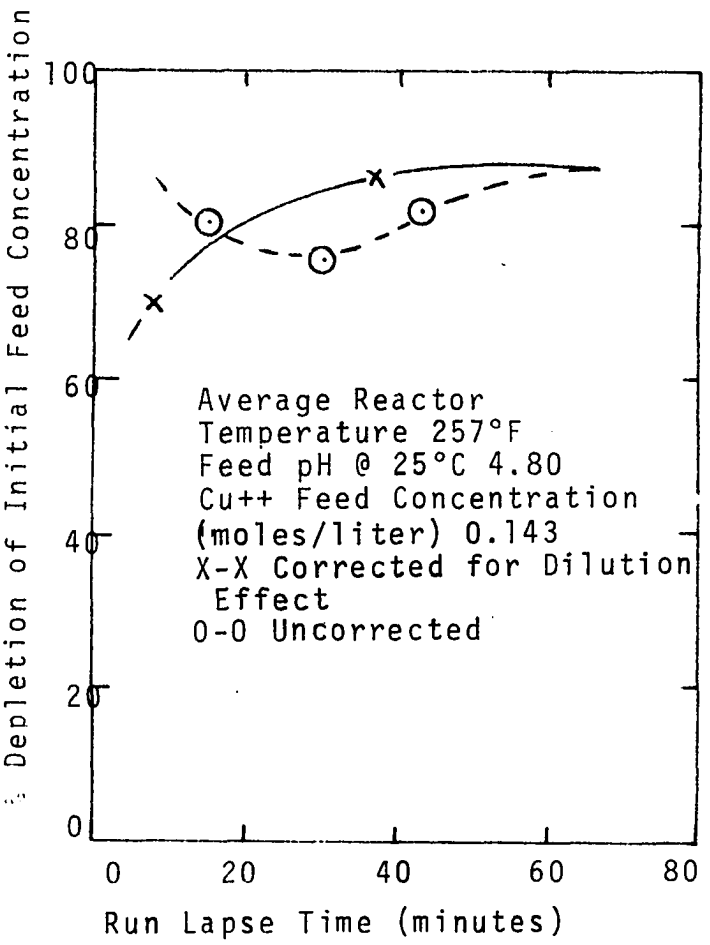

Figure 38. Lapse Time versus Depletion (Run 21)

Run 22 Observations and Notes

1. Non-isothermal reactor.
2. Same acid leach feed solution used in prior three runs.
3. Ammonium hydroxide pretreatment, similar to Runs 19 and 21 was used to increase the reactor feed solution pH to approximately 5.
4. Operation during 110 minute run was very smooth and a steady-state feed depletion of 84 percent was achieved at an average reaction temperature of 250°F.
5. Reactor volume determination revealed approximately 30 cc of the original clean reactor volume (180 cc) was occupied by solids.
6. Following this run, the tubular reactor was removed and dissected for subsequent inspection.
7. Deposits of various compositions were noted at different reactor positions. The lower 15 inch section of the reactor was relatively free of deposits. The reactor section between 15 and 18 inches from the lower end contained spherical nodule deposits on a thin wall deposit of cuprous oxide. The six inch section between 18 and 24 inches from the lower reactor end was composed of a cuprous oxide deposit increasing to approximately 0.06 inches in thickness. The 3 inch section between 24 and 27 inches from the lower end of the reactor included a green deposit of copper basic salt on a sub-layer of cuprous

Run 22 Observations and Notes (continued)

oxide. Approximately 29 inches from the lower end of the reactor, the basic salt deposit disappeared. The cuprous oxide deposit continued upward to the normal reactor operating level and reached a maximum thickness of approximately 0.125 inches.

8. Lapse time versus depletion plot is given in Figure 39.

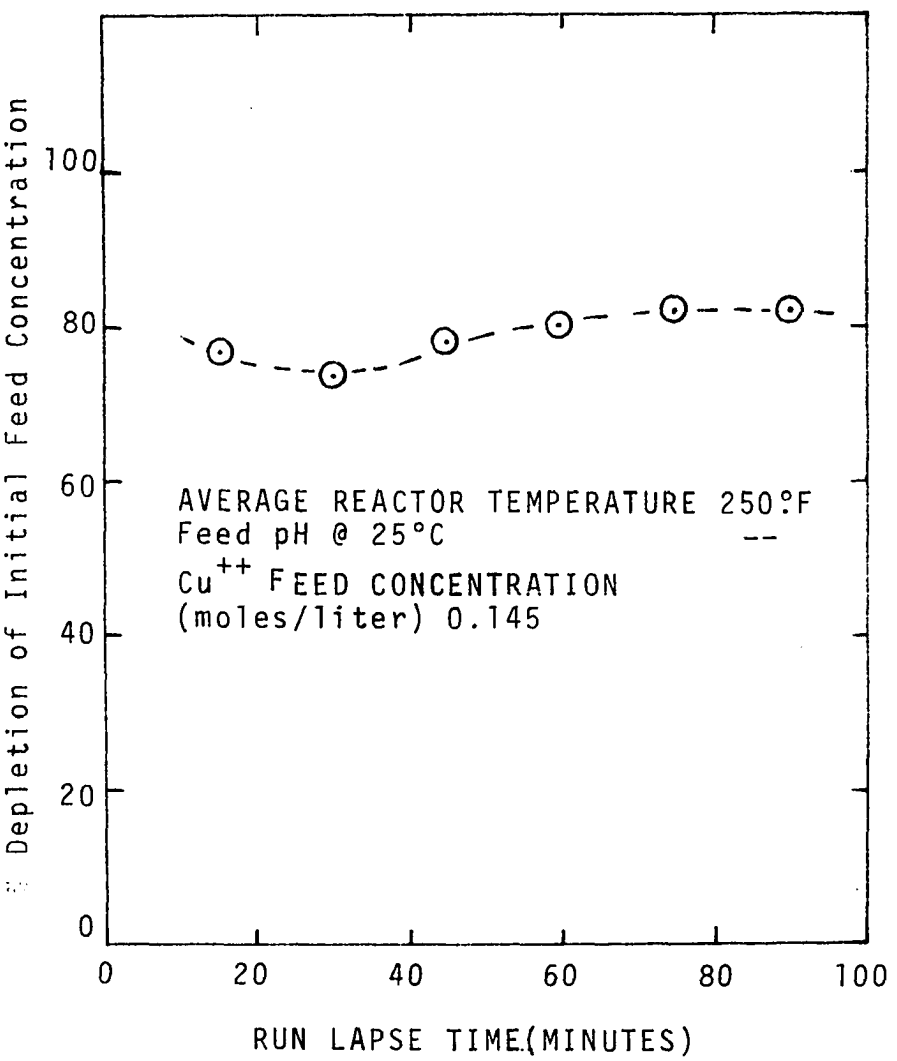

Figure 39. Lapse Time versus Depletion (Run 22)

APPENDIX B

ANALYTICAL TECHNIQUES

This appendix briefly describes the analytical techniques summarized in Table 4.

Specific Gravity

Specific gravity of liquids and slurries was determined by the following procedure:

1. Sample was allowed to equilibrate to room temperature.

2. A clean and dry 50 ml flask was accurately weighed to four decimal places using a Type 10, Ainsworth, electronic balance and the weight was recorded.

3. An accurate 10 ml portion of sample was obtained with a pipet and transferred to the weighed flask.

4. The flask and sample was reweighed to four decimal places and the weight was recorded.

5. Corresponding relation between sample weight (obtained by difference of weights in steps 2 and 4) and volume provided sample specific gravity (density).

Hydrogen Ion Concentration (pH)

A Orion Research, Model 401, specific ion meter was used in conjunction with a silver chloride reference electrode to measure pH. The following procedure was used:

1. Sample was allowed to equilibrate to room temperature.

2. pH meter and electrode was calibrated using buffer solutions of 1, 7, and 11 pH.

3. After calibration, sample pH was measured and recorded.

Free Ammonia Analysis

Free ammonia or the complexed ammonia was determined using the following procedure (14):

1. Aliquot 5 ml pipet sample was transferred to 125 ml flask.

2. Five drops of methyl orange indicator were added to aliquot sample.

3. Solution was titrated with a standardized 0.1 molar sulfuric acid solution. Volume of acid required to change solution color from yellow to red was recorded.

4. Standardized acid strength and recorded acid volumes were used to calculate the free ammonia concentrations of liquid and slurry samples.

Iodimetric Titration

Iodimetric titration was used to analyze for copper ion concentrations in liquid, solid, and liquid-solid samples. The procedure recommended by Pierie, Sawyer and Haenisch (27) was used and is briefly described below:

1. A sample (5 to 10 ml) of the copper solution was accurately obtained using a pipet.

2. When solids were analyzed, a weighed sample of the solid was first dissolved in nitric acid. One gram of urea was added to the dissolved sample and the solution was boiled for one minute and then cooled.

3. Ammonia was added to the solution, from step 1 or 3, until the solution showed a deep blue color.

4. Acetic acid was added (about 5 ml) to buffer the solution.

5. Potassium iodide (about 5 grams) was added and the sample allowed to stand for a couple of minutes.

6. The sample was titrated with a standard solution of sodium thiosulfate until the iodine color began to fade. Starch indicator was added and the titration was continued until the white starch end point was reached.

7. Based on the volume of standard sodium thiosulfate used in the titration, the equivalents of sodium thiosulfate and consequently equivalents of copper in the sample were obtained.

EDTA Titration

EDTA (ethylenediammetetraacetic acid) analyses were used for determining nickel and iron concentrations in all sample phases. The following procedure for nickel was described by Homer (14):

1. A 5 ml sample of liquid solution was accurately obtained using a pipet.

2. When solids were analyzed, a weighed sample of the solid was first dissolved in nitric acid.

3. The solution from step 1 or 2 was adjusted to a pH of 9 using ammonium hydroxide.

4. Murexide indicator was added to the buffered solution (less than four crystals).

5. The solution was titrated with standardized EDTA to the murexide end point.

6. The nickel concentration in the sample was calculated from the volume of standard EDTA used in step 5.

The following procedure for iron analysis was described by Homer (14):

1. A 5 ml sample of liquid solution or a weighed sample of solid dissolved in nitric acid was obtained.

2. Six molar sodium hydroxide was added drop-wise until a deep red-brown Fe-OH precipitate of $Fe(OH)_3$ was formed.

3. The precipitate from step 2 was redissolved with 6M HNO_3 and four drops excess added.

4. 25 ml of 0.02 M EDTA (an excess) was added to the solution of step 3 .

5. Three drops of xylenol orange indicator were added after the iron complexing in step 4 was complete (approximately one minute).

6. The excess EDTA was back titrated with standard Bi(III) solution to the xylenol orange end point.

7. The concentration of iron was determined by calculating the difference in original EDTA added (25 ml) and the excess EDTA titrated with Bi(III).

X-ray Diffraction

Solid samples were analyzed using the Norelco X-ray unit located in the School of Geology. The following analysis procedure was followed:

1. The solid samples were allowed to dry in an oven at approximately 110°C.

2. The dry solids were ground to a fine powder using a mortar and pestle.

3. A small portion of the solid sample was placed on a vaseline slide and exposed to X-rays from the Norelco unit.

4. The corresponding X-ray pattern peaks were resolved and compared to standards published by the American Society of Testing Materials.

Sieve Analysis

Nickel powders produced by continuous hydrogen reduction were analyzed for particle size distribution. The equipment used for this analysis is located in the School of Geology. The following procedure was followed:

1. The solid powder (approximately 100 grams) was dried in an oven at approximately 110°C and allowed to cool in a dessicator to room temperature.

2. The dry, temperature equilibrated sample was weighed to the nearest 0.1 grams using an electronic balance.

3. The sieve trays were cleaned and tare weights of each tray were obtained to the nearest 0.1 gram.

4. The clean and weighed sieve trays were sequentially stacked; largest mesh size on top and the minus 250 mesh pan on bottom.

5. The sieve sample was placed in the top sieve tray.

6. The sample and sieve tray system was attached to a vibrator table and the particles were separated into their respective size fractions.

7. Sieving was complete when the gross weight of each tray in successive weight determinations was relatively constant.

8. The final particle size distribution was obtained by subtracting the tare weight of each sieve tray from its

final gross weight, thus determining the amount of product larger than each mesh size.

Electron Microscope

The microscopic solid analyses in this investigation were made in the School of Geology by Mr. W. H. Bellis, using a JSM-2 scanning electron microscope.

APPENDIX C

CALIBRATION PLOTS

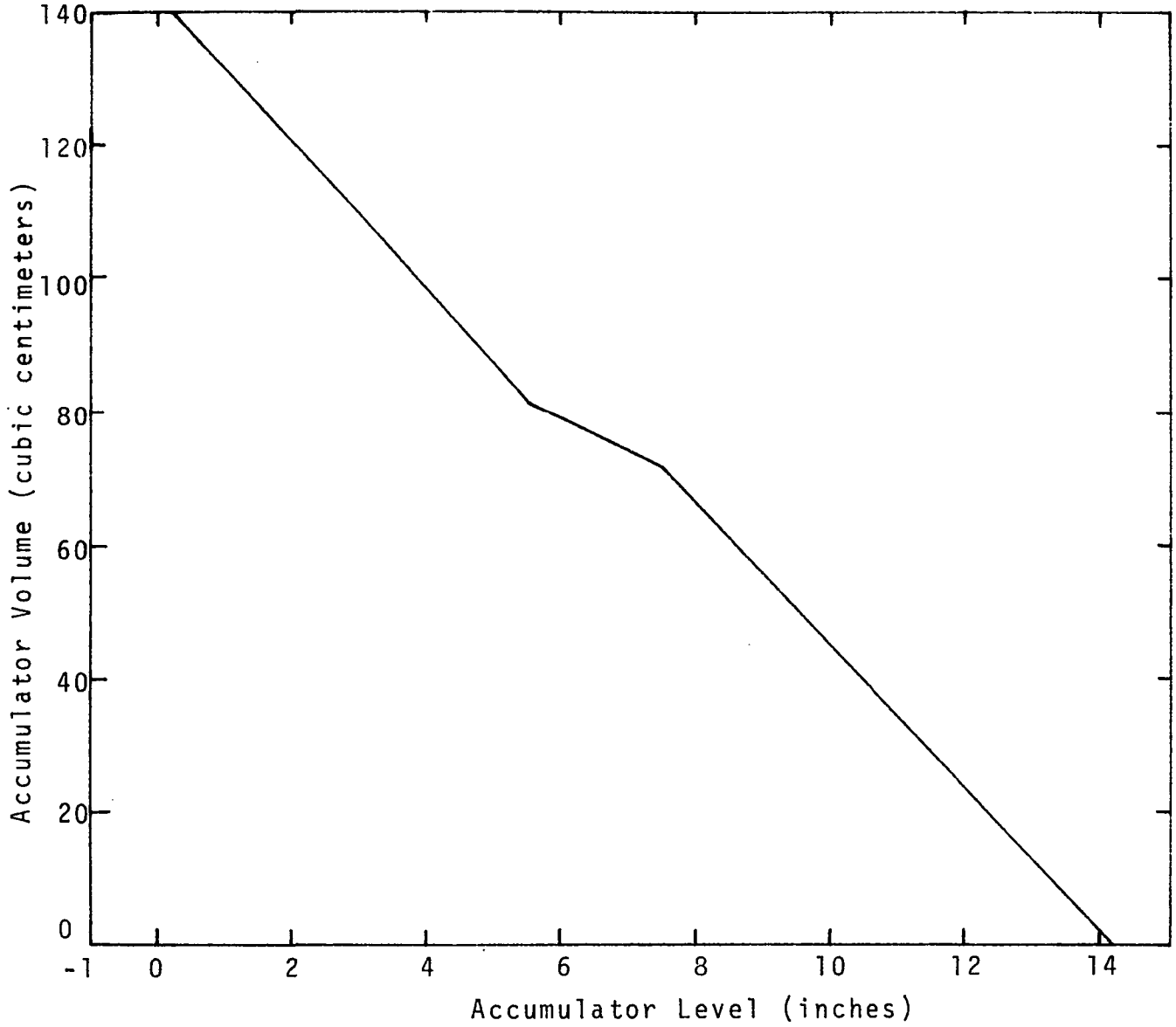

Figure 40. Pretreatment Accumulator Calibration

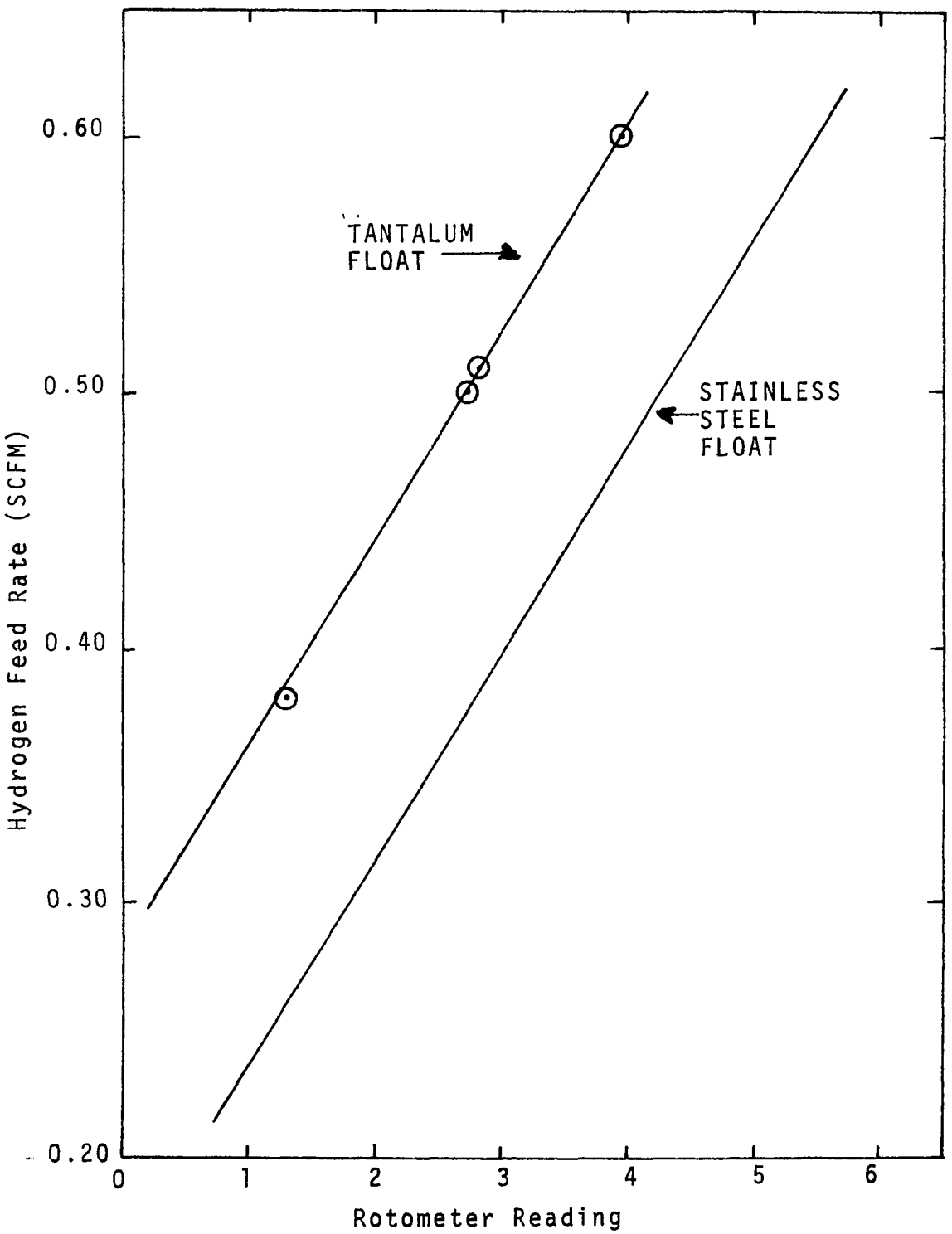

Figure 41. Feed Hydrogen Rotometer Calibration at 625 psig Operating Pressure.

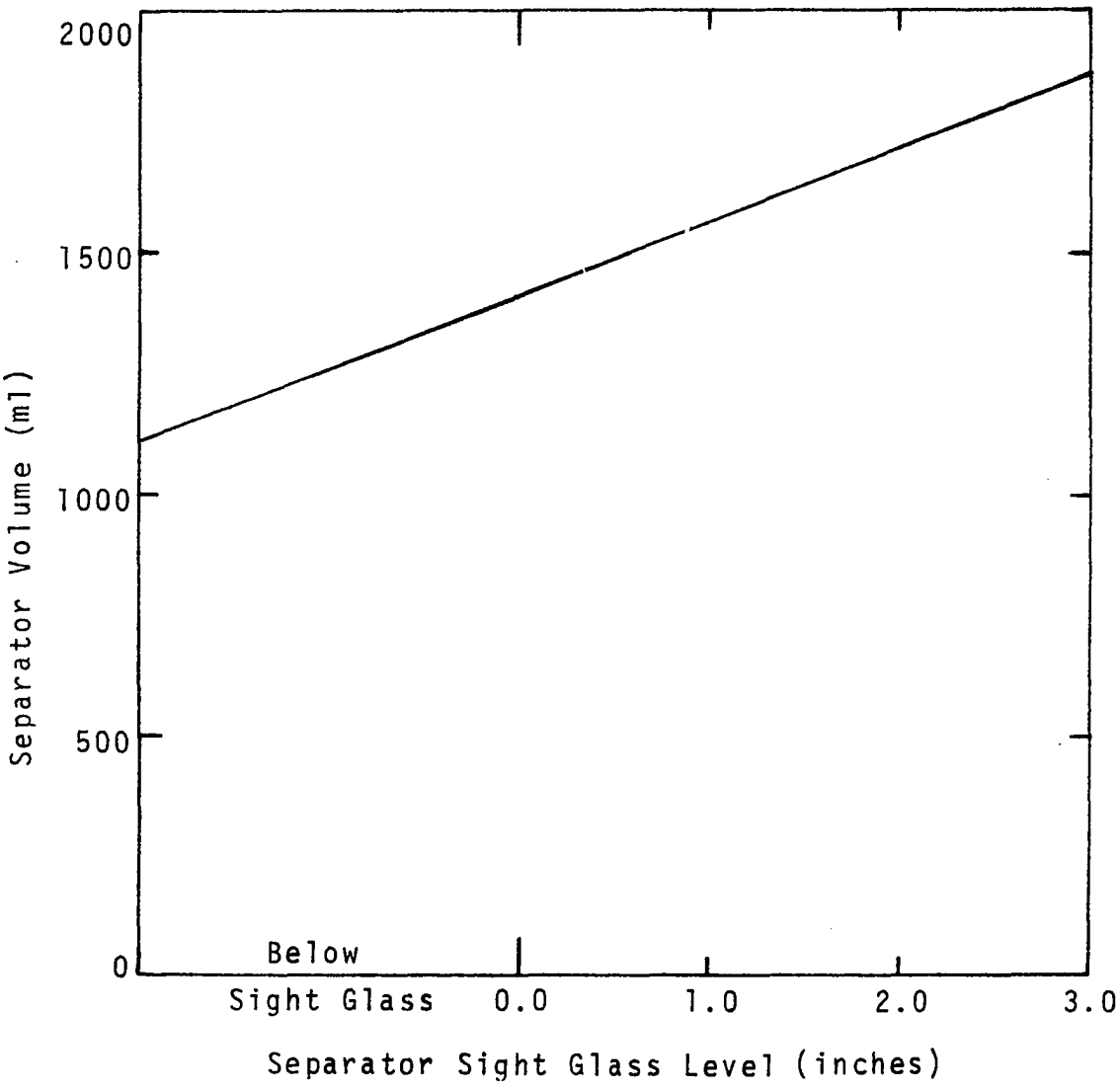

Figure 42. High Pressure Separator Liquid Volume Calibration

APPENDIX D

DATA SHEETS FROM RUN 13

Table 7

Run 13 Data Sheet

Lapse Time (minutes)		High Pressure Separator Level (inches)	Product Gas Rate (SCFM)	Operating Pressure (psig)	Pretreatment Accumulator Level (inches)	Feed Accumulator Weight (grams)	Reactor Top Process Temperature (°F)	Feed Hydrogen Rotometer Pressure Reading (psig)		Samples Feed	Samples Product	Run Notes
Start	0	1.0	--	510	14.0	26400	380	625	0.5	F-1	p-1	prod. to A-1
	15	0	0.26	509	13.4	24800	384	625	0.5		p-2	
	30	0	0.29	503	11.9	23400	384	625	0.5		p-3	
	45	1.0	0.29	520	10.5	21950	394	625	0.5		p-4	Inc. Acid Rate
	60	0	0.25	525	7.5	20500	395	625	0.5		p-5	
	75	1.5	0.31	529	3.3	19000	395	625	0.5	F-2	p-6	
	90	0.5	0.28	508	12.8	17500	392	625	0.5		p-7	Acid Accum @85, 2→14"
	105	0.7	0.26	516	9.8	16000	396	625	0.5		p-8	Inc. Acid Rate
	120	0.7	0.29	514	3.6	14550	397	625	0.5		p-9	prod. to A-2
	135	0.5	0.29	514	11.2	13100	396	625	0.5		p-10	Acid Accum @126, 2→14"
	150	0.9	0.29	500	5.2	11650	395	625	0.5		p-11	Inc. Acid Rate
	165	0.4	0.29	503	11.3	10225	396	625	0.5		p-12	Acid Accum @159, 2→14"
	180	0.2	0.28	505	3.2	8750	395	625	0.5	F-3	p-13	prod. sample taken 165-185
End	186	0.8	0.26	511	0.5	8350	395	625	0.5		--	prod. to A-3
Run Average		--	0.28	512	5.0 g/min	97.0 g/min	392	625	0.5			

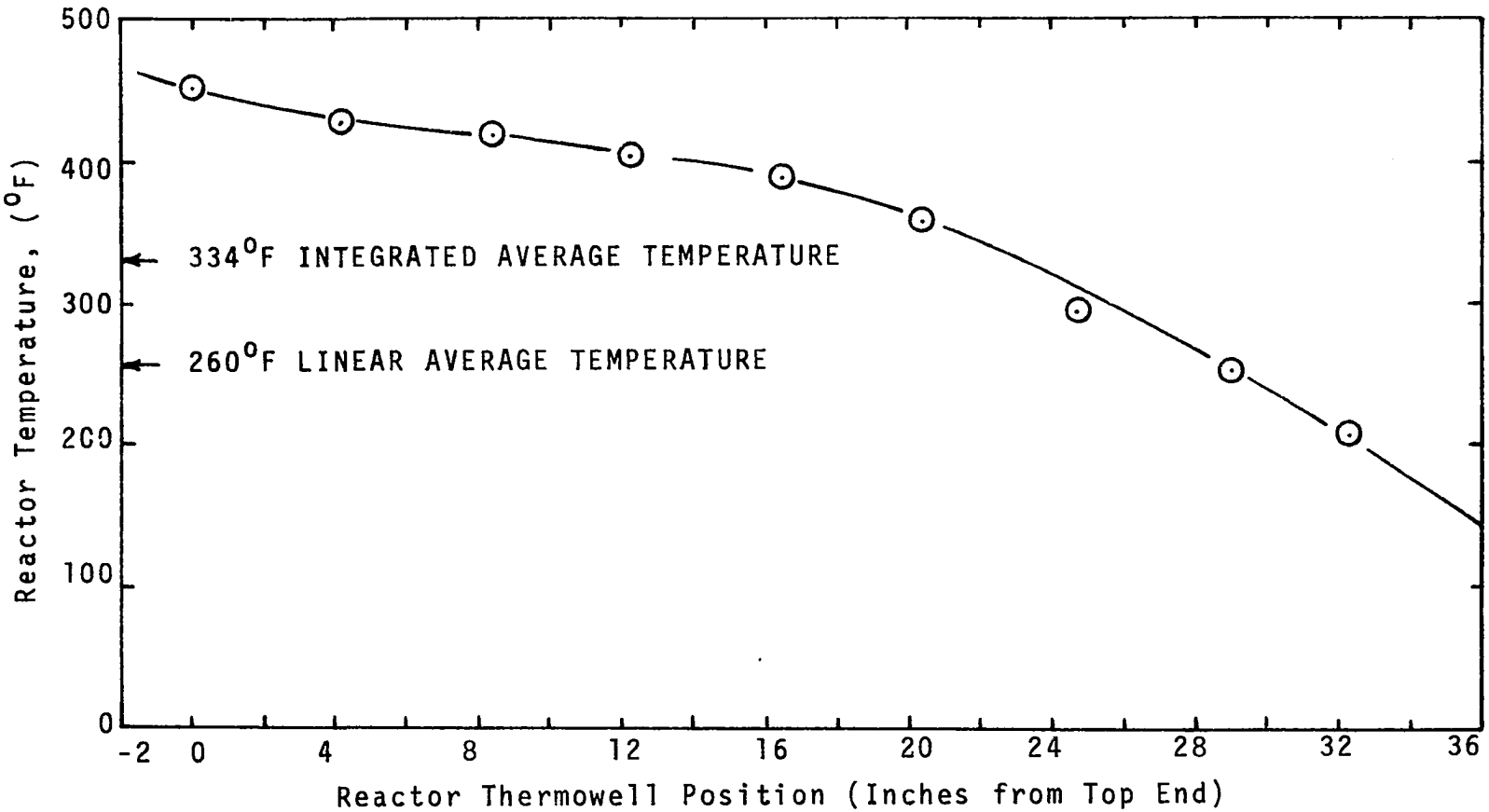

Figure 43. Non-isothermal Reactor Temperature Profile (Run 13).